

TECHNISCHE UNIVERSITÄT MÜNCHEN

Lehrstuhl für Grundwasserökologie

**Distribution and dynamics of contaminant degraders  
and microbial communities in stationary and non-  
stationary contaminant plumes**

Giovanni Piloni

Vollständiger Abdruck der von der Fakultät Wissenschaftszentrum Weihenstephan für Ernährung, Landnutzung und Umwelt der Technischen Universität München zur Erlangung des akademischen Grades eines

Doktors der Naturwissenschaften

genehmigten Dissertation.

Vorsitzende(r): Univ.-Prof. Dr. S. Scherer

Prüfer der Dissertation:

1. Univ.-Prof. Dr. R. Meckenstock
2. Univ.-Prof. Dr. J. P. Geist

Die Dissertation wurde am 16.12.2010 bei der Technischen Universität München eingereicht und durch die Fakultät Wissenschaftszentrum Weihenstephan für Ernährung, Landnutzung und Umwelt am 03.03.2011 angenommen.



## Zusammenfassung

Weltweit sind mehr als zwei Milliarden Menschen für ihre tägliche Wasserversorgung auf Grundwasser angewiesen. Bedauerlicherweise ist Grundwasser einer ständigen Belastung durch eine Vielfalt an anthropogenen Substanzen ausgesetzt. Der mikrobielle Abbau von Schadstoffen ist eine der nachhaltigsten und effektivsten Strategien zur Sanierung von belastetem Grundwasser.

Jedoch sind in vielen Fällen die Identität und Physiologie der am Abbau von Schadstoffen beteiligten Mikroben, sowie der ökologischen Prinzipien, die ihre Aktivität steuern, noch kaum verstanden. Ein solches Wissen ist aber essentiell, um eine langfristige Prognose dieser wichtigen Ökosystemdienstleistungen zu ermöglichen. Grundwasserleiter werden als überaus stabile Lebensräume angesehen, die auch nach anthropogener Verschmutzung durch ein niedriges Reaktionsvermögen und geringe Dynamik gekennzeichnet sind.

Diese Dissertation erlaubt wesentliche neue Einblicke in die Ökologie anaerober Kohlenwasserstoff-Abbauer in belasteten Grundwasserleitern. Eine vergleichende Untersuchung von Wasser- und Sedimentproben aus einem mit Teer-Öl kontaminierten Standort zeigte zunächst, dass bis zu 98 % der bakteriellen Zellen im Sediment zu finden waren. Gleichzeitig durchgeführtes Fingerprinting bakterieller Gemeinschaften zeigte über die Schadstofffahne hindurch wichtige Unterschiede, aber auch Gemeinsamkeiten, in der Verteilung mikrobieller Gemeinschaften in Sediment und Wasser über die Tiefe. Eine umfassendere Aussage zu natürlichen Schadstoffminderungsprozessen konnte aus den Sedimentproben abgeleitet werden.

Am gleichen Standort wurde eine hochgradig spezialisierte Toluol-abbauende mikrobielle Gemeinschaft am unteren Rand der BTEX-Fahne nachgewiesen. Obwohl der Schadstoffabbau mit einer ausgeprägten Sulfid-Bildung gekoppelt war, wurde „spezialisierte“ mikrobielle Gemeinschaft sowohl durch *Desulfobulbaceae* und *Geobacteraceae* (beide *Deltaproteobacteria*) dominiert. Somit galt es, die mutmaßliche Rolle beider Gruppen beim Toluol-Abbau am Standort zu hinterfragen. In dieser Arbeit werden die Mikroben, welche am unteren sulfidogenen Fahnenrand in Flingern für den

Abbau von Toluol wirklich verantwortlich sind, über „DNA-stable isotope probing“ (DNA-SIP) erstmals eindeutig identifiziert. Frische Sedimentproben wurden mit  $^{13}\text{C}$ -Toluol und Sulfat oder Eisen(III) als alternativen Elektronenakzeptoren inkubiert. Die mit  $^{13}\text{C}$ -angereicherte markierte DNA zeigte, dass *Desulfobulbaceae* unter Sulfat-reduzierenden Bedingungen für die Oxidation von Toluol verantwortlich waren. Sulfatreduzierer innerhalb der *Clostrida*, verwandt mit *Desulfosporosinus* spp., wurden ebenfalls als markiert gefunden. Dagegen wurde unter Eisen-reduzierenden Bedingungen ganz klar keine markierte DNA von *Geobacter* spp. nachgewiesen. Hier wurden neue, mit *Georgfuchsia* spp. (*Betaproteobacteria*) und *Thermincola* (*Clostridia*) verwandte Toluol-Abbauer gefunden. Diese Ergebnisse ordnen die Schlüsselfunktion des anaeroben Toluolabbaus innerhalb einer „spezialisierten“ mikrobiellen Gemeinschaft in einem kontaminierten Grundwasserleiter eindeutig zu. Sie erlauben zudem erste Hypothesen zu funktioneller Redundanz und ökologischer Nischenbildung innerhalb der anaeroben Schadstoffabbauer an diesem Standort.

Schließlich wurden über eine noch nie dagewesene Zeitreihe an Probenahmen in Zeit und Raum vor Ort bisher völlig unbeobachtete Dynamiken der anaeroben Abbauer aufgedeckt. Diese waren scheinbar durch hydraulische Veränderungen des Grundwasserspiegels vor Ort beeinflusst, und sind bislang völlig unbeobachtet. Zum Teil wurden diese Ergebnisse durch die in dieser Arbeit etablierten Amplicon-Pyrosequencing Methoden ermöglicht, die hier zum ersten Mal für Grundwasser-Ökosysteme angewendet wurden. Demnach waren die Toluol-Abbauer von der hydraulischen Dynamik, welche zwischen den drei Probennahme-Zeitpunkten (Februar 2006, September 2008 und Juni 2009) beobachtet wurde, stark beeinflusst und sie reagierten in einer unerwarteten Art und Weise. Nach einer Verschiebung des Grundwasserspiegels wurde ein dramatischer Zusammenbruch der bestehenden, zu den *Desulfobulbaceae* gehörenden Toluol-Abbauer beobachtet (Sep. 2008), welcher mit einem vorübergehenden Verlust der biologischen Abbau-Aktivität verbunden war. Danach (Juni 2009) stellte sich eine funktionell redundante, aber ökologisch unterschiedliche Population von Abbauern innerhalb des Genus *Desulfosporosinus* ein, wodurch die ursprünglich dominierende Abbauer-Population ersetzt wurde. Somit „versicherte“ letztlich die funktionelle Redundanz innerhalb der Abbauer den Prozess der natürlichen Schadstoffminderung gegen hydraulische Störungen.

Diese Ergebnisse zeigen, dass Grundwasserleiter weitaus dynamischere Lebensräume darstellen als es gegenwärtig erkannt wird. Dies erfordert ein neues Verständnis der ökologischen Parameter, welche Mikroorganismen in Grundwasser-Ökosystemen beeinflussen. In dieser Dissertation wird vorgeschlagen, dass das Konzept der „Disturbance Ecology“, bereits gut etabliert für andere aquatische Lebensräume, auch für Grundwasser-Ökosysteme anwendbar ist. Nur wenn die Häufigkeit solcher ökologischer Störungen für natürliche Schadstoffminderungsprozesse genau eingeschätzt werden kann, sind solide Vorhersagen für das langfristige Verhalten von kontaminierten Grundwasserleitern überhaupt möglich.

## Abstract

More than two billion people worldwide depend on groundwater for their daily water supply. Unfortunately, groundwater is subject to constant contamination by a huge variety of harmful anthropogenic compounds. One of the most sustainable and cost-effective remediation strategies for contaminated aquifers is microbially mediated contaminant removal. However, in many cases, the identity, physiology, and the ecological principles governing contaminant degraders and natural attenuation, very relevant to predict ecosystem services, are still poorly understood. Aquifers are in fact classically perceived as extremely stable environments, characterized by low reactivity and dynamics even after anthropogenic pollution.

This thesis contributes substantial novel insights into the ecology of anaerobic hydrocarbon (toluene, in specific) degraders in contaminated aquifers. First, a comparative water vs. sediment screening at a tar-oil contaminated field site revealed sediment samples to harbour >98% of bacterial cells. Parallel bacterial community fingerprinting showed important distinctions, but also similarities in depth-resolved microbial community distribution in sediments and water throughout the contaminant plume, with generally more comprehensive information on natural attenuation gained from sediment samples.

Furthermore, at the same site, a highly specialized toluene-degrading microbial population was previously found to dominate at the lower fringe of the BTEX plume. Although pronounced sulphide production associated contaminant degradation to sulphate reduction, the degrader community was dominated by both deltaproteobacterial *Desulfobulbaceae* and *Geobacteraceae*. Thus the putative role of both lineages in on site toluene degradation remained to be elucidated. Here, I unambiguously identify the microbes actually responsible for toluene-oxidation at the sulfidogenic lower plume fringe of the Flingern site using DNA-SIP. Fresh sediment slurries were incubated with <sup>13</sup>C-toluene and sulphate or ferric iron as alternative electron acceptor. Analyses of <sup>13</sup>C-enriched DNA revealed TRM1-related *Desulfobulbaceae* populations to be highly relevant in toluene oxidation under sulphate reducing condition. Clostridial sulphate-

reducers related to *Desulfosporosinus* spp. were also found. In contrast, labelled DNA of *Geobacter* spp. was not detected under iron reducing condition. Here, novel hydrocarbon degraders related to *Georgfuchsia* spp. (*Betaproteobacteria*) and *Thermincola* (*Clostridia*) were retrieved. These findings clearly affiliate key toluene-degrading functions within a highly specialised, low-evenness degrader community in a contaminated aquifer, and at the same time give rise to hypotheses about functional redundancy and ecological niche partitioning amongst on site degraders.

Finally, via an unprecedented time series of on site depth-resolved microbial community monitoring, previously unrecognized dynamics of on-site degrader populations as driven by hydraulic fluctuations of the groundwater table were unravelled. In part, these results were facilitated by novel amplicon pyrosequencing strategies established in this thesis, and applied, for the first time, to groundwater ecosystems. Hence, degrader populations in the lower plume fringe were affected by and unexpectedly reacted to hydraulic dynamics observed over the three sediment sampling points (February 2006, September 2008 and June 2009). After a pronounced shift of the groundwater table, a dramatic collapse of the standing *Desulfobulbaceae* toluene degrader population was observed (Sep. 2008), connected to a transient loss of biodegradation activity. Subsequently (Jun 2009), a functionally redundant but ecologically distinct population of *Desulfosporosinus* degraders re-established and replaced the initial degraders, and thus ultimately insured natural attenuation against hydraulic disturbance.

These results demonstrate that aquifers are much more dynamic environments than currently perceived. This calls for a new understanding of the ecological controls of hydraulic disturbance on microbes in groundwater ecosystems. In this thesis, I propose that the concept of “disturbance ecology”, already established for other aquatic ecosystems, also applies to groundwater ecosystems. If the frequency of such intrinsic disturbances on natural attenuation can be estimated in the future, much more sound predictions of the time scales required for aquifer ecosystem recovery at contaminated sites will become possible.





## **Table of Contents:**

<b>Zusammenfassung</b>	<b><i>i</i></b>
<b>Abstract</b>	<b><i>iv</i></b>
<b>1. Introduction</b>	<b>1</b>
1.1. Global relevance of groundwater systems	1
1.2. Anthropogenic pollution of groundwater systems	2
1.3. Microbe-mediated remediation of groundwater pollution	3
1.4. The Düsseldorf Flingern site	7
1.5. Aims of the present study	9
1.6. References	10
<b>2. High resolution analysis of contaminated aquifer sediments and groundwater- what can be learned in terms of natural attenuation?</b>	<b>15</b>
2.1. Abstract	15
2.2. Introduction	16
2.3. Materials and method	18
2.3.1 Site description	18
2.3.2 Groundwater sampling	18
2.3.3 Sediment sampling	19
2.3.4 Sample preparation and geochemical analysis	19
2.3.5 Stable isotope analysis of sulfate	20
2.3.6 Determination of bacterial cell numbers	21
2.3.7 Bacterial community fingerprinting	21
2.4. Results	22
2.4.1 Distribution of contaminants	22
2.4.2 Physical-chemical conditions and redox-specific parameters	23
2.4.3 Direct cell counts and enzyme activities	25
2.4.4 Depth-resolved analysis bacterial communities	27
2.5. Discussion	30
2.6. References	38
<b>3. Electron acceptor-dependent identification of key anaerobic toluene degraders at a tar-oil contaminated aquifer by Pyro-SIP</b>	<b>42</b>
3.1. Abstract	42
3.2. Introduction	43
3.3. Material and Methods	44
3.3.1. Sampling site and sample acquisition	44

3.3.2.	Incubation of sediments	45
3.3.3.	Process measurements	45
3.3.4.	Nucleic acid extraction and ultracentrifugation	45
3.3.5.	Analyses of density-resolved DNA fractions	46
3.3.6.	Amplicon Pyrosequencing from SIP microcosms	46
<b>3.4.</b>	<b>Results</b>	<b>48</b>
3.4.1	Exposure of aquifer sediments to <sup>13</sup> C-toluene	48
3.4.2	Detection and identification of <sup>13</sup> C-labelled degraders	49
3.4.3	<i>BssA</i> genes detected in SIP gradient fractions	55
<b>3.5.</b>	<b>Discussion</b>	<b>56</b>
<b>3.6.</b>	<b>References</b>	<b>59</b>
<b>4.</b>	<b><i>Disturbance ecology controls natural attenuation in contaminated aquifers</i></b>	<b>62</b>
4.1.	Abstract	62
4.2.	Introduction	62
4.3.	Materials and Methods	64
4.3.1	Samples acquisition	64
4.3.2	Geochemical analyses of groundwater samples	64
4.3.3	DNA extraction	64
4.3.4	Microbial community fingerprinting	65
4.3.5	Quantification of genetic signatures (qPCR)	65
4.3.6	16S rRNA amplicons ultra-deep pyrosequencing	66
4.4.	Results and Discussion	68
4.5.	References	77
<b>5.</b>	<b><i>General conclusions and outlooks</i></b>	<b>81</b>
5.1.	References	84
<b><i>Authorship clarifications</i></b>		<b><i>I</i></b>
Publications in peer reviewed journals		II
<b><i>Appendix</i></b>		<b><i>III</i></b>
Supporting data tables		IV
Lebenslauf - Giovanni Piloni		XV
Selected contributions to national and international scientific meetings		XVI
Acknowledgments		XVII





## 1. Introduction

### 1.1. Global relevance of groundwater systems

An aquifer is a geological formation capable of yielding useful groundwater supplies to wells and springs. All aquifers have two fundamental characteristics: a capacity for groundwater storage and a capacity for groundwater flow. But different geological formations vary widely in the degree to which they exhibit these properties and their areal extent can vary from a few km<sup>2</sup> to many thousands of km<sup>2</sup>. The most significant elements of hydrogeological diversity are: 1) major variation of aquifer unit storage capacity between unconsolidated granular sediments and highly-consolidated fractured rocks; 2) wide variation in aquifer saturated thickness between different depositional types, resulting in a wide range of groundwater flow potentials (15).

As a water supply for our society groundwater has a number of essential advantages when compared with surface water: it is of higher quality, better protected from possible pollution, less subject to seasonal fluctuations, and much more uniformly spread over large regions than surface water (fig. 1.1).

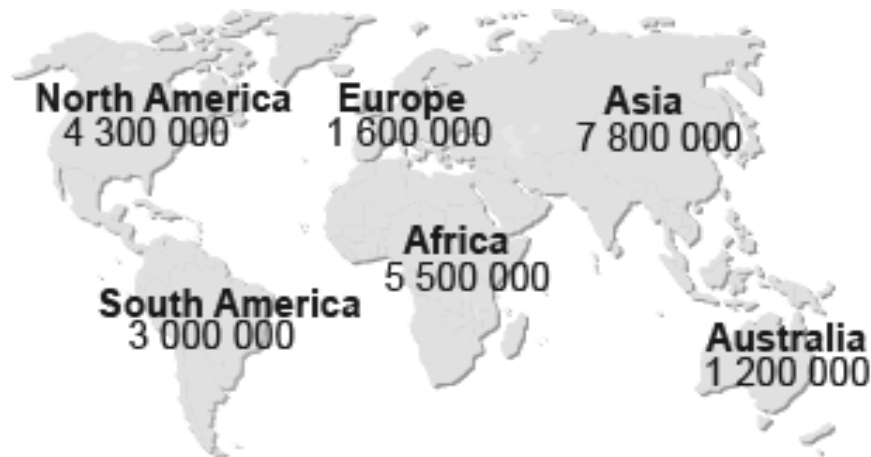


Fig. 1.1: Global distribution of groundwater by region. Numbers represent the km<sup>3</sup> of groundwater in that region.

Very often groundwater is available in places where there is no surface water: it is the only source of potable water supply for some countries in the world (Denmark, Malta, Saudi Arabia,

etc.). Water supply in European cities such as Budapest, Copenhagen, Hamburg, Munich, Rome and Vienna is completely or almost completely based on groundwater and for others like Amsterdam and Brussels it provides for more than half of the total water demand (52). Groundwater is closely interrelated with other components of the environment, as underground part of the 'water cycle'. In humid climates, large volumes of water seep into groundwater after rainfalls: this contributes actively to the water cycle, feeding streams, springs and wetlands during periods of less rainfall. In semi-arid and arid climates, any exchange between the surface water and groundwater regimes is largely reduced, because the small volume of seepage from occasional rainfalls only rarely penetrates the thick and dry (unsaturated) soils. In these areas groundwater resources are only minimally recharged. Therefore, any climate and atmospheric change inevitably cause consequences in the groundwater regime, resources and quality. Moreover, intensive groundwater exploitation by concentrated water well systems can result in a decrease in surface water discharge, land surface subsidence, and vegetation oppression due to groundwater withdrawal.

## **1.2. Anthropogenic pollution of groundwater systems**

Various human activities can significantly impact aquifer ecosystems, especially by groundwater depletion and pollution. Groundwater pollution in most cases is a direct result of environmental pollution. Groundwater is polluted mainly by sulphates, chlorides, nitrogen compounds (nitrates, ammonia, and ammonium), petroleum products, phenols, iron compounds, and heavy metals (copper, zinc, lead, cadmium and mercury) (60).

Petroleum constituents are amongst the most prevalent anthropogenic contaminants found in aquifers. Petroleum is a complex mixture of hydrocarbons, commonly classified into four groups: alkanes (saturated hydrocarbons), alkenes, alkynes and aromatic hydrocarbons (54). Aromatic hydrocarbons, subdivided into volatile aromatics, collectively indicated as BTEX (benzene, toluene, ethyl benzene, xylene) and polycyclic aromatic hydrocarbons (PAHs), are of particular concern, due to their toxicity which constitutes a serious threat to public health. BTEX have attracted much research focus as model compounds to investigate hydrocarbon degradation in laboratory systems as well as in the field (22, 33, 48). Especially, toluene degradation has been studied in detail since the last decade (4).

Various reasons could bring aromatic hydrocarbon into groundwater, e.g. oil spills from drilling wells, leaks from pipes, storage tanks or gasworks stations. The fate of aromatic

hydrocarbon contaminants depends on the hydraulic characteristics of the aquifer and the chemical properties of the pollutants. Volatilization, sorption, and mixing processes (dilution, diffusion dispersion) can facilitate decreasing contaminant concentrations. Solubility can, instead, cause persistence of contaminant within the aquifer water body (fig.1.2).

### 1.3. Microbe-mediated remediation of groundwater pollution

The demand for clean water will increase in the near future with global population growth. Thus, wherever protection strategies for groundwater resources have failed, remediation remains the only option in order to restore water supplies for populations. Over the last decades there has been an increasing interest in biological methodologies, collectively indicated as **bioremediation**, which may help to reduce the risks of organic pollutants and to effectively restore polluted sites. These methodologies, usually considered environment-friendly treatments, are essentially based on processes mediated by living organisms (mainly microorganisms), which can degrade or transform contaminants to less toxic or nontoxic products, with mitigation or elimination of environmental contamination. The different biotic and abiotic processes contributing to contaminant removal from environments under natural conditions are summarized as “natural attenuation” (NA), of which microbial contaminant degradation is the only sustainable component.

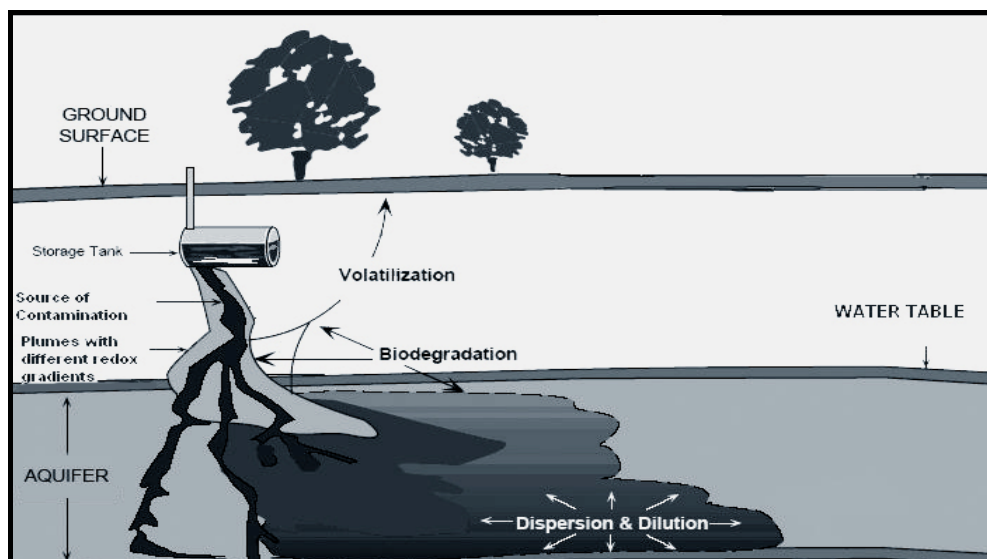


Fig. 1.2: Petroleum dispersion from a storage tank to ground water and occurrence of abiotic and biotic processes.

Amongst different remediation strategies, NA is the most convenient, if effective, because it does not depend on the introduction of nutrients (biostimulation) or microorganisms (bioaugmentation) into environments. However, NA is often limited by the slow growth and low activity of intrinsic microorganisms, especially within mostly anoxic impacted groundwater systems. Other limitations may be relevant as well (e.g. bioavailability, mixing, electron acceptors), but the most important effective limitations of natural attenuation are far from clear to date. Therefore, the mechanisms behind and controls of biotic contaminant degradation are of special interest for the understanding of natural attenuation, and also for the development of effective bioremediation strategies.

The rapid oxygen consumption in groundwater upon contaminant impact and the absence of photosynthesis allow spatial and temporal successions from aerobic utilization of the contaminants to anaerobic ones. When a tar-oil contamination event occurs (fig. 1.2), in fact, the contaminant plume is spreading out from the point source along the main groundwater flow direction, forming zones of different redox regimes along as well as transversal to the flow direction after a certain period of time (13). These redox zones are largely occupied by specialized microorganisms under stationary conditions, which oxidize contaminating hydrocarbons with respiration on locally available electron acceptors to depletion. For the electron acceptors, the redox regimes vary from aerobic (microaerophilic) conditions in the outskirts of the plume, over nitrate-, manganese-, iron-, and sulphate reduction to methanogenesis near the centre of the plume (4), in accordance with decreasing thermodynamic yields.

The understanding of the controls of degradation requires detailed information on the responsible intrinsic microbes, as well as their physiological and biochemical capabilities. Most of the current knowledge about the microbes involved in the removal of petroleum compounds from groundwater is linked to cultivation studies. Many biogeochemical pathways involved in aerobic and anaerobic degradation of petroleum compounds and the genes/proteins taking part in these processes are well known. A two step process is involved in the aerobic degradation of aromatic hydrocarbon (fig. 1.3) (20). The initial oxidative attack of BTEX converts the compound into a catechol structure, which is subsequently cleaved. Initial oxidative attack consists of direct oxidation of the aromatic ring via a mono- or di-oxygenase. Ring cleavage occurs by catechol 2, 3- dioxygenases after which the structure is further degraded into the Krebs cycle intermediates.



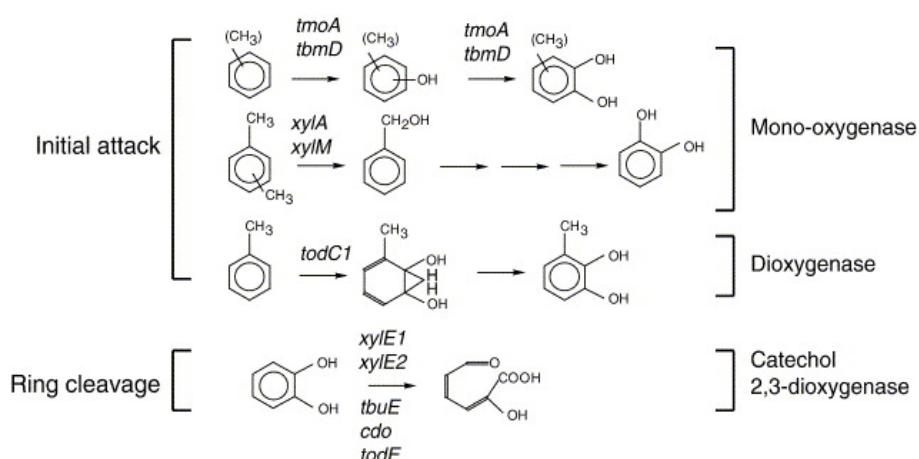


Fig. 1.3: Schematic 2-steps pathway of BTEX aerobic degradation. Catabolic enzymes involved in each step, for different aromatic compounds are reported in italic (20).

Studies on aerobic degradation (5, 20) characterized microbes isolated from contaminated environment mainly as belonging to the *Gammaproteobacteria* (mostly *Pseudomonas*) and *Actinobacteria*. Phylogeny of amino acid sequences of key proteins involved shows that they can be divided into specific families and subfamilies with significant sequence homology, indicating a common ancestry.

The anaerobic degradation of BTEX compounds (18, 48) like toluene (xylene) starts with the addition of fumarate, forming benzylsuccinate (methylbenzylsuccinate) (17, 19, 54). The reaction is catalyzed by the enzyme **benzylsuccinate synthase**, a glyceryl-radical enzyme (like e.g. pyruvate formate lyase), with a  $\alpha_2\beta_2\gamma_2$  composition and codified by the *bss* operon (*bssDCABEFGH*) (27), in which the product of the first gene (*bssD*) is an activating enzyme, the three further genes (*bssCAB*) form the subunits of the holoenzyme and the remaining ones (*bssEFGH*) are of unknown function. The product of the reaction, benzylsuccinate, is converted to benzylsuccinyl-CoA by a CoA transfer with succinyl-CoA and further metabolized through a series of  $\beta$ -oxidation-like reactions to benzoyl-CoA. Benzoyl-CoA is the central metabolite of the anaerobic degradation of aromatic compounds and is dearomatized by benzoyl-CoA reductase (enzyme codified by the *bcrABCD* operon) by two-electron reduction (yielding cyclohexa-1, 5-diene-1-carboxyl-CoA), prior to ring cleavage (48).

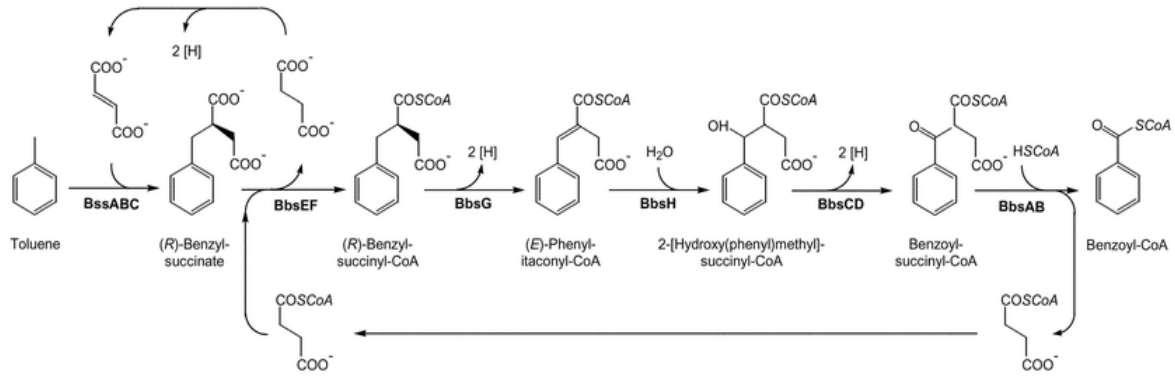


Fig. 1.4: Proposed initial anaerobic activation of toluene to Benzoyl-CoA (24). The different steps are explained in the text and the names of the involved enzymes are given in bold.

The *bss* enzyme was shown to be irreversibly inactivated in the presence of molecular oxygen by oxygenolytic cleavage of the  $\alpha$  subunit (1) and it is under a double regulation system (26) from the enzymes *tdiSR* (toluene degradation inducing Sensor and Regulation) that is active both in the regulation of the *bss* operon and of the *bbsA-H* operon, a *bss* downstream region that codes enzymes for the above mentioned further steps of the pathway, involving the modified  $\beta$ -oxidation of benzyl succinate to benzoyl-CoA and the recycling of fumarate from succinyl-CoA (24). The anaerobic pathway for toluene degradation has been elucidated primarily in three denitrifying strains, *Thauera aromatica* K172 (21), *T. aromatica* T1 (46), and *Azoarcus* sp. strain T (1), but is also common to different respiratory guilds (table 1.1) of anaerobic microorganism, such as iron reducers, sulphate reducers and apparently also fermenters active in methanogenic environments. Hence, the *bssA* gene has been successfully established as assay for the specific, cultivation-independent detection, identification and also quantification of anaerobic toluene and hydrocarbon degraders in environmental samples (55, 57).

Tab. 1.1: Equations and Gibbs energies (kJ/mol from electron donor) for toluene oxidation over different anoxic electron acceptors (modified form (18)).

Electron Acceptor	Equation	$\Delta G^{\circ}$
nitrate	$C_7H_8 + 7.2 NO_3^- + 0.2 H^+ \rightarrow 7 HCO_3^- + 3.6 N_2 + 0.6 H_2O$	-3554
iron(III)	$C_7H_8 + 94 Fe(OH)_3 \rightarrow 7 FeCO_3 + 29 Fe_3O_4 + 145 H_2O$	-3398
sulfate	$C_7H_8 + 4.5 SO_4^{2-} + 3 H_2O \rightarrow 7 HCO_3^- + 4.5 HS^- + 2.5 H^+$	-205
carbon dioxide	$C_7H_8 + 7.5 H_2O \rightarrow 4.5 CH_4 + 2.5 HCO_3^- + 2.5 H^+$	-131

Amongst the iron reducing aromatic hydrocarbon degraders, most of the studies seem to point out the relevance of members of  $\delta$ -*Proteobacteria* and especially of the genus *Geobacter* (10, 23, 42, 50), whereas sulphate reducing bacteria seem more diversely occurring in different contaminated habitats (38), with relatives of deltaproteobacterial *Desulfobulbaceae* often characteristic of tar-oil contaminated environments (32, 36, 40). Moreover, recent evidences from stable isotope probing experiments (25, 56) increased the perception about the importance of *Clostridia* in anoxic aromatic hydrocarbon degradation with both sulphate and iron as electron acceptors. Purification of anaerobic aromatic-oxidizing strains resulted, however, problematic due to the toxicity of the substrate, the relatively slow growth of the microbes and the possibility of syntrophies could establish between complementary guilds (25, 32). Therefore, information about phylotypes and physiological processes might be responsible for remediation of the contaminated sites could be gained by culture-independent analyses of the *in situ* geochemistry and molecular ecology. This approach, if conducted with the appropriate spatial and temporal resolution, can be very powerful tool to open the “black box” linking the observed processes to the responsible key-players (44, 53).

In the environment, aromatic hydrocarbon degraders use primarily the energetically most favourable electron acceptor (table 1.1). Nitrate is normally used quickly in anoxic environments like porous aquifers (29) and degradation activities thus normally proceed over iron and sulphate reduction. Even if thermodynamically more favourable (30), iron reduction is *in situ* often less suitable for microorganisms due to limited availability of Fe(III) species (2, 3, 51). Furthermore, iron and sulphate reducing processes are often overlapping in the environment (41, 43, 47), due to the abiotic reactions between the different oxidative states of the two electron acceptors (12, 14, 39) and to the ability of both iron- and sulphate-reducing bacteria to grow also with the respective not specific electron acceptor (11, 28, 37, 49).

#### **1.4. The Düsseldorf Flingern site**

The investigation site of the present thesis is a tar oil-contaminated aquifer in Düsseldorf Flingern (river Rhine valley, western Germany). The sandy sediments of the aquifer show an almost homogeneous composition over depth. Low permeability Tertiary fine sand layers confine the aquifer at a depth of about 15 m below ground surface. Groundwater moves from east to west with a flow velocity ranging between 0.5 and 2 m/d, following a hydraulic gradient

of about 6 ‰ (6). From 1893 until 1967, benzene, gas, coke, and different tar oil components were industrially produced in the area.

Second World War destructions and gasworks deconstruction after 1968 caused a significant release of aromatic hydrocarbons into the subsurface, resulting in concentrations of more than 100 mg/l of BTEX and ~20 mg/l of PAHs. To reduce the extent of the contaminant plume, which initially exhibited a length of about 600 m and a width of 100 m, several remediation actions (excavation, pumping and bioaugmentation) were launched since 1996. Even if the treatments reduced the plume extension to approx. 200 × 40 m, the target soil sanitation threshold of 2 mg/kg for BTEX and 5 mg/kg for PAH was not achieved and considerable amounts of mono- and polycyclic aromatic hydrocarbons are still detectable within groundwater and sediment (8).

To understand the localization and dynamics of degradation processes occurring at the Flingern aquifer, a unique high-resolution multilevel monitoring well has been previously installed at the site and fine-scale biogeochemical data were collected both for the contaminant and redox conditions of sediment and water (6, 8). The site is characterized of different gradient zones, with the unsaturated zone from 0 to 5.70 m depth and the saturated zone, under the water table, subdivided into capillary fringe and plume core (from ~6.30 to 6.65), sulfidogenic lower plume fringe (between 6.80 and 7.35 m), and deeper, partially PAH contaminated zones (7.50 - 12.7 m). Net biodegradation in aquifers has been hypothesized to take place mostly at the interfaces between plume compartments (plume fringes), where the local conditions of simultaneously available electron acceptors and donors are permissive. Therefore, the sulfidogenic lower plume fringe, in which the toluene is quantitatively degraded, is of particular interest.

The intrinsic microbial communities and the specific degraders responsible for toluene degradation have been characterized, localized and quantified in the sediment (55, 57). The different plume compartments allow for the growth of well-adapted microbial assemblages highly specialized to the specific processes feasible within their micro-habitat under stationary conditions. Previous evidence from the site had shown a highly active anaerobic toluene-degrading microbial community to be established at the lower sulfidogenic fringe of the BTEX plume (7, 55). Even if toluene degradation at the site is thought to be depend on sulphate reduction (6, 55), this community is co-dominated by microbes within the *Desulfobulbaceae* and the *Geobacteraceae*. Both deltaproteobacterial lineages are known to harbour anaerobic toluene degraders; however, these are either sulphate or iron-reducing degraders (31, 32). At the same

time, the dominating *bssA* cluster (putatively called “F1”) was more closely related to geobacterial *bssA* than to that of other known sulphate-reducing degraders (57). Moreover, recent studies indicate that some members of the *Peptococcaceae* (*Clostridia*), also relevant constituents of the above described lower plume fringe degrader community (7, 55), carry a previously unrecognised capacity for BTEX degradation under iron- (25) and sulphate-reducing conditions (56).

The above mentioned studies are amongst the few to show (55, 58) that *in situ* degradation activities establish, qualitatively and quantitatively, especially in “hot spots” localised in overlapping counter-gradients between highly contaminated zones and surrounding reservoirs of available electron acceptors. The establishment of such hot spots can be understood as a primary contribution to the restoration of groundwater ecosystems after contamination. Yet, the biogeochemical and ecological factors that control biodegradations in such hot spots (or hot zones) are still far from fully understood. In example, such specialized degrader populations and their degradation activities are interwoven with on-site hydrodynamics. In fact, one of the most important abiotic parameters affecting contaminant plumes is hydraulically driven fluctuations of the groundwater table (16). Hydrodynamics have been previously hypothesized to positively affect net reactive capacities in porous media by increasing the mixing (34). However, in contrast, if locally established degrader populations cannot cope with such plume dynamics, a negative effect on net biodegradation could be predicted. Currently, although a small number of reports on microbial population variability in aquifers is available (45, 59), the effects of hydrodynamics on dedicated degrader populations have been completely neglected.

### 1.5. Aims of the present study

In order to address some of the above mentioned knowledge gaps, three research goals for this thesis were defined as follows:

1. **Which details on aquifer degrader communities are accessible in sediment vs. groundwater-based analyses?** This project addresses differences in degraders relative abundance between the sediment and interstitial water compartments as semi-quantitative variation and statistics of genetic fingerprinting signatures of degrader populations in Flingern.

2. **Do the key toluene degraders established at the Flingern lower plume fringe belong to the *Desulfobulbaceae* or the *Geobacteraceae*?** DNA-based Stable Isotope Probing (SIP) of microbial key players responsible for anaerobic toluene degradation under sulphate or iron reducing conditions was performed. Thus, I aim to assign functionalities for the concomitant presence of *Desulfobulbaceae* and *Geobacteraceae* in the sulphidogenic gradient zone beneath the contaminant plume (7, 55) and to unambiguously affiliate site-specific anaerobic hydrocarbon degradation genes (“F1” *bssA*) previously associated to the iron reducer *Geobacter* (57);
  
3. **What effects are imposed by hydraulic dynamics on in situ degrader populations and degradation processes?** The response of total microbial communities and anaerobic aromatic hydrocarbon degraders to hydraulic disturbance is unravelled. By following on site qualitative and quantitative changes in degrader populations over 4 years of sampling, surprising and previously completely neglected effects of ecosystem disturbance on microbes and processes involved in contaminant removal are revealed.

## 1.6. References

1. **Achong, G. R., A. M. Rodriguez, and A. M. Spormann.** 2001. Benzylsuccinate Synthase of *Azoarcus* sp. Strain T: Cloning, Sequencing, Transcriptional Organization, and Its Role in Anaerobic Toluene and m-Xylene Mineralization. *J. Bacteriol.* **183**:6763-6770.
2. **Albrechtsen, H.-J., G. Heron, and T. H. Christensen.** 1995. Limiting factors for microbial Fe(III) -reduction in a landfill leachate polluted aquifer (Vejen, Denmark). *FEMS Microbiology Ecology* **16**:233-247.
3. **Albrechtsen, H. J., and T. H. Christensen.** 1994. Evidence for microbial iron reduction in a landfill leachate-polluted aquifer (Vejen, Denmark). *Applied Environmental Microbiology* **60**.
4. **Anderson, R. T., and D. R. Lovley.** 1997. Ecology and biogeochemistry of in situ groundwater bioremediation, p. 289-350, *Advances in Microbial Ecology*, Vol 15, vol. 15.
5. **Andreoni, V., and L. Gianfreda.** 2007. Bioremediation and monitoring of aromatic-polluted habitats. *Applied Microbiology and Biotechnology* **76**:287-308.
6. **Anneser, B., F. Einsiedl, R. U. Meckenstock, L. Richters, F. Wisotzky, and C. Griebler.** 2008. High-resolution monitoring of biogeochemical gradients in a tar oil-contaminated aquifer. *Applied Geochemistry* **23**:1715-1730.

7. **Anneser, B., G. Pilloni, A. Bayer, T. Lueders, C. Griebler, F. Einsiedl, and L. Richters.** 2010. High Resolution Analysis of Contaminated Aquifer Sediments and Groundwater-What Can be Learned in Terms of Natural Attenuation? *Geomicrobiology Journal* **27**:130 - 142.
8. **Anneser, B., L. Richters, and C. Griebler.** 2008. Application of high-resolution groundwater sampling in a tar oil-contaminated sandy aquifer. Studies an small-scale abiotic gradients, p. 107-122. *In* C. Press/Balkema (ed.), *Advances in Subsurface Pollution of Porous Media: Indicators, Processes and Modelling* Candela, L. Vadillo, I. Elorza, F.J., Leiden, NL.
9. **Beller, H. R., D. Grbic-Galic, and M. Reinhard.** 1992. Microbial degradation of toluene under sulfate-reducing conditions and the influence of iron on the process. *Appl. Environ. Microbiol.* **58**:786-793.
10. **Botton, S., M. van Harmelen, M. Braster, J. R. Parsons, and W. F. M. Roling.** 2007. Dominance of Geobacteraceae in BTX-degrading enrichments from an iron-reducing aquifer. *FEMS Microbiology Ecology* **62**:118-130.
11. **Brock, T. D. a. G., J.** 1976. Ferric iron reduction by sulfur- and iron-oxidizing bacteria. *Appl. Environ. Microbiol.* **32**:567-571.
12. **Canfield, D. E., R. Raiswell, and S. H. Bottrell.** 1992. The reactivity of sedimentary iron minerals toward sulfide. *Am J Sci* **292**:659-683.
13. **Christensen, T. H., P. L. Bjerg, S. A. Banwart, R. Jakobsen, G. Heron, and H.-J. Albrechtsen.** 2000. Characterization of redox conditions in groundwater contaminant plumes. *Journal of Contaminant Hydrology* **45**:165-241.
14. **Dos Santos Afonso, M., and W. Stumm.** 1992. Reductive dissolution of iron(III) (hydr)oxides by hydrogen sulfide. *Langmuir* **8**:1671-1675.
15. **Foster, S., A. Tuinhof, K. Kemper, H. Garduño, and M. Nanni.** 2008. Characterization of Groundwater Systems, key concepts and frequent misconceptions. *GW-Mate*, Briefing note 2.
16. **Fretwell, B. A., W. G. Burgess, J. A. Barker, and N. L. Jefferies.** 2005. Redistribution of contaminants by a fluctuating water table in a micro-porous, double-porosity aquifer: Field observations and model simulations. *J. Contam. Hydrol.* **78**:27-52.
17. **Harwood, C. S., G. Burchhardt, H. Herrmann, and G. Fuchs.** 1998. Anaerobic metabolism of aromatic compounds via the benzoyl-CoA pathway. *FEMS Microbiology Reviews* **22**:439-458.
18. **Heider, J., A. M. Spormann, H. R. Beller, and F. Widdel.** 1998. Anaerobic bacterial metabolism of hydrocarbons. *FEMS Microbiology Reviews* **22**:459-473.
19. **Heider, J. a. F. G.** 1997. Review: Anaerobic metabolism of aromatic compounds. *Eur. J. Biochem.* **243** 577-596.
20. **Hendrickx, B., H. Junca, J. Vosahlova, A. Lindner, I. Ruegg, M. Bucheli-Witschel, F. Faber, T. Egli, M. Mau, M. Schlomann, M. Brennerova, V. Brenner, D. H. Pieper, E. M. Top, W. Dejonghe, L. Bastiaens, and D. Springael.** 2006. Alternative primer sets for PCR detection of genotypes involved in bacterial aerobic BTEX degradation: Distribution of the genes in BTEX degrading isolates and in subsurface soils of a BTEX contaminated industrial site. *Journal of Microbiological Methods* **64**:250-265.
21. **Hermuth, K., B. Leuthner, and J. Heider.** 2002. Operon structure and expression of the genes for benzylsuccinate synthase in *Thauera aromatica* strain K172. *Archives of Microbiology* **177**:132-138.
22. **Jahn, M. K., S. B. Haderlein, and R. U. Meckenstock.** 2005. Anaerobic Degradation of Benzene, Toluene, Ethylbenzene, and o-Xylene in Sediment-Free Iron-Reducing Enrichment Cultures. *Appl. Environ. Microbiol.* **71**:3355-3358.

23. **Kane, S. R., H. R. Beller, T. C. Legler, and R. T. Anderson.** 2002. Biochemical and genetic evidence of benzylsuccinate synthase in toluene-degrading, ferric iron-reducing *Geobacter metallireducens*. *Biodegradation* **13**:149-54.
24. **Kube, M., J. Heider, J. Amann, P. Hufnagel, S. Kühner, A. Beck, R. Reinhardt, and R. Rabus.** 2004. Genes involved in the anaerobic degradation of toluene in a denitrifying bacterium, strain EbN1. *Archives of Microbiology* **181**:182-194.
25. **Kunapuli, U., T. Lueders, and R. U. Meckenstock.** 2007. The use of stable isotope probing to identify key iron-reducing microorganisms involved in anaerobic benzene degradation. *ISME J.*
26. **Leuthner, B., and J. Heider.** 1998. A two-component system involved in regulation of anaerobic toluene metabolism in *Thauera aromatica*. *FEMS Microbiology Letters* **166**:35-41.
27. **Leuthner, B., C. Leutwein, H. Schulz, P. Horth, W. Haehnel, E. Schiltz, H. Schagger, and J. Heider.** 1998. Biochemical and genetic characterization of benzylsuccinate synthase from *Thauera aromatica*: a new glyceryl radical enzyme catalysing the first step in anaerobic toluene metabolism. *Molecular Microbiology* **28**:615-628.
28. **Li, Y.-L. e. a.** 2007. Reduction of Iron Oxides Enhanced by a Sulfate-Reducing Bacterium and Biogenic H<sub>2</sub>S. *Geomicrobiology Journal* **23**:103–117.
29. **Lovley, D. R.** 1997. Potential for anaerobic bioremediation of BTEX in petroleum-contaminated aquifers. *Journal of Industrial Microbiology and Biotechnology* **18**:75-81.
30. **Lovley, D. R., and F. H. Chapelle.** 1995. Deep Subsurface Microbial Processes. *Reviews of Geophysics* **33**:365-381.
31. **Mahadevan, R., D. R. Bond, J. E. Butler, A. Esteve-Nunez, M. V. Coppi, B. O. Palsson, C. H. Schilling, and D. R. Lovley.** 2006. Characterization of Metabolism in the Fe(III)-Reducing Organism *Geobacter sulfurreducens* by Constraint-Based Modeling. *Appl. Environ. Microbiol.* **72**:1558-1568.
32. **Meckenstock, R. U.** 1999. Fermentative toluene degradation in anaerobic defined syntrophic cocultures. *FEMS Microbiology Letters* **177**:67-73.
33. **Meckenstock, R. U., R. J. Warthmann, and W. Schafer.** 2004. Inhibition of anaerobic microbial o-xylene degradation by toluene in sulfidogenic sediment columns and pure cultures. *FEMS Microbiology Ecology* **47**:381-386.
34. **Miller, S. R., A. L. Strong, K. L. Jones, and M. C. Ungerer.** 2009. Bar-Coded Pyrosequencing Reveals Shared Bacterial Community Properties along the Temperature Gradients of Two Alkaline Hot Springs in Yellowstone National Park. *Appl. Environ. Microbiol.* **75**:4565-4572.
35. **Moser, D. P., and K. H. Nealson.** 1996. Growth of the Facultative Anaerobe *Shewanella putrefaciens* by Elemental Sulfur Reduction. *Appl. Environ. Microbiol.* **62**:2100-2105.
36. **Müller, S., C. Vogt, M. Laube, H. Harms, and S. Kleinstüber.** 2009. Community dynamics within a bacterial consortium during growth on toluene under sulfate-reducing conditions. *FEMS Microbiology Ecology* **70**:586-596.
37. **Neal, A. e. a.** 2001. Iron sulfides and sulfur species produced at hematite surfaces in the presence of sulfate-reducing bacteria. *Geochimica et Cosmochimica Acta*, **Vol. 65**,:223–235.
38. **Perez-Jimenez, J. R., and L. J. Kerkhof.** 2005. Phylogeography of Sulfate-Reducing Bacteria among Disturbed Sediments, Disclosed by Analysis of the Dissimilatory Sulfite Reductase Genes (*dsrAB*). *Appl. Environ. Microbiol.* **71**:1004-1011.
39. **Poulton, S. W., M. D. Krom, and R. Raiswell.** 2004. A revised scheme for the reactivity of iron (oxyhydr)oxide minerals towards dissolved sulfide. *Geochimica et Cosmochimica Acta* **68**:3703-3715.



40. **Rabus, R., and F. Widdel.** 1995. Conversion studies with substrate analogues of toluene in a sulfate-reducing bacterium, strain Tol2. *Archives of Microbiology* **164**:448-451.
41. **Rioux, J., and D. Fortin.** 2003. Microbial activity of iron-reducing bacteria and sulfate reducing bacteria isolated from mine tailings in the presence of various electron donors. (unpublished results).
42. **Rooney-Varga, J. N., R. T. Anderson, J. L. Fraga, D. Ringelberg, and D. R. Lovley.** 1999. Microbial Communities Associated with Anaerobic Benzene Degradation in a Petroleum-Contaminated Aquifer. *Appl. Environ. Microbiol.* **65**:3056-3063.
43. **Roychoudhury, A., and G. L. Merret.** 2006. Redox pathways in a petroleum contaminated shallow sandy aquifer: Iron and sulfate reductions. *Science of the Total Environment* **366** 262–274.
44. **Schroth, M. H., J. Kleikemper, C. Bolliger, S. M. Bernasconi, and J. Zeyer.** 2001. In situ assessment of microbial sulfate reduction in a petroleum-contaminated aquifer using push-pull tests and stable sulfur isotope analyses. *Journal of Contaminant Hydrology* **51**:179-195.
45. **Sheridan, K. H., R. F. Lisa, G. W. Toby, W. A. Elizabeth, T. M. Jennifer, T. L. David, W. H. David, and J. F. Larry.** 2004. Spatial and temporal changes in microbial community structure associated with recharge-influenced chemical gradients in a contaminated aquifer. *Environmental Microbiology* **6**:438-448.
46. **Song, B., L. Y. Young, and N. J. Palleroni.** 1998. Identification of denitrifier strain T1 as *Thauera aromatica* and proposal for emendation of the genus *Thauera* definition. *Int J Syst Bacteriol* **48**:889-894.
47. **Sorensen, J.** 1982. Reduction of Ferric Iron in Anaerobic, Marine Sediment and Interaction with Reduction of Nitrate and Sulfate. *Appl. Environ. Microbiol.* **43**:319-324.
48. **Spormann, A. M., and F. Widdel.** 2000. Metabolism of alkylbenzenes, alkanes, and other hydrocarbons in anaerobic bacteria. *Biodegradation* **11**:85-105.
49. **Thamdrup, B., K. Finster, J. W. Hansen, and F. Bak.** 1993. Bacterial Disproportionation of Elemental Sulfur Coupled to Chemical Reduction of Iron or Manganese. *Appl. Environ. Microbiol.* **59**:101-108.
50. **Tobler, N. B., T. B. Hofstetter, K. L. Straub, D. Fontana, and R. P. Schwarzenbach.** 2007. Iron-Mediated Microbial Oxidation and Abiotic Reduction of Organic Contaminants under Anoxic Conditions. *Environ. Sci. Technol.* **41**:7765-7772.
51. **Tuccillo, M. E., I. M. Cozzarelli, and J. S. Herman.** 1999. Iron reduction in the sediments of a hydrocarbon-contaminated aquifer. *Applied Geochemistry* **14**:655-667.
52. **UNESCO.** 2004. Groundwater resources of the world and their use. IHP-VI SERIES ON GROUNDWATER **6**.
53. **Whiteley, A. S., M. Manefield, and T. Lueders.** 2006. Unlocking the 'microbial black box' using RNA-based stable isotope probing technologies. *Current Opinion in Biotechnology* **17**:67-71.
54. **Widdel, F., and R. Rabus.** 2001. Anaerobic biodegradation of saturated and aromatic hydrocarbons. *Current Opinion in Biotechnology* **12**:259-276.
55. **Winderl, C., B. Anneser, C. Griebler, R. U. Meckenstock, and T. Lueders.** 2008. Depth-Resolved Quantification of Anaerobic Toluene Degradation and Aquifer Microbial Community Patterns in Distinct Redox Zones of a Tar Oil Contaminant Plume. *Appl. Environ. Microbiol.* **74**:792-801.
56. **Winderl, C., H. Penning, F. von Netzer, R. U. Meckenstock, and T. Lueders.** 2010. DNA-SIP identifies sulfate-reducing Clostridia as important toluene degraders in tar-oil-contaminated aquifer sediment. *ISME J.*

57. **Winderl, C., S. Schaefer, and T. Lueders.** 2007. Detection of anaerobic toluene and hydrocarbon degraders in contaminated aquifers using benzylsuccinate synthase (bssA) genes as a functional marker. *Environmental Microbiology* **9**:1035-1046.
58. **Wu, X.-J., J.-L. Pan, X.-L. Liu, J. Tan, D.-T. Li, and H. Yang.** 2009. Sulfate-reducing bacteria in leachate-polluted aquifers along the shore of the East China Sea. *Canadian Journal of Microbiology* **55**:818-828.
59. **Yagi, J. M., E. F. Neuhauser, J. A. Ripp, D. M. Mauro, and E. L. Madsen.** 2009. Subsurface ecosystem resilience: long-term attenuation of subsurface contaminants supports a dynamic microbial community. *ISME J* **4**:131-143.
60. **Zektser, I. S., B. Marker, J. Ridgway, L. Rogachevskaya, G. Vartanyan, and R. Dzhamalov.** 2006. *Environmental Aspects of Groundwater Pollution*, p. 183-193, *Geology and Ecosystems*. Springer US.

## 2. High resolution analysis of contaminated aquifer sediments and groundwater-what can be learned in terms of natural attenuation?

B. Anneser<sup>a</sup>, G. Pilloni<sup>a</sup>, A. Bayer<sup>a</sup>, T. Lueders<sup>a</sup>, C. Griebler<sup>a</sup>, F. Einsiedl<sup>b</sup>, L. Richters<sup>c</sup>.

<sup>a</sup> Institute of Groundwater Ecology, Helmholtz Zentrum München, Neuherberg, Germany; <sup>b</sup> Department of Environmental Engineering, Technical University of Denmark, Kgs., Lyngby, Denmark; <sup>c</sup> Stadtwerke Düsseldorf AG, Duesseldorf, Germany.

*Geomicrobiology Journal*, **27**:130–142, 2010.

### 2.1. Abstract

High-resolution depth-resolved monitoring was applied to groundwater and sediments samples in a tar oil contaminated aquifer. Today, it is not fully clear, whether groundwater-based lines of evidence are always sufficient to adequately assess natural attenuation (NA) potentials and processes going on *in situ*. Our data unveiled small-scale heterogeneities, steep physical-chemical and microbial gradients, as well as hot spots of contaminants and biodegradation in the supposedly homogeneous sandy aquifer. The comparison of basic geochemical data revealed a fairly good agreement between sediment and groundwater samples. Nevertheless, a comprehensive understanding of both BTEX and PAH distribution, as well as redox processes involving insoluble electron acceptors, *i.e.* iron reduction, clearly asks for consideration of both, sediment and groundwater analysis. A thin BTEX plume right below the groundwater table was visible only in groundwater, while significant amounts of PAHs were present in sediments from deeper zones of the aquifer. Indications for sulfate reduction as a dominant process involved in

BTEX degradation were largely obtained from groundwater, while the role of iron reduction in degradation and possible sulfide oxidation at the capillary fringe and the upper BTEX plume fringe, as well as in deeper PAH-contaminated zones was evident from sediments. Moreover, sediment analyses were essential to meaningfully recover cellular abundances and distribution, activity and composition of the bacterial community.

Sediments harbored >97.7% of microbial cells and displayed enzyme activities 5 to 6 orders of magnitude higher than groundwater samples. Bacterial community T-RFLP fingerprints revealed important distinctions, but also similarities in depth-resolved microbial community distribution in sediments and water. An apparently highly specialized degrader population was found to dominate the lower BTEX plume fringe. However, even though sediment data seemed to comprise most community information found also in groundwater, this relation did not apply *vice versa*. In summary, our results show that groundwater sampled at an appropriate scale may contain sufficient information to identify and localize dominant redox reactions, but clearly fails to unravel natural attenuation potentials. This clearly emphasizes the importance of both groundwater and sediment samples for truly assessing natural attenuation potentials and activities at organically contaminated aquifers.

## **2.2. Introduction**

Contaminations with complex mixtures of petroleum hydrocarbons are known to exhibit a long-term persistence in soils and aquifers, and may be detectable even after thousands of years (15). In many cases, a complete remediation of contaminations fails, despite application of vigorous physical-technical remediation (e.g. air sparging, thermal treatment or pump and treat techniques) or biostimulation approaches. The monitoring of natural attenuation (NA) is therefore often chosen as a cost- and labour-efficient strategy to follow the transport and fate of pollutants in subsurface environments (8). Consequently, there's a growing interest to predict the spread and development of contaminant plumes and to understand intrinsic degradation behavior. NA is controlled by a complex interplay of physical, chemical and biological reactions, which are in turn affected by sediment-porewater interactions (36). The distribution and transport of contaminants in groundwater, the distribution and structure of microbial degrader populations,

as well as actual biodegradation activities are at least partially determined by sediment and groundwater characteristics.

The monitoring of NA at a given site usually involves the investigation of a limited set of groundwater parameters (i.e. contaminants, redox species), but rarely also considers geochemical and microbiological analyses of sediments, or both groundwater and sediments (14, 27, 28). For aquifer microbial populations, however, it is known that the major part occurs associated to sediments (e.g. (1, 3, 19, 21)), and activities are often found higher for attached cells (e.g. (2, 23, 35)). Previous studies have also revealed that considerable discrepancy in microbial community composition and biodegradation potential can prevail between sediment and groundwater samples of the same location (9, 27, 28, 40). It is therefore not fully clear, whether monitoring of groundwater is sufficient to adequately assess *in situ* NA processes and potentials at a specific site. It is frequently hypothesized that most degradation processes in aquifers are catalyzed by attached microbial populations (25, 28, 40). However, respective data sets comparing NA process information obtainable in sediment vs. water samples taken at a given site are extremely rare. Due to the considerable efforts associated with borehole drilling and installation of multi-level monitoring wells, only a limited number of studies is available where both groundwater and sediment analysis have been conducted in parallel today. Furthermore, the spatial resolution of sampling may often not be sufficient to adequately recover small-scale sediment heterogeneities and the reactive biogeochemical gradient zones at the fringes of contaminant plumes (6, 9, 14, 24, 52). In this study, we present a comprehensive data set comparing the biogeochemistry and microbiology of groundwater and sediment samples from a tar oil-contaminated sandy aquifer.

Temporally and spatially closely connected sampling allowed a direct comparison of both sediment and groundwater characteristics and enabled us to localize and scrutinize NA potentials. In particular, the distribution of contaminants and redox reaction products in groundwater and sediments was assessed in relation to the abundance, activity, diversity and distribution of bacteria present in different zones of the contaminated aquifer. Important distinctions in the two different data sets were more than evident. While distinct abiotic features may be sufficiently recovered by groundwater monitoring, this study especially points out the importance of sediment matrix-based information for assessing major microbial NA potentials.

## **2.3. Materials and method**

### **2.3.1 Site description**

The investigated area is a Quaternary sandy aquifer at a former gasworks site in Düsseldorf-Flingern, Germany. Release of tar oil compounds during operation and break-down of the plant resulted in the development of a contaminant plume with concentrations of up to 100 mg L<sup>-1</sup> of monoaromatic and 10 mg L<sup>-1</sup> of polycyclic aromatic hydrocarbons (PAHs) dissolved in groundwater. In the course of several remediation actions launched since 1995 the major part of the tar oil phases was removed. Nevertheless, residual amounts still can be detected in sediments and groundwater, forming a hydrocarbon plume of about 200 × 40 m in horizontal dimension. For detailed information on site characteristics see (5, 6, 16).

### **2.3.2 Groundwater sampling**

In February 2006, groundwater was collected from a specially designed high-resolution multi-level well (HR-MLW), which extends from 3m to 12m below land surface (bls) and exhibits sampling filter spacings of 2.5cm, 10cm and 30cm. For geochemical analyses, groundwater was sampled at vertical intervals of 2.5 – 10cm from 6.38m (groundwater table) down to 8.1m below land surface (bls) in 100 mL pre-washed narrow neck glass bottles and immediately processed for the analysis of a number of biotic and abiotic parameters, as described below. Water samples for microbial community analyses were sampled from only 5 selected depths down to 9m bls. Here, water was collected in autoclaved 1 L glass bottles, sealed on site to minimize oxygen exposure, and transported to the lab within 24 h under cooling (<10°C). In the lab, ~750 mL per depth were filtered over 0.22 µm cellulose acetate filters (Corning Inc., NY, USA), which were immediately frozen until DNA extraction. A detailed description of the HR-MLW as well as information on the sampling procedure and the materials and instruments used is given in (5, 6).

### 2.3.3 Sediment sampling

One week after sampling groundwater, two boreholes were drilled in a distance of approximately 0.5 m downgradient and, respectively, 1.5 m adjacent to the HR-MLW by means of hollow-stem auger drilling. Sediment liners were obtained in one meter segments down to a depth of 14 m (Liner 1) and 11 m (Liner 2), respectively. Right after retrieving the sediment liners they were transferred into an aluminum box and subsampled immediately under argon atmosphere for a selected set of parameters. Sediment sub cores from selected depths were immediately fixed for individual parameter measurements (see below), or frozen on dry ice for subsequent DNA extraction and molecular community analyses (52).

### 2.3.4 Sample preparation and geochemical analysis

Groundwater collected in 100ml glass bottles was immediately processed for measuring specific conductivity, pH and redox potential as well as for the analysis of dissolved iron and sulfide species, which is described in detail in (5). Total reduced inorganic sulfur was extracted from sediment samples fixed in 20% (w/v) zinc acetate using HCl-Cr(II) solution (1M Cr(II)-HCl in 12M anoxic HCl), according to the protocol of (47). Under maintenance of anoxic conditions, reduced inorganic sulfur species were converted to hydrogen sulfide during 30 hours of intensive shaking at room temperature. The liberated H<sub>2</sub>S was trapped in a 10 % zinc acetate solution and subsequently analyzed analogous to groundwater sulfide measurements (5).

Groundwater samples dedicated to the analysis of dissolved mono- and polycyclic aromatic hydrocarbons were amended with NaOH (0.1 M final concentration) to stop biological activity. BTEX concentrations were measured via GC-MS by headspace analysis; the less soluble polycyclic aromatic hydrocarbons (PAH) were determined by liquid injection analysis. Major anions (SO<sub>4</sub><sup>2-</sup>, HPO<sub>4</sub><sup>3-</sup>) and cations were analyzed via ion chromatography (Dionex DC-100, Idstein, Germany). Further details on analytical procedures are given in (5).

Sediment total organic matter (TOM) was calculated from the loss in weight of dried sediment after combustion of the organic content at 450°C for 4 h. Amorphous, ready available sedimentary iron was extracted in duplicates with 30 mL of 0.5 M HCl from 2 mL of sediment during 24 hours of intensive shaking at room temperature (2). Likewise, crystalline iron phases were obtained by 5 M HCl extraction over a period of 21 days. The extracted Fe(II) was measured analogous to groundwater samples (5). Concentrations of ferric iron species were

determined after reduction of total iron to Fe(II) using hydroxylamine hydrochloride (HACl; 10% w/w in 1M HCl) as reductant. The amount of HACl-reducible Fe(III) was calculated as the difference of Fe(II) determined in the HCl and HACl extracts (31, 32).

PAHs adsorbed to the sediment were extracted with acetone and amended with an internal standard mixture containing deuterated acenaphthene, chrysene, perylene and phenanthrene species (Internal Standards Mix 25, Ehrenstorfer, Augsburg, Germany) at a final concentration of 25 mg L<sup>-1</sup>. Aromatic hydrocarbons were determined in a GC-MS applying the settings as described in (52).

*In situ* microbial activity was assessed by determining the enzymatic hydrolysis rates of two fluorogenic substrates, *i.e.* MUF-P (4-methylumbelliferyl phosphate) and MUF-Glc (4-methylumbelliferyl β-D-glucoside) (17, 22). Enzyme assays of both groundwater and sediment samples were performed in 4 mL Supelco glass vials. For each sample, three replicates and one control were prepared. Groundwater was filled immediately after sampling into the vials avoiding headspace. Sediment samples were transferred in aliquots of 1 mL into vials, which have been prefilled with anoxic, low-ionic strength (1:500 dilution) freshwater medium (51). The substrates MUF-P or MUF-Glc (both Sigma, Taufkirchen, Germany) were added to a final concentration of 225 μM to groundwater samples and 1 mM to sediment samples, respectively. After incubation at *in situ* temperature (16°C ± 1°C) for 18 hours, groundwater samples were stopped by addition of ammonium glycine buffer (pH 10.5) at a ratio of 1:10. Enzyme activity within sediment samples was terminated after 22 hours of incubation (16°C ± 1°C) by adding 100 μL of an alkaline solution (2M NaOH/0.4M EDTA) to each sample. Controls for background fluorescence were treated analogously, but inactivated prior to incubation. Fluorescence was determined in a luminescence spectrometer (Aminco Bowman Series 2, Thermo Scientific) at 455 nm emission and 365 nm excitation.

### **2.3.5 Stable isotope analysis of sulfate**

Stable sulfur (<sup>34</sup>S/<sup>32</sup>S) and oxygen (<sup>18</sup>O/<sup>16</sup>O) isotope ratios of sulfate dissolved in groundwater were determined from samples collected in 100 mL vessels containing 10 mL of a 20% (w/v) Zn-acetate solution for precipitation of sulfide. Procedures for the recovery of sulfate and details on isotope measurements are described elsewhere in detail (6).



### **2.3.6 Determination of bacterial cell numbers**

From sediment liners stored at -20°C, 0.5 mL sample aliquots were fixed with 2.5% glutardialdehyde and kept at 4°C until further preparations. After replacement of the glutardialdehyde by 1.5 mL PBS, cells were released from sediment using a swing mill (Retsch, MM 200; 3 min, 20 Hz) and separated from abiotic particles via density gradient centrifugation. The layer containing the bulk (about 80%) of bacterial cells was collected and cells were stained with SYBR green I (Molecular Probes, Invitrogen, Karlsruhe, Germany) at a ratio of 1:10,000. Total cell counts were quantified in a flow cytometer (LSR II, Becton Dickinson, Heidelberg, Germany) equipped with a 488 nm and 633 nm laser, using TruCount beads (TruCount Tubes, Becton Dickinson) as internal standard. Instrument settings were as follows: forward scatter (FSC) 350 mV, side scatter (SSC) 300 – 370 mV, B530 (bandpass filter 350 nm) 500–580 mV. All parameters were collected as logarithmic signals. For minimization of background noise, the threshold was adjusted to 200 mV each for FSC and SSC. Calculations of total bacterial cell numbers were performed as described in (37). Loss of cells due to sediment freezing was accounted for applying a correction factor determined from fresh and frozen sediments from a later sampling at the same site.

### **2.3.7 Bacterial community fingerprinting**

DNA was extracted from 9 different sediment depths of Liner 1 (6, 6.4, 6.65, 6.9, 7.1, 7.6, 7.8, 8.1 and 9.2 m) and available corresponding groundwater filtrates (6.38, 6.46, 6.83, 7.1, 8.1 and 9.0 m). The extraction protocols used for sediments (~1 g wet weight) and filters were as previously described (10, 52), using a CTAB extraction buffer (54) modified as follows: 100 mM Tris, 100 mM Na-EDTA, 95 mM Na<sub>2</sub>HPO<sub>4</sub>, 750 mM NaCl, 1% CTAB, pH 7.80. Extracted DNA was stored frozen (-20°C) until further analyses. Terminal restriction fragment length polymorphism (T-RFLP) analysis of bacterial 16S rRNA gene amplicons was done with primers Ba27f-FAM / 907r and *MspI* digestion as previously described (52). Data evaluation and principal component analyses (PCA) was performed as reported elsewhere (33, 52).

## 2.4. Results

### 2.4.1 Distribution of contaminants

The spread of major contaminants (e.g. benzene, toluene, ethylbenzene and xylenes; BTEX) in groundwater of the investigated aquifer section was restricted to a narrow zone stretching from right below the groundwater table (ca. 6.4m bsl at time of sampling) to a depth of approximately 8.1m bsl, describing a vertically thin plume with a maximum BTEX concentration of 58 mg L<sup>-1</sup> at 6.7 m depth (Fig. 2.1A).

Toluene constituted the main fraction of monoaromatic hydrocarbons, accounting for about 75 % of total BTEX concentrations. For naphthalene, the major dissolved PAH component, a similar depth profile was found with a maximum concentration of 16 mg L<sup>-1</sup> at 6.75 m bsl (Fig. 2.1A). Out of the 16 EPA-PAHs, only acenaphthene and fluorene were further detected in groundwater, with lowest concentrations in the area of the BTEX plume and slightly increased values (< 1 mg L<sup>-1</sup>) further down (> 7m bsl) (data not shown).

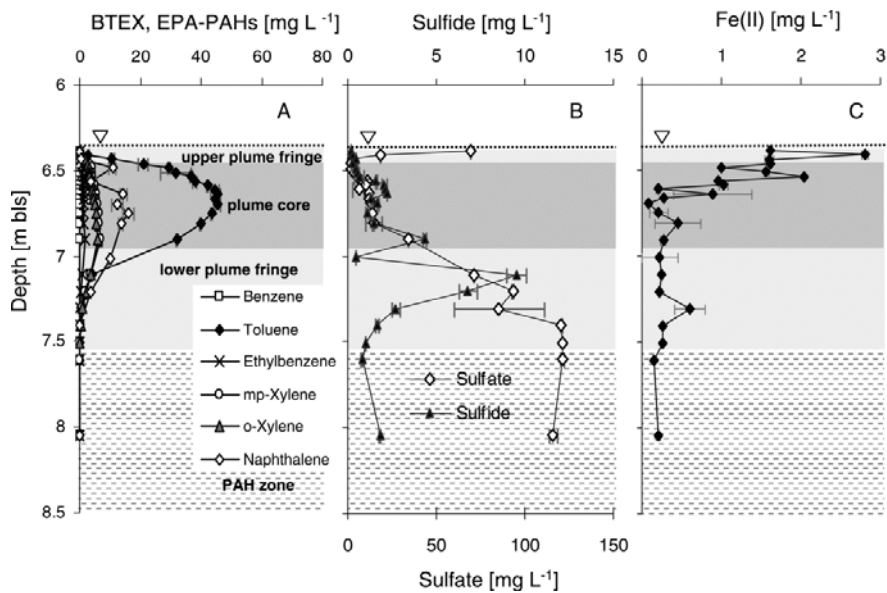


Fig. 2.1: Small-scale distribution of (A) contaminants, (B) sulfate and sulfide, and (C) ferrous iron in groundwater sampled from the HR-MLW; values represent means of duplicate measurements  $\pm$  SD.

Sediment samples contained no detectable amounts of BTEX, but exhibited distinct peaks for individual PAHs such as naphthalene, acenaphthene and fluorene. In detail, concentration maxima within Liner 1 were found at 6.65 m and 8.8 m bls (Fig. 2.2A). Both maxima were mainly contributed by naphthalene, with the upper peak located directly within the center of the plume, and the lower in an area where no BTEX and only minor concentrations of PAHs, *i.e.* acenaphthene and fluorene, could be detected in groundwater. Interestingly, no other of the 16 EPA-PAHs were found or, if yet, they were below the detection limits of the respective extraction and analysis protocols (*i.e.*  $20 \mu\text{g L}^{-1}$  for groundwater and  $6.8 \mu\text{g kg}^{-1}$  wwt for sediments). The distribution patterns of total PAHs within Liner 2 were found to be quite similar to Liner 1 for the upper layers of the saturated zone, yet concentrations of individual components partly differed. Additionally, a PAH-impacted layer that was not present in Liner 1 was detected at 10.2 m bls (Fig. 2.2B), thus pointing at lateral sediment heterogeneities.

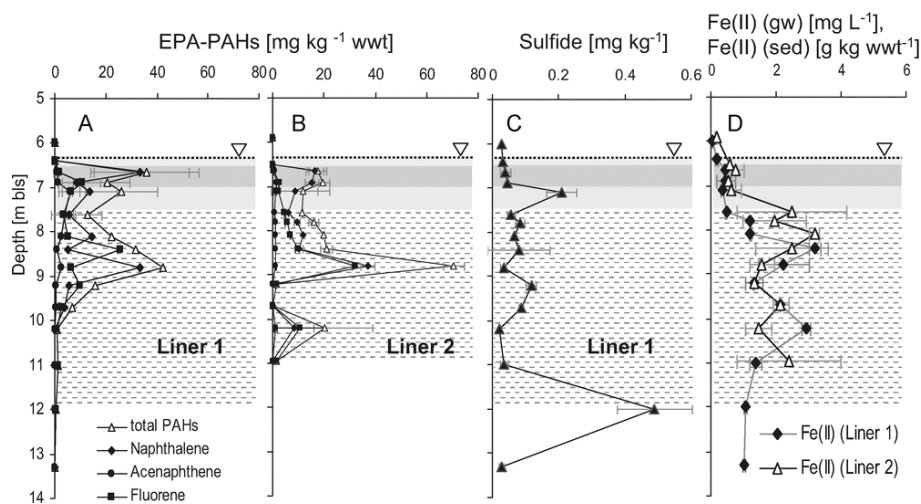


Fig. 2.2: (A) Vertical distribution of (A, B) contaminants, (C) sulfide, and (D) ferrous iron in sediments in relation to BTEX (grey area) and PAH (shaded area) contamination zones, respectively; values represent means of duplicate measurements  $\pm$  SD.

#### 2.4.2 Physical-chemical conditions and redox-specific parameters

The redox potential ( $E_h$ ) in groundwater rapidly declined with depth from -20 mV at the uppermost sampling point to a value of -235 mV in the plume center (6.81m; Tab. 2.1). A trend opposite to  $E_h$  was observed for pH, starting at a value of 7.07 right below groundwater table and

2. High resolution analysis of contaminated aquifer sediments and groundwater-what can be learned in terms of natural attenuation?

a maximum of 7.46 at 6.81m bls (Tab. 2.1). Likewise, specific conductivity ranging from 1030 to 1215  $\mu\text{S cm}^{-1}$  showed an increasing trend with depth (Tab. 2.1). Dissolved inorganic phosphate was available all across the investigated aquifer section, with lowest concentrations of 70  $\mu\text{g L}^{-1}$  at the water table and peak values of up to 2.1  $\text{mg L}^{-1}$  in the plume center (Tab. 2.1). No nitrate (detection limit of 0.1  $\text{mg L}^{-1}$ ) could be detected in groundwater at time of sampling. Sulfate, the most important dissolved electron acceptor, was almost absent in the BTEX plume center, yet its availability increased rapidly with declining contaminant concentrations at the upper and lower plume fringe (Fig. 2.1B). At a depth of 7.4 m bls, sulfate leveled off to a concentration of about 120  $\text{mg L}^{-1}$ .

Tab. 2.1: Hydrogeochemistry and stable isotope ratios of groundwater sampled from the HR-MLW.

Depth [m]	pH	Redox [mV]	Specific conductivity [ $\mu\text{S cm}^{-1}$ ]	$\text{HPO}_4^{2-}$ [ $\text{mg L}^{-1}$ ]	SD	$\delta^{34}\text{S}$ [‰]	SD	$\delta^{18}\text{O}$ [‰]	SD
6.39	7.07	-20	1096			5.5	0.04	2.1	0.18
6.41		-100	1030	0.07					
6.46	7.13	-100	1053	0.54	0.02				
6.56	7.27	-150	1052	2.05	0.18				
6.67	7.4	-190	1081	1.19	0.17				
6.75	7.43	-195	1094	1.07	0.38				
6.81	7.46	-235	1138	1.18		42.4	0.17	15.2	0.04
7.11	7.42	-230		0.44	0.05	25.0	0.20	12.6	0.13
7.41	7.39	-197	1215	0.95	0.12				
8.05	7.43	-229	1166	0.57	0.06	15.9	0.02	11.1	0.11
9.05						12.5	0.02	10.7	0.05

Stable isotope values of sulfate, *i.e.*  $^{34}\text{S}/^{32}\text{S}$  and  $^{18}\text{O}/^{16}\text{O}$ , determined for selected depths indicated the occurrence of bacterial sulfate reduction in the contaminated aquifer (Tab. 2.1). Concomitant with declining concentrations of organics and increasing sulfate concentrations at the lower plume fringe, distinct peaks of dissolved sulfide were observed, reaching a maximum of almost 10  $\text{mg L}^{-1}$  at 7.11 m bls (Fig. 2.1B). Lower amounts of sulfide were detected in the

plume core and scarcely any dissolved sulfide was found within the first centimeters beneath the capillary fringe. There, however, elevated concentrations of dissolved Fe(II) were measured, followed by a steep decline until approximately constant concentrations of about  $0.3 \text{ mg L}^{-1}$  were attained at 6.9 m bls (Fig. 2.1C).

In contrast, ferrous iron extracted from the sediments (0.5M HCl) exhibited lowest concentrations within the BTEX contamination area but exhibited a pronounced increase with depth, reaching concentrations of up to  $3.2 \text{ g kg}^{-1}$  wwt beneath 8 m bls (Fig. 2.2D). With the exception of local peaks at 10.2 m (Liner 1) and 9.2 m (Liner 2) bls, the recovery of ready extractable Fe(III) from saturated sediments was considerably lower compared to that of Fe(II), i.e. always  $< 1 \text{ g kg}^{-1}$  in Liner 1 and, respectively,  $< 2 \text{ g kg}^{-1}$  wwt in Liner 2 (data not shown). Only low amounts of crystalline Fe(II) averaging  $1 \text{ mg kg}^{-1}$  were obtained by extraction with 5M HCl; in contrast, concentrations of Fe(III) released by this harsh extraction exhibited clearly higher values of up to  $5.5 \text{ g kg}^{-1}$  wwt (data not shown). Total reduced inorganic sulfur extracted from sediment samples of Liner 1 revealed concentrations in the range of  $0.02 - 0.5 \text{ g sulfide per kg (wwt)}$ , with pronounced peaks at 7.1 and 12 m depth (Fig. 2.2C). Unfortunately, no sulfide values are available from Liner 2 sediments. Total organic matter (TOM) content in dried sediments of both liners ranged between 0.2 and 0.6% (dwt), with a mean value of 0.34% in Liner 1 and 0.39% in Liner 2.

### 2.4.3 Direct cell counts and enzyme activities

In sediments of Liner 1, bacterial cell counts exhibited two distinct peaks of  $4.1 \times 10^7$  and  $6.8 \times 10^7 \text{ cells g}^{-1}$  wwt at the upper and lower fringe of the BTEX plume, separated by a local minimum of  $8.8 \times 10^6 \text{ cells g}^{-1}$  wwt in the plume center (Fig. 2.3). Background numbers in the less contaminated zone below 8 m bls averaged at  $6.8 \times 10^6 \text{ cells g}^{-1}$  wwt. In contrast, direct cell counts in sediments of Liner 2 exhibited one dominant peak of  $4.8 \times 10^7 \text{ cells g}^{-1}$  wwt at the upper plume fringe (Fig. 2.3) and only a less distinct increase of cell number at the lower plume fringe. With depth, cell numbers decreased significantly down to background concentrations of  $6.9 \times 10^6 \text{ cells g}^{-1}$  wwt below 8 m bls. Unfortunately, no bacterial cell numbers are available from groundwater from this sampling event.

## 2. High resolution analysis of contaminated aquifer sediments and groundwater-what can be learned in terms of natural attenuation?

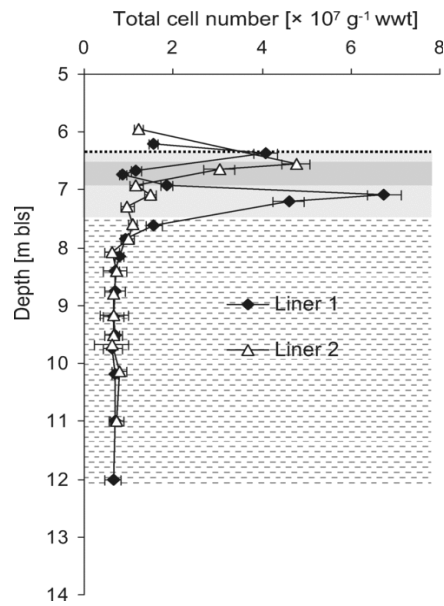


Fig. 2.3: Total number of bacteria in sediments from Liner 1 and 2 in relation to BTEX- and PAH-contaminated zones; values represent means of triplicate measurements  $\pm$  SD.

Both sediment and groundwater samples exhibited maximum rates of substrate conversion at the uppermost sampling depths. Up to 1.9 mmol MUF-P were hydrolyzed by phosphatases per kilogram sediment (wwt) and hour in Liner 2 (Fig. 2.4C). Turnover rates in Liner 1 reached maximum values of 1.2 mmol kg<sup>-1</sup> wwt h<sup>-1</sup> (Fig. 2.4B). At 6.9 m bls, the activity started to level off at 180  $\mu\text{mol kg}^{-1}$  wwt h<sup>-1</sup> (Liner 2) and 60  $\mu\text{mol kg}^{-1}$  wwt h<sup>-1</sup> (Liner 1) on average. The gradient of MUF-P in groundwater samples was less pronounced and the activities were significantly lower, showing values of max. 32 nmol l<sup>-1</sup> h<sup>-1</sup> directly below the water table (Fig. 2.4A), which corresponds to 10.9 nmol kg<sup>-1</sup> h<sup>-1</sup> wwt assuming a sediment porosity of 34%. Consequently, phosphatase activities in sediments were found up to six orders of magnitude higher than in groundwater. Sediment  $\beta$ -glucosidase activities were comparable for both liners according to the individual depth zones (Fig. 2.4B+C). Hydrolysis rates of MUF-Glc in groundwater exhibited slightly elevated values at the upper and lower fringe of the BTEX plume (Fig. 2.4A). Similar to MUF-P turnover, sediment activities outreached groundwater activities by five orders of magnitude.

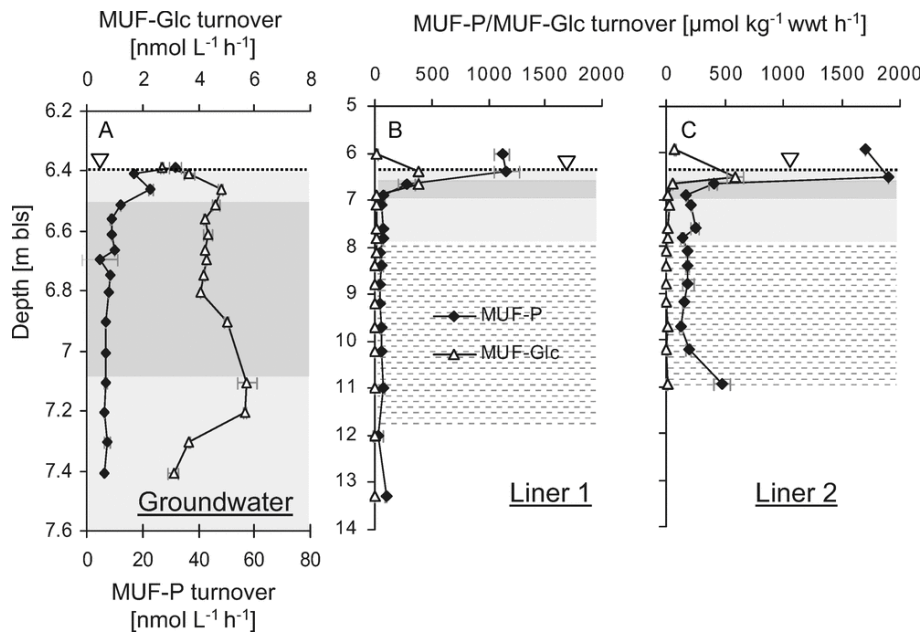


Fig. 2.4: Microbial enzyme activities in (A) groundwater and sediments of (B) Liner 1 and (C) Liner 2 in relation to BTEX (grey) and PAH (shaded) contaminated zones. Values represent means of triplicate measurements  $\pm$  SD.

#### 2.4.4 Depth-resolved analysis bacterial communities

T-RFLP analysis of bacterial communities indicated pronounced shifts in structure and diversity of total bacterial communities with depth (fingerprints are not shown). For groundwater, the Shannon-Wiener diversity  $H'$  as inferred from relative T-RF abundances was highest at the level of the capillary fringe/groundwater table and dropped to local minima within the lower plume fringe (7.1 m) (Fig. 2.5A). For sediments,  $H'$  was very similar with depth, except at the lower part of the plume core, where a slightly increased local maximum of bacterial diversity was observed. A total of 77 distinct T-RFs was retrieved from both sediment and water samples, of which 21 peaks were unique for the sediment and 17 for the water samples. However, with the exception of the uppermost samples from near the capillary fringe,  $H'$  was always lower in water samples than in corresponding sediments.

2. High resolution analysis of contaminated aquifer sediments and groundwater-what can be learned in terms of natural attenuation?

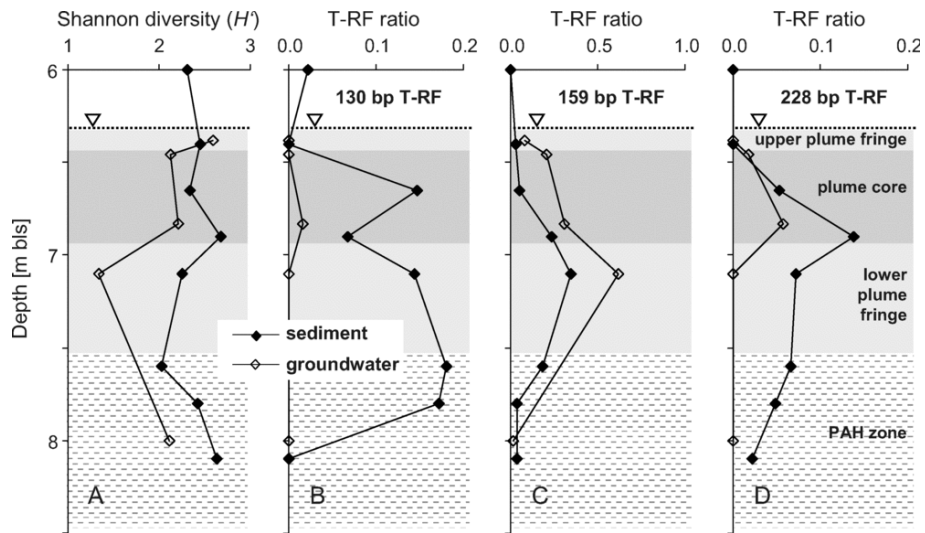


Fig. 2.5: Depth-distribution of (A) bacterial T-RFLP fingerprinting Shannon-Wiener diversity  $H'$  and relative T-RF abundance of characteristic T-RFs; i.e. related to (B) *Geobacter* spp. (130 bp), (C) *Desulfocapsa* spp. (159 bp), and (D) clostridial sulphate reducers and fermenters (228 bp) in sediments and corresponding groundwater samples of the Flingern site. The putative affiliation of the T-RFs is in accordance to previously published clone libraries from the same site (52).

To further elucidate these distinctions, we compared the depth-distribution of the relative abundance of selected T-RFs previously identified to represent important components of the degrader community. Respective results for sediment samples taken in 2005 revealed that especially the 130, 159, and 228 bp T-RFs represented dominating members of the contaminant-degrading bacterial community established in the lower plume fringe. As shown in a previous study by 16S rRNA gene cloning, these T-RFs were affiliated to microbes related to *Geobacter* spp., *Desulfocapsa* spp., and also clostridial sulphate reducers and fermenters (52). Albeit semi-quantitative, this assessment revealed pronounced distinctions in distribution patterns (Fig. 2.5). T-RF abundances of over 15% were observed for 130 bp peaks (*Geobacter*-related microbes) in sediments of the plume core and over the lower plume fringe. In groundwater samples, however, this T-RF was only detected in one depth (6.83 m) and was thus almost not detectable over the entire depth transect (Fig. 2.5B). In contrast, the 159 bp T-RF (*Desulfocapsa*-related) showed a very similar distribution with depth in both sample sets, with clear abundance maxima in the lower plume fringe at 7.1 m (Fig. 2.5C). The 159 bp T-RF was always of a higher relative abundance in groundwater than in sediments (~62 vs. ~35%, respectively). Finally, the 228 bp T-RF (putatively representing clostridial sulphate reducers and fermenters) was present at a



maximum frequency of ~14% and ~6% in both sediments and water of the lower plume core, respectively (Fig. 2.5D).

To comparatively assess total bacterial community variance over depth in both sample sets, PCA statistics of the T-RFLP data set was conducted. The percentage of total community variability explained by the two primary PC factors inferred was no less than 59% (Fig. 2.6). Surprisingly, data reduction indicated congruent community dynamics with depth over the different zones of the Flinger plume. As observed previously (52), especially the populations of the lower fringe zone were resolved in ordination, indicating similar community patterns for both sediments and groundwater samples in these depths. As observed before for the loading of PCA factors on specific T-RFs (52), the distinction of the lower plume fringe degrader community was largely attributed to a high abundance of the 159 bp T-RF (factor loadings not shown). In summary, PCA illustrated similar community dynamics (clockwise shifts in virtual ordination) with depth for both sample sets, but dynamics (i.e. distinctions) with depth were more pronounced for groundwater samples (Fig. 2.6).

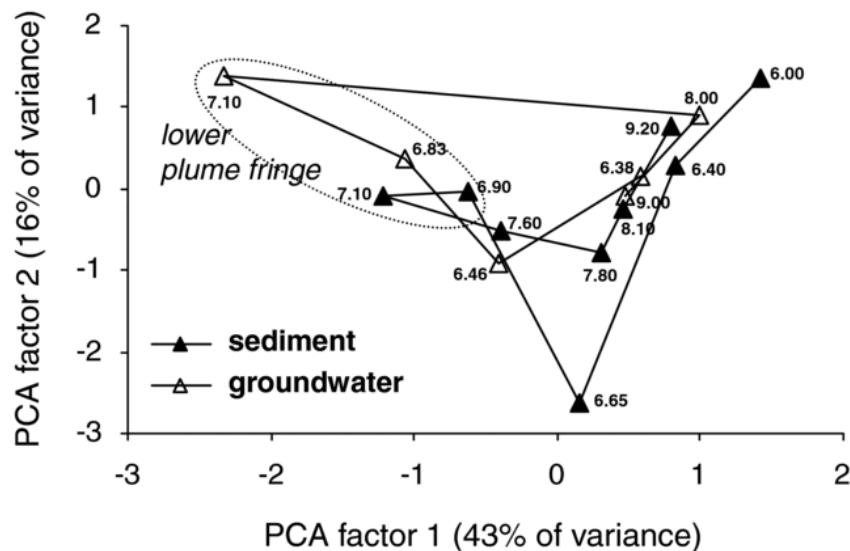


Fig. 2.6: Ordination of PCA factor scores for T-RFLP fingerprinting of sediment and water samples comprising the overall variance in depth-resolved bacterial community composition. The depths at which specific fingerprints were retrieved are indicated next to the ordination points.

## 2.5. Discussion

Efficient biodegradation of organic contaminants in the subsurface requires two elements: (1) microbial populations with degradative capabilities, and (2) favourable geochemical and hydrological conditions (36). Then, *vice versa*, biodegradation processes are suggested to cause significant changes in groundwater and sediment properties, which include: (i) a rapid depletion of the energetically most favorable electron acceptors (*i.e.* oxygen and nitrate) (4, 11), (ii) the appearance of metabolites and reaction products (e.g. reduced sulfur and iron species as shown in Fig. 2.3, Fig. 2.4), (iii) increase in pH and alkalinity owing to proton consumption during anaerobic oxidation of organic compounds, and (iv) a decrease in redox potential as well as a change in specific conductivity due to the conversion of individual ions such as sulfate (12, 14). Some of these indicators may easily be followed in groundwater samples, however, some may clearly call for sediment data. For example, with respect to important redox processes (distribution of major electron acceptors and reaction products) information from groundwater samples is limited to dissolved chemical species. The role of solid electron acceptors such as ferric iron and the turnover of contaminants adsorbed to the sediment matrix can only be assessed directly in sediments, or indirectly via soluble metabolites and end products in groundwater. In contrast, major dissolved electron donors cannot be adequately monitored via sediment samples, and only partial information on intrinsic microbial communities and respective activities is obtainable from groundwater. As we discuss in the following, both, groundwater and sediments needs to be addressed when assessing NA potential in an organically polluted aquifer.

### ***Small scale physical-chemical heterogeneities in groundwater and sediments***

Steep concentration gradients in groundwater clearly delineated a fine-scale vertical zonation of the BTEX plume. As obvious from Fig. 2.1A, only the extraordinarily high-resolution of groundwater sampling allowed depicting the small-scale and steep geochemical gradients, which could not have been resolved by a conventional multi-level well with a vertical resolution of 0.5 to 1 m. However, groundwater samples did not provide comprehensive information regarding the PAH contamination. This is not surprising, as PAHs exhibit a high tendency to adsorb to the sediment matrix. A recent study (38) found up to 90% of PAHs adsorbed and only a small fraction dissolved in groundwater. Naphthalene, due to its comparably low molecular weight and high solubility (15), showed a similar distribution in groundwater as

the monoaromatic hydrocarbons. Compared to the maximally  $16 \text{ mg L}^{-1}$  of naphthalene dissolved in groundwater (=  $5.4 \text{ mg per kg soil}$ ; Tab. 2.2), maximally ~6 to 7-fold increased amounts were found sorbed to the sediments (Fig. 2.2A+B). Sorption of PAHs to the sediment matrix is substantially influenced by the presence of organic matter, which is commonly regarded to be negligible in sandy aquifers, where mean organic carbon contents are in the range of only about 0.1 % (7, 30). Nevertheless, due to their hydrophobicity, the higher molecular weight PAHs acenaphthene and fluorene are strongly retained. In the Flingern aquifer, despite the relatively low soil organic carbon content of ~ 0.3% (dry weight), concentrations of acenaphthene were 10 to 20-fold, fluorene concentrations even 100-fold higher in sediments than in groundwater.

The relation between adsorbed ( $C_s$ ) and dissolved concentrations ( $C_w$ ) can be expressed by the solid water distribution coefficient  $K_D$  of a given compound, according to:

$$K_D = \frac{C_s [mg \text{ kg}^{-1}]}{C_w [mg \text{ kg}^{-1}]} \quad (1)$$

In soil-water systems,  $K_D$  is also defined by the product of the organic carbon – water distribution coefficient  $K_{oc}$  and the fraction  $f_{oc}$  of organic compounds in solution (7):

$$K_D = K_{oc} \times f_{oc} \quad (2)$$

Using literature  $K_{oc}$  values (Tab. 2.3) and measured  $f_{oc}$  (= 0.3%) and  $C_w$  in eq. 1 and 2, the theoretically adsorbed contaminant concentration  $C_s$  can be calculated (Tab. 2.2). Measured concentrations of fluorene and naphthalene adsorbed to the sediment matrix exceeded calculated results by a factor of 5 and 2.5, respectively.

2. High resolution analysis of contaminated aquifer sediments and groundwater-what can be learned in terms of natural attenuation?

Tab. 2.3: Sorption properties and aqueous solubilities  $S_i$  of selected aromatic hydrocarbons.

Compound	log $K_{ow}$	log $K_{oc}$	$S_i$ at 25°C [mg L <sup>-1</sup> ] <sup>a</sup>
Toluene	2.69 <sup>c</sup>	2.18 <sup>d</sup>	534.8
Naphthalene	3.36 <sup>b</sup>	2.94 <sup>b</sup>	31.7
Acenaphthene	3.98 <sup>c</sup>	3.66 <sup>c</sup>	3.93
Fluorene	4.18 <sup>c</sup>	3.86 <sup>c</sup>	1.98

$S_i$  = aqueous solubility of organic compound  $i$ ,  $K_{ow}$  = octanol-water coefficient,  $K_{oc}$  = organic carbon-water coefficient

<sup>a</sup> Eberhardt and Grathwohl (2002)

<sup>b</sup> Appelo and Postma (2005)

<sup>c</sup> USACE (2002)

<sup>d</sup> Szabo et al. (1990)

Amounts of acenaphthene determined in the sediment agreed fairly well to theoretical values, overestimating the actual mean concentration by 10% (Tab. 2.2). Calculated maximum toluene concentrations adsorbed to the sediment matrix amounted to ~6.8 mg kg<sup>-1</sup>, but neither toluene nor other BTEX compounds were detected in sediment samples of the Flingern site. Apparently, the sorption capacity of the sediment matrix for these substances was lower than expected. In conclusion, sediment samples alone would lead to inconclusive information on the BTEX contamination.

Tab. 2.2: Measured and calculated maximum concentrations of aromatic hydrocarbons in sediment and groundwater of the Flingern aquifer.

Compound	Liner 1 <sup>b</sup>		Liner 2 <sup>b</sup>	Calculated <sup>c</sup>
	Groundwater [mg L <sup>-1</sup> ] <sup>a</sup>		Sediment [mg kg <sup>-1</sup> ]	
Toluene	45 (15.3)	-	-	6.80
Naphthalene	16 (5.4)	33.5	37	13.94
Acenaphthene	0.9 (0.31)	6	1.6	4.11
Fluorene	0.7 (0.24)	26	32	5.07

<sup>a</sup> parentheses indicate the corresponding sedimentary concentrations in mg kg<sup>-1</sup>

<sup>b</sup> maximum concentrations measured in the respective sediment liners

<sup>c</sup> theoretically sorbed contaminant concentration calculated from max. contaminant concentrations measured in groundwater

Considering the inaccuracies associated with the collection of sediments by liner coring, the differences in the distribution patterns of contaminants may also partly be ascribed to on site heterogeneities. “Hot spots” of pollutants and preferential flow paths in heterogeneous sediments may foster a diffuse spreading of contaminants. In the source zone, which is located ~ 15 m upstream of the sampling area (6), the dense non-aqueous phase liquids (DNAPLs) are likely to seep down due to their higher density and molecular weight, which may explain the accumulation of PAHs in deeper zones in contrast to the lighter BTEX compounds.

### ***Biodegradation via sulfate reduction***

A significant enrichment of both  $^{18}\text{O}$  and  $^{34}\text{S}$  isotopes in groundwater sulfate proved microbial sulfate reduction to occur throughout the BTEX-contaminated zone, with pronounced activities across the lower plume fringe (Tab. 2.1; see also (5)). Inverse gradients of dissolved sulfate and sulfide (Fig. 2.1B), which are regarded as indicators of ongoing sulfate reduction, support this hypothesis. Further geochemical evidence for bacterial sulfate reduction derived from a distinct peak of reduced inorganic sulfur extracted from sediment samples, which again hints at high sulfate reduction activity at 7.1 m bls, marking the transition between heavily and less contaminated groundwater in the lower plume fringe (Fig. 2.2C). The lack of sulfide at the upper plume fringe is most likely attributed to scavenging of sulfide by both complexation and reoxidation reactions with Fe(II) (14, 26, 43).

### ***Iron reduction and iron cycling processes***

Iron reduction has previously been shown to occur at the Flingern site (16). Groundwater analysis revealed iron reducing activity being most pronounced at the upper and lower plume fringe (5, 16). Elevated concentrations of dissolved Fe(II) measured in groundwater samples hint at significant iron reduction in the upper 20 cm of the saturated zone (Fig. 2.1C). However, only sediment analysis could show that considerable amounts of readily extractable ferric iron are actually present in this zone (data not shown). At the interface between the unsaturated and saturated zone, cycling of iron species is likely to proceed at high rates. Transient hydraulic conditions causing a fluctuating groundwater table govern regular periods of re-oxidation and reduction, providing a regeneration of sedimentary electron acceptors (46, 48). A minor secondary peak of ferrous iron in groundwater was observed at the lower plume fringe. This pattern has already been observed in previous investigations at that site (5, 6).

From a thermodynamic point of view, iron reduction is considered to be energetically more favorable than sulfate reduction (30). Nevertheless, bacterial iron reduction in organically contaminated porous aquifers is frequently limited by the availability of Fe(III) species (2, 45). In the sediments of Liner 1 and 2, extractable ferric iron did only exceptionally account for more than 1 g kg<sup>-1</sup> wwt. Crystalline Fe(III) species, on the other hand, were available at two to fourfold higher concentrations all across the anoxic aquifer section, with maxima above and below the BTEX plume (data not shown). Although bacteria are theoretically capable of using crystalline Fe(III) as electron acceptor (39), these are only slowly converted and less attractive to microorganisms owing to their stability and inaccessibility. It has to be considered, furthermore, that only a small ratio of the ferrous iron is found dissolved in groundwater, while the major part remains associated with to sediment surfaces. This can further decrease the availability of sedimentary Fe(III) to attached bacteria.

Interestingly, readily extractable ferrous iron in sediments exhibited highest values (3-4 g kg<sup>-1</sup> wwt) below the BTEX plume (Fig. 2.2D). Sediment data thus points at an undepleted reservoir of ferric iron in deeper zones of the aquifer. Independent from depth the amount of Fe(II) associated with the sediment in the saturated zone accounted for >99%, while less than 1% was found dissolved in groundwater. A similar distribution of Fe(II) between groundwater and sediment matrix was also reported for other aquifers (2, 31). Elevated concentrations of Fe(II) and concurrent low sulfide concentrations, as found near the capillary fringe, point also at sulfide oxidation with ferric iron, a topic which needs further investigations.

### ***Microbial patterns in groundwater and sediments***

It has repeatedly been shown that cells attached to surfaces can account for 90 to 99.99% of the microbial biomass in porous aquifers. The sediment cell counts, therefore, matched well general findings. However, the two biomass peaks in Liner 1 and 2 (here the lower one was less pronounced) impressively mirrored zones of highest biodegradation activities as indicated by redox gradients. Unfortunately, no data on the number of suspended cells were available for the February 2006 sampling campaign due to accidental loss of sample vials. Thus no direct sediment-groundwater comparisons could be performed for this particular parameter. However, the sediment data obtained may be well compared with groundwater data from a sampling campaign six months later (6). The general distribution of bacteria in groundwater was highly similar to the sediment pattern reported here. In detail, the total number of cells was highest in the uppermost sampling point in the upper plume fringe zone, exhibiting  $1.2 \times 10^6$  cells mL<sup>-1</sup>. In

the plume core, cell numbers were ten times less with an average value of  $2.1 \times 10^5 \text{ mL}^{-1}$ , but increased again to  $5 \times 10^5 \text{ mL}^{-1}$  at the lower plume fringe. Further down, a slight decrease of cell numbers to  $3.2 \times 10^5 \text{ mL}^{-1}$  was observed, interrupted by another distinct peak ( $6.8 \times 10^5 \text{ mL}^{-1}$ ) right in the area of highest PAH concentrations in the sediment (6). Comparing total cell counts in groundwater and sediments on a volume basis (assuming a sediment active porosity of 34%) revealed between 97.7 and 99.8% of the cells attached to the sediments. Similar values are reported from an aquifer at a landfill site, where 98.3% of the cells were found attached (40). Also (9) emphasized the ecological role of sediments, which harbored cell numbers approximately one magnitude higher compared to groundwater.

Assuming a sediment surface area of 22 (coarse sand) to  $450 \text{ cm}^2 \text{ g}^{-1}$  (fine sand) (2, 29) and a mean area of  $0.5 \mu\text{m}^2$  covered by a typical bacterial cell in groundwater (19),  $4.4 \times 10^9$  to  $9 \times 10^{10}$  attached cells  $\text{g}^{-1}$  would be required to form a closed unicellular biofilm. In fact, the highest bacterial abundance determined from our sediment samples, i.e. at the lower plume fringe in Liner 1 (Fig. 2.3), accounts for a surface coverage of only 0.08 to 1.6%. This colonization density is comparable with other studies in aquifers (18, 19) and marine sands (50, 53). In such a case it is questionable, however, whether the term ‘biofilm’ is appropriate or whether we should rather refer to single cells and microcolonies. On the other hand, the maximal total direct cell counts of 4.1 to  $4.8 \times 10^7$  cells  $\text{g}^{-1}$  wwt reported here for the upper sediment layers account for only ~20% of the maximally  $2.4 \times 10^8$  bacterial 16S rRNA genes  $\text{g}^{-1}$  wwt detected via qPCR in similar depths upon sediment sampling in 2005 (52). This number, consequently, would result in a surface coverage of 0.3 to 5.5%. It is likely that both quantification methods carry intrinsic biases, thus although they may be well suited to compare microbial distributions over depth, any absolute interpretations in terms of sediment carrying capacities should be treated with caution.

Indeed, the total cellular distribution did not reveal much about microbial activities and ongoing biodegradation processes. Hydrolysis rates of extracellular phosphatases (MUF-P substrate) and glucosidases (MUF-Glc substrate) (17) revealed microbial activities 5-6 orders of magnitude higher in sediments compared to groundwater (Fig. 2.4). Again, highest values were obtained from the interface between the unsaturated and saturated zone, i.e. the capillary zone and upper plume fringe. As alkaline phosphatases are subject to catabolite repression by their product phosphate (13), the high phosphatase activity in this zone corresponds well with the local decrease in phosphate concentration. Recycling of electron acceptors and mixing with electron donors from the contaminated area make the capillary fringe a favorable place for

biodegradation (41, 42). Higher activities of attached vs. suspended communities have been shown in a number of studies (2, 23, 28, 35). However, with  $\beta$ -glucosidase activity (28) also found the opposite pattern. Concluding, when comparing the gradients in Fig. 2.3 and Fig. 2.4 it can be seen that zones of enhanced microbial activity matched well zones with highest biomass concentration. High biomass zones in contaminated aquifers may thus be a good proxy for zones of pronounced NA activities.

### ***Bacterial community shifts in sediment and water***

Shifts in bacterial community composition over a depth transect of the Flingern BTEX-plume have been observed before for sediment samples taken in June 2005 (52). Hence, an apparently highly specialized degrader population dominated by deltaproteobacterial and clostridal iron reducers, sulfate reducers and fermenters was found to dominate the lower plume fringe. In the present study, we repeated these analyses for selected sediment depths sampled in February 2006, but, more importantly, aimed to compare sedimentary community fingerprints to those obtained from corresponding groundwater samples. Depth-resolved fingerprinting of bacterial communities in water and sediments revealed that only ~50% of all detected T-RFs were shared between water and sediment samples. This is evidence that even if very close corresponding depths are sampled, the two compartments are partially separated on the microscale, and that not all aquifer microbes are equally detectable in both.

This comparison may provide valuable insights on the ecology of the different microbes, as exemplified e.g. by the comparative distribution pattern of the *Geobacter*-related T-RF (130 bp). This T-RF was practically not detected in groundwater, which may be attributed to the preference of these microbes to insoluble electron acceptors such as ferric iron and elemental sulfur, and hence to a lifestyle attached to mineral surfaces (49). In contrast, other microbes putatively more dependent on dissolved electron acceptors, such as the *Desulfocapsa*-relatives represented by the 159 bp T-RF, were consistently distributed with depth in both sediment and water samples, but always detected in higher ratios in groundwater. Moreover, the maximal abundance of this T-RF was surprisingly congruent to the peak of sulfide (Fig. 2.1B). This may be an indication that the distribution of these specific microbes is clearly correlated to the localization of sulfate reducing processes within the Flingern aquifer. We are fully aware that the inference of peak abundances in T-RFLP fingerprinting allow only for a semi-quantitative assessment of community composition and provide no absolute abundances of specific populations (20, 34, 44). Nevertheless, we are confident to demonstrate important distinctions,



but also similarities in depth-resolved microbial community distribution in sediments and water at the site using this approach. A significant correlation between community structure and degree of contamination was also observed in sediments of a leachate-impacted aquifer (9).

Over depth, the non-shared T-RFs appeared mainly in the deeper PAH zone (56% of all singletons). Thus, the upper zones dominated by the BTEX plume seem to impose much stronger selective pressures on the microorganisms, leading to a more uniform appearance of bacteria in both compartments. This was also reflected in the congruent depth-related bacterial community shifts identified in PCA, which supports both strategies to provide relevant information on depth-resolved microbial distribution patterns. Up to now, researchers have been well aware that only a minor fraction of total aquifer microbiota are found in groundwater itself (3, 19, 27). Although we do not provide a direct quantitative comparison of microbial abundance in groundwater and sediments for the same sampling date, this is to our knowledge the first systematic evaluation of the congruence of physical-chemical and microbial community patterns found in both compartments.

We show that major microbial community indicators such as total diversity or the relative abundance of selected community members are distributed in similar, however not identical patterns. Sediment samples always seem to comprise most genetic information found also in the water, but this relation is not correct *vice versa*. Nevertheless, as ~50% of all T-RF peaks were shared between both compartments, both strategies can be considered appropriate to detect spatial and temporal distinctions in the microbial community composition at contaminated sites.

In summary, the data presented in this study emphasize the importance of considering both groundwater and sediment parameters for assessing natural attenuation potential and activities at organically contaminated aquifers. Unlike groundwater samples, which provide only a momentary snapshot of dissolved reactants and dependant microbes *in situ*, sediment analyses allowed more profound insights into the history of the aquifer and into long-term processes occurring at a site, not only in the aquatic, but also the sedimentary compartments.

## 2.6. References

1. **Albrechtsen, H.-J., and A. Winding.** 1992. Microbial biomass and activity in subsurface sediments from Vejlen, Denmark. *Microbial Ecology* **23**:303-317.
2. **Albrechtsen, H. J., and T. H. Christensen.** 1994. Evidence for microbial iron reduction in a landfill leachate-polluted aquifer (Vejlen, Denmark). *Applied Environmental Microbiology* **60**.
3. **Alfreider, A., M. Krössbacher, and R. Psenner.** 1997. Groundwater samples do not reflect bacterial densities and activity in surface systems. *Water Research* **31**:882-840.
4. **Anderson, R. T., and D. R. Lovley.** 1997. Ecology and biogeochemistry of in situ groundwater bioremediation, p. 289-350, *Advances in Microbial Ecology*, Vol 15.
5. **Anneser, B., F. Einsiedl, R. U. Meckenstock, L. Richters, F. Wisotzky, and C. Griebler.** 2008. High-resolution monitoring of biogeochemical gradients in a tar oil-contaminated aquifer. *Applied Geochemistry* **23**:1715-1730.
6. **Anneser, B., L. Richters, and C. Griebler.** 2008. Application of high-resolution groundwater sampling in a tar oil-contaminated sandy aquifer. Studies an small-scale abiotic gradients, p. 107-122. *In* C. Press/Balkema (ed.), *Advances in Subsurface Pollution of Porous Media: Indicators, Processes and Modelling* Candela, L. Vadillo, I. Elorza, F.J., Leiden, NL.
7. **Appelo, C. A., and D. Postma.** 2005. *Geochemistry, Groundwater and Pollution*, Second Edition. Taylor & Francis, Leiden, The Netherlands.
8. **Bamforth, S. M., and I. Singleton.** 2005. Bioremediation of polycyclic aromatic hydrocarbons: current knowledge and future directions. *Journal of Chemical Technology & Biotechnology* **80**:723-736.
9. **Brad, T., B. M. van Breukelen, M. Braster, N. M. van Straalen, and F. M. Röling.** 2008. Spatial heterogeneity in sediment-associated bacterial and eukaryotic communities in a landfill leachate-contaminated aquifer. *FEMS Microbiology Ecology* **65**:534-543.
10. **Brielmann, H., C. Griebler, S. I. Schmidt, R. Michel, and T. Lueders.** 2009. Effects of thermal energy discharge on shallow groundwater ecosystems. *FEMS Microbiology Ecology* **68**:273-286.
11. **Christensen, T. H., P. L. Bjerg, S. A. Banwart, R. Jakobsen, G. Heron, and H.-J. Albrechtsen.** 2000. Characterization of redox conditions in groundwater contaminant plumes. *Journal of Contaminant Hydrology* **45**:165-241.
12. **Christensen, T. H., P. Kjeldsen, P. L. Bjerg, D. L. Jensen, J. B. Christensen, A. Baun, H.-J. Albrechtsen, and G. Heron.** 2001. Biogeochemistry of landfill leachate plumes. *Applied Geochemistry* **16**:659-718.
13. **Coolen, M. J. L., and J. Overmann.** 2000. Functional Exoenzymes as Indicators of Metabolically Active Bacteria in 124,000-Year-Old Sapropel Layers of the Eastern Mediterranean Sea. *Appl. Environ. Microbiol.* **66**:2589-2598.
14. **Cozzarelli, I. M., J. S. Herman, M. J. Baedecker, and J. M. Fischer.** 1999. Geochemical heterogeneity of a gasoline-contaminated aquifer. *Journal of Contaminant Hydrology* **40**:261-284.
15. **Eberhardt, C., and P. Grathwohl.** 2002. Time scales of organic contaminant dissolution from complex source zones: coal tar pools vs. blobs. *Journal of Contaminant Hydrology* **59**:45-66.
16. **Eckert, P.** 2001. Untersuchungen zur Wirksamkeit und Stimulation natrlicher Abbauprozesse in einem mit gaswerksspezifischen Schadstoffen kontaminierten Grundwasserleiter. **Bochum: PhD thesis** 123.

17. **Freeman, C., G. Liska, N. Ostle, S. Jones, and M. Lock.** 1995. The use of fluorogenic substrates for measuring enzyme activity in peatlands. *Plant and Soil* **175**:147-152.
18. **Griebler, C., B. Mindl, and D. Slezak.** 2001. Combining DAPI and SYBR Green II for the Enumeration of Total Bacterial Numbers in Aquatic Sediments. *Internat. Rev. Hydrobiol.* **86**:453-465.
19. **Griebler, C., B. Mindl, D. Slezak, and M. Geiger-Kaiser.** 2002. Distribution patterns of attached and suspended bacteria in pristine and contaminated shallow aquifers studied with an in situ sediment exposure microcosm. *Aquatic Microbial Ecology* **28**:117-129.
20. **Hartmann, M., and F. Widmer.** 2008. Reliability for detecting composition and changes of microbial communities by T-RFLP genetic profiling. *FEMS Microbiology Ecology* **63**:249-260.
21. **Hazen, T., L. Jiménez, G. López de Victoria, and C. Fliermans.** 1991. Comparison of bacteria from deep subsurface sediment and adjacent groundwater. *Microbial Ecology* **22**:293-304.
22. **Hendel, B., and J. Marxsen.** 1997. Measurement of Low-level Extracellular Enzyme Activity in Natural Waters Using Fluorogenic Model Substrates. *Acta hydrochimica et hydrobiologica* **25**:253-258.
23. **Holm, N., A. Cairns-Smith, R. Daniel, J. Ferris, R. Hennet, E. Shock, B. Simoneit, and H. Yanagawa.** 1992. Marine hydrothermal systems and the origin of life: future research. *Orig Life Evol Biosph.* **22**:181-242.
24. **Kao, C. M., S. Kota, B. Ress, M. A. Barlaz, and R. C. Borden.** 2001. Effects of subsurface heterogeneity on natural bioremediation at a gasoline spill site. *Water Sci Technol* **43**:341-348.
25. **Kölbel-Boelke, J., P. Hirsch, W. G. Characklis, and P. A. Wilderer.** 1989. Comparative physiology of biofilm and suspended microorganisms in the groundwater environment. . *Structure and Function of Biofilms* . **John Wiley Chichester** 221-238.
26. **Kostka, J. E., A. Roychoudhury, and P. Van Cappellen.** 2002. Rates and controls of anaerobic microbial respiration across spatial and temporal gradients in saltmarsh sediments. *Biogeochemistry* **60**:49-76.
27. **Lehman, R. M., F. S. Colwell, and G. A. Bala.** 2001. Attached and Unattached Microbial Communities in a Simulated Basalt Aquifer under Fracture- and Porous-Flow Conditions. *Appl. Environ. Microbiol.* **67**:2799-2809.
28. **Lehman, R. M., and S. P. O'Connell.** 2002. Comparison of Extracellular Enzyme Activities and Community Composition of Attached and Free-Living Bacteria in Porous Medium Columns. *Appl. Environ. Microbiol.* **68**:1569-1575.
29. **Leichtfried, M.** 1985. Organic matter in gravel streams (Project Ritrodat-Lunz). *Verh Int Ver Limnol* **22**:2058-2062.
30. **Lovley, D. R., and F. H. Chapelle.** 1995. Deep Subsurface Microbial Processes. *Reviews of Geophysics* **33**:365-381.
31. **Lovley, D. R., and E. J. P. Phillips.** 1988. Novel Mode of Microbial Energy Metabolism: Organic Carbon Oxidation Coupled to Dissimilatory Reduction of Iron or Manganese. *Appl. Environ. Microbiol.* **54**:1472-1480.
32. **Lovley, D. R., and E. J. P. Phillips.** 1987. Rapid Assay for Microbially Reducible Ferric Iron in Aquatic Sediments. *Appl. Environ. Microbiol.* **53**:1536-1540.
33. **Lueders, T., and M. W. Friedrich.** 2002. Effects of Amendment with Ferrihydrite and Gypsum on the Structure and Activity of Methanogenic Populations in Rice Field Soil. *Appl. Environ. Microbiol.* **68**:2484-2494.
34. **Lueders, T., and M. W. Friedrich.** 2003. Evaluation of PCR Amplification Bias by Terminal Restriction Fragment Length Polymorphism Analysis of Small-Subunit rRNA and

- mcrA Genes by Using Defined Template Mixtures of Methanogenic Pure Cultures and Soil DNA Extracts. *Appl. Environ. Microbiol.* **69**:320-326.
35. **Madsen, E. L., and W. C. Ghiorse.** 1993. Groundwater microbiology: subsurface ecosystem processes. *Aquatic Microbiology-An Ecological Approach*, 167-213.
36. **McGuire, J. T., E. W. Smith, D. T. Long, D. W. Hyndman, S. K. Haack, M. J. Klug, and M. A. Velbel.** 2000. Temporal variations in parameters reflecting terminal-electron-accepting processes in an aquifer contaminated with waste fuel and chlorinated solvents. *Chemical Geology* **169**:471-485.
37. **Nebe-von-Caron, G., P. J. Stephens, C. J. Hewitt, C. R. Powell, and R. A. Badley.** 2000. Analysis of bacterial function by multi-colour fluorescence flow cytometry and singel cell sorting. *Journal of Microbiological Methods* **42**:97-114.
38. **Paissé, S., F. Coulon, M. Goñi-Urriza, L. Peperzak, T. J. McGenity, and R. Duran.** 2008. Structure of bacterial communities along a hydrocarbon contamination gradient in a coastal sediment. *FEMS Microbiology Ecology* **66**:295-305.
39. **Roden, E. E., and J. M. Zachara.** 1996. Microbial Reduction of Crystalline Iron(III) Oxides: Influence of Oxide Surface Area and Potential for Cell Growth. *Environ. Sci. Technol.* **30**:1618-1628.
40. **Roling, W. F. M., B. M. van Breukelen, M. Braster, B. Lin, and H. W. van Verseveld.** 2001. Relationships between Microbial Community Structure and Hydrochemistry in a Landfill Leachate-Polluted Aquifer. *Appl. Environ. Microbiol.* **67**:4619-4629.
41. **Ronen, D., H. Scher, and M. Blunt.** 2000. Field observations of a capillary fringe before and after a rainy season. *Journal of Contaminant Hydrology* **44**:103-118.
42. **Sinke, A. J. C., O. Dury, and J. Zobrist.** 1998. Effects of a fluctuating water table: column study on redox dynamics and fate of some organic pollutants. *Journal of Contaminant Hydrology* **33**:231-246.
43. **Stumm, W., and J. J. Morgan.** 1996. *Aquatic Chemistry* John Wiley & Sons Inc , New York
44. **Thies, J. E.** 2007. Soil Microbial Community Analysis using Terminal Restriction Fragment Length Polymorphisms. *Soil Sci. Soc. Am. J.* **71**:579-591.
45. **Tuccillo, M. E., I. M. Cozzarelli, and J. S. Herman.** 1999. Iron reduction in the sediments of a hydrocarbon-contaminated aquifer. *Applied Geochemistry* **14**:655-667.
46. **Ulrich, G. A., G. N. Breit, I. M. Cozzarelli, and J. M. Suflita.** 2003. Sources of Sulfate Supporting Anaerobic Metabolism in a Contaminated Aquifer. *Environmental Science & Technology* **37**:1093-1099.
47. **Ulrich, G. A., L. R. Krumholz, and J. M. Suflita.** 1997. A rapid and simple method for estimating sulfate reduction activity and quantifying inorganic sulfides. *Appl Environ Microbiol* **63**:4626.
48. **Ulrich, G. A., D. Martino, K. Burger, J. Routh, E. L. Grossman, J. W. Ammerman, and J. M. Suflita.** 1998. Sulfur cycling in the terrestrial subsurface: Commensal interactions, spatial scales, and microbial heterogeneity. *Microbial Ecology* **36**:141-151.
49. **Weber, K. A., L. A. Achenbach, and J. D. Coates.** 2006. Microorganisms pumping iron: anaerobic microbial iron oxidation and reduction. *Nat Rev Micro* **4**:752-764.
50. **Weise, W., and G. Rheinheimer.** 1977. Scanning electron microscopy and epifluorescence investigation of bacterial colonization of marine sand sediments. *Microbial Ecology* **4**:175-188.
51. **Widdel, F., and F. Bak.** 1992. Gram negative mesophilic sulfate reducing bacteria. In: Balows A, Trüper HG, Dworkin M, Harder W and Schleifer K-H (eds). *The Prokaryotes*, 2nd edn Springer: New York, NY, pp 3352–3378.

52. **Winderl, C., B. Anneser, C. Griebler, R. U. Meckenstock, and T. Lueders.** 2008. Depth-Resolved Quantification of Anaerobic Toluene Degraders and Aquifer Microbial Community Patterns in Distinct Redox Zones of a Tar Oil Contaminant Plume. *Appl. Environ. Microbiol.* **74**:792-801.
53. **Yamamoto, N., and G. Lopez.** 1985. Bacterial abundance in relation to surface area and organic content of marine sediments. *Journal of Experimental Marine Biology and Ecology* **90**:209-220.
54. **Zhou, J., M. A. Bruns, and J. M. Tiedje.** 1996. DNA recovery from soils of diverse composition. *Appl. Environ. Microbiol.* **62**:316-322.

### 3. Electron acceptor-dependent identification of key anaerobic toluene degraders at a tar-oil contaminated aquifer by Pyro-SIP

Giovanni Pilloni<sup>1</sup>, Frederick von Netzer<sup>1</sup>, Marion Engel<sup>2</sup> and Tillmann Lueders<sup>1\*</sup>

<sup>1</sup> Institute of Groundwater Ecology, Helmholtz Zentrum München - German Research Center for Environmental Health, Neuherberg, Germany

<sup>2</sup> Department of Terrestrial Ecogenetics, Institute of Soil Ecology, Helmholtz Zentrum München - German Research Center for Environmental Health

*FEMS Microbiology Ecology* (accepted 2 March 2011)

#### 3.1. Abstract

Bioavailability of electron acceptors is probably the most limiting factor in the restoration of anoxic, contaminated environments. The oxidation of contaminants such as aromatic hydrocarbons, particularly in aquifers, often depends on the reduction of ferric iron or sulphate. We have previously detected a highly active fringe zone beneath a toluene plume at a tar-oil contaminated aquifer in Germany, where a specialized community of contaminant degraders co-dominated by *Desulfobulbaceae* and *Geobacteraceae* had established. Although on-site geochemistry links degradation to sulphidogenic processes, dominating catabolic (benzylsuccinate synthase alpha-subunit, *bssA*) genes detected *in situ* appeared more related to those of *Geobacter* spp. Therefore, a stable isotope probing (SIP) incubation of sediment samples with <sup>13</sup>C<sub>7</sub>-toluene and comparative electron acceptor amendment was performed. We

introduce pyrosequencing of templates from SIP microcosms as a powerful new strategy in SIP gradient interpretation (Pyro-SIP).

Our results reveal the central role of *Desulfobulbaceae* for sulphidogenic toluene degradation *in situ*, and affiliate the detected *bssA* genes to this lineage. This and the absence of  $^{13}\text{C}$ -labelled DNA of *Geobacter* spp. in SIP gradients preclude their relevance as toluene degraders *in situ*. In contrast, *Betaproteobacteria* related to *Georgfuchsia* spp. became labelled under iron-reducing conditions. Furthermore, secondary toluene degraders belonging to the *Peptococcaceae* detected in both treatments suggest the possibility of functional redundancy amongst anaerobic toluene degraders on site.

### 3.2. Introduction

Groundwater, a primary resource of drinking water, is subject to notorious contamination by a huge variety of anthropogenic compounds. Amongst them petroleum derivatives, especially aromatic ones, are significantly persistent. Therefore, degradation of compounds such as benzene, toluene, ethylbenzene and xylenes (BTEX) by intrinsic aquifer microbial communities, specifically under anaerobic conditions, is of particular interest for the comprehension and prediction of natural attenuation. Anaerobic BTEX degradation is known to occur under different terminal electron accepting processes such as nitrate, iron or sulphate reduction, and methanogenesis (1, 7). However, the co-occurrence of, or competition between different degrader guilds *in situ* is not well understood. Clearly, the dominance of a given degrader lineage is assumed to be dictated by electron acceptor availability.

Previous evidence from a tar-oil contaminated aquifer site in Germany has shown establishment of a highly active anaerobic toluene-degrading microbial community at the lower fringe of a BTEX plume (3, 31). Even though toluene degradation at the site is presumed to be driven by sulphate reduction (2, 31), this community is co-dominated by microbes affiliated to the *Desulfobulbaceae* and the *Geobacteraceae*. Both deltaproteobacterial lineages are known to harbour anaerobic toluene degraders, but these are either sulphate- or iron-reducers (13, 22). At the same time, the dominating anaerobic toluene degradation genes (benzylsuccinate synthase alpha-subunit, *bssA*) detected at the site were more closely related to *Geobacter*-affiliated *bssA* than to other known sulphate-reducing degraders (33). However, the utility of the *bssA* gene as a phylogenetic marker is not robust, as cases of lateral gene transfer of this gene have been

reported (27, 33). Moreover, recent studies indicate that certain members of the *Peptococcaceae* (*Clostridia*), also relevant constituents of the respective lower plume fringe community (3, 31), carry a previously unrecognised capacity for toluene degradation under iron- (15) and sulphate-reducing conditions (32).

To resolve this dilemma and to assign phylogenetically key toluene-degrading functionality and genes at this site, we conducted a stable isotope probing (SIP) experiment with fresh sediment samples taken *in situ* from the degradation-active lower plume fringe. Sediments were incubated in microcosms under amendment of  $^{13}\text{C}_7$ -toluene and either sulphate or ferric iron as electron acceptor. SIP allows direct identification of environmental microorganisms degrading and assimilating carbon from a  $^{13}\text{C}$ -labelled hydrocarbon and, if conducted for DNA, affiliation of respective degradation genes (21). We hypothesize that if both *Desulfobulbaceae* and *Geobacteraceae*-related degraders are important in toluene degradation *in situ*, both will become labelled in the respective SIP incubations. However, if only one of the two lineages is important in the breakdown of toluene *in situ*, only this will be labelled while respiring the appropriate electron acceptor. In contrast, a different degrader lineage, not dominating (or important) *in situ*, could become detectable using the other oxidant. We test this hypothesis using a new combination of DNA-stable isotope probing and high throughput pyrosequencing of amplicons from SIP incubations to identify the key toluene-degrading lineage in these sediments.

### 3.3. Material and Methods

#### 3.3.1. Sampling site and sample acquisition

Sampling was performed within a well studied (2, 3, 31) tar-oil contaminated aquifer in Düsseldorf-Flingern, Germany in September 2008. Sediments ranging between 6.9 and 7.75 m below ground surface were sampled from intact direct-push liners and immediately dispensed into 1 L glass bottles full of anoxically autoclaved (under  $\text{N}_2/\text{CO}_2$ ) deionised water. Bottles were directly closed without gaseous headspace to minimise oxygen exposure of sediments and transported to the laboratory under cooling (4°C).



### 3.3.2. Incubation of sediments

Replicates (~8 g wet weight) of homogeneously mixed sediment material were transferred (in an anoxic tent) into sterile 120 ml serum bottles containing 50 ml of artificial anoxic groundwater medium as previously described (32). To ensure constantly low *in situ*-like concentrations of toluene during SIP incubation, 0.3 g of Amberlite XAD7 absorber resin in each microcosm was loaded with a total of 1 mM of either non-labelled ( $^{12}\text{C}$ ) or fully labelled  $^{13}\text{C}_7$  toluene (Sigma-Aldrich, Munich, Germany) (32). Parallel incubation series were amended with either 10 mM of sodium sulphate, or 40 mM of amorphous Fe(III) oxyhydroxide prepared by titration of a solution of  $\text{FeCl}_3$  to a pH of 7 with NaOH (19). Twelve replicate microcosms for each treatment were set up. Abiotic control bottles (autoclaved 3 times), amended with each electron acceptor and unlabelled toluene, were also prepared to exclude the occurrence of abiotic redox reactions. The bottles were incubated statically for over 4 months in the dark at  $16^\circ\text{C}$ , which was close to *in situ* aquifer temperatures of  $14^\circ\text{C}$  -  $16^\circ\text{C}$ .

### 3.3.3. Process measurements

Liquid and gaseous samples were taken from replicate  $^{12}\text{C}$ - and  $^{13}\text{C}$ -toluene and control bottles to monitor toluene degradation weekly. Aqueous toluene and sulphide concentrations were determined as described previously (32). Fe(II) was monitored from 100  $\mu\text{l}$  liquid subsamples also as described previously (5), using a Cary 50 Bio UV-Vis photometer (Varian, Darmstadt, Germany) at a wavelength of 508 nm. The formation of  $^{13}\text{CO}_2$  was followed via gas chromatography combustion-isotope ratio mass spectrometry (GC-C-IRMS) on 15  $\mu\text{l}$  samples taken from the head space of each bottle, as described previously (32).

### 3.3.4. Nucleic acid extraction and ultracentrifugation

At selected time points, a pair of bottles ( $^{12}\text{C}$  &  $^{13}\text{C}$ ) for each electron acceptor series (sulphate, ferric iron) was sacrificed for DNA-SIP analyses. Sediment and biomass were collected by centrifugation at 4000 rpm at  $4^\circ\text{C}$  for 10 min with a Megafuge 1.0 R (Heraeus Instruments, Hanau, Germany). Pellets were frozen immediately at  $-20^\circ\text{C}$  until DNA extraction. DNA was extracted as previously described (31) with minor modifications concerning the last 30% PEG-precipitation step (~12h instead of ~4h, in order to increase the yield). For each single

extract, several replicate extractions were pooled in max. 100  $\mu$ l of elution buffer (Qiagen) and stored frozen (-20°C) for downstream analyses.

Approximately 1  $\mu$ g of PicoGreen (Invitrogen)-quantified DNA extracts were loaded into a gradient medium of CsCl (average density 1.71 g ml<sup>-1</sup>, Calbiochem., Merck, Darmstadt, Germany) in gradient buffer (0.1 M Tris-HCl at pH 8, 0.1 M KCl, 1mM EDTA) and centrifuged (44500 rpm, ~65 h) as described in detail elsewhere (21, 32). Thirteen fractions from each gradient were collected from ‘heavy’ to ‘light’ using a Perfusor V syringe pump (B.Braun, Melsungen, Germany). Refractometric measurements of fractions buoyant density (BD) and the recovery of DNA from gradient fractions were also performed as published (21).

### 3.3.5. Analyses of density-resolved DNA fractions

Recovered DNA from CsCl gradient fractions was analysed by bacterial 16S rRNA gene targeted qPCR in the presence of 0.1 x SYBR Green as described (16)., Most fractions from each gradient were selected for bacterial 16S rRNA gene targeted T-RFLP fingerprinting. FAM-labelled amplicons were generated with the primers Ba27f (5’FAM-aga gtt tga tcm tgg ctc ag-3’) and 907r (5’-ccg tca att cct ttg agt tt-3’) in a Mastercycler ep gradient (Eppendorf, Hamburg, Germany) with the following cycling conditions: initial denaturation (94°C, 5 min) followed by 24 or 28 cycles of denaturation (94°C, 30 s), annealing (52°C, 30 s), and elongation (70°C, 60 s). Each 50  $\mu$ l PCR reaction contained 1x PCR buffer, 1.5 mM MgCl<sub>2</sub>, 0.1 mM dNTPs, 1.25 U recombinant Taq polymerase (all from Fermentas, St. Leon-Rot, Germany), 0.2  $\mu$ g  $\mu$ l<sup>-1</sup> BSA (Roche, Penzberg, Germany), 0.5  $\mu$ M of each primer (Biomers, Ulm, Germany), and 1  $\mu$ l of template DNA. Amplicons were restricted using *MspI* and separated by capillary electrophoresis as reported (33). Electropherograms were evaluated as described (31).

In addition, density-resolved DNA was also subjected to bacterial *bssA* gene fingerprinting. This was conducted with the 7772f / 8546r-FAM primer pair as described (32), but with a PCR annealing temperature of 58°C (33). Amplicons were digested with *TaqI* and PCR chemistry and the remaining procedures were as for 16S fingerprints.

### 3.3.6. Amplicon Pyrosequencing from SIP microcosms

Amplicon pyrosequencing was performed on unfractionated total DNA extracted from <sup>13</sup>C-microcosms. Barcoded amplicons for multiplexing were prepared with the primers Ba27f (5’-aga

gtt tga tcm tgg etc ag-3') and Ba519r (5'-tat tac cgc ggc kgc tg-3') (17) extended as amplicon fusion primers with respective primer A or B adapters, key sequence and multiplex identifiers (MID) as recommended by 454/Roche (<http://454.com/products-solutions/experimental-design-options/amplicon-sequencing.asp>).

Amplicons were generated with the same cycling conditions as described above for T-RFLP. Each 50 µl PCR reaction contained 1x PCR buffer, 1.44 mM MgCl<sub>2</sub>, 0.1 mM dNTPs, 1% DMSO, 1.25 U Taq polymerase (all from FastStart High Fidelity Taq DNA Polymerase kit, Roche), 0.32 µg µl<sup>-1</sup> BSA (Roche), 0.3 µM of each MID-primer (Biomers), and 1 µl of template DNA. Amplicons were purified and pooled as specified by the manufacturer. Emulsion PCR, emulsion breaking and sequencing were performed applying the GS FLX Titanium chemistry following protocols and using a 454 GS FLX pyrosequencer (Roche) as recommended by the developer. For this study, 2 amplicons were sequenced in a pool of 14 mixed amplicons on 1/8<sup>th</sup> of a FLX picotiter plate. Quality filtering of the pyrosequencing reads was performed using the automatic amplicon pipeline of the GS Run Processor (Roche), with a modification concerning the valley filter (vfScanAllFlows false instead of TiOnly) to extract sequences.

Afterwards, reads were further quality-trimmed using the Trim function of Greengenes (8) with the following settings: good quality score 20, window size 40 bp, window threshold 90%. Subsequently, reads were batched per sample based on MID-identifiers with BioEdit (10) and reads with inferior read length (<250 bp) were excluded from further analysis. Total community composition was classified via read affiliation using the RDP classifier (29) at a confidence threshold of 70%. Read abundance percentage of classified lineages was recorded.

For downstream analysis of sequenced amplicon pools (T-RF prediction, phylogenetic inference), matching sequences from forward- and reverse-reads were assembled into contigs with the SeqMan II software (DNASTar) using assembly thresholds of at least 98% sequence similarity over a 50 bp match window. Contigs without at least one forward and one reverse read were not considered for further analysis. Selected dominating amplicon contigs were then integrated into an ARB (20) database (version SSURef-95, July 2008). Sequences were aligned using automated aligners in the ARB\_EDIT4 editor. For phylogenetic affiliation, a 'backbone' tree based on selected full-length (>1200 bp) reference sequences of cultivated and uncultivated taxa was constructed using quartet puzzling as previously described (15). Subsequently, shorter sequences including the selected amplicon contigs were added to the tree using the ARB parsimony tool, thereby maintaining overall tree topology.

T-RFs of amplicon contigs were predicted using ARB\_EDIT4. Possible deviations between predicted and measured T-RFs were handled by referring to our previous thorough verification of lineage-specific T-RFs by direct T-RFLP analysis of cloned amplicons generated from the same contaminated site (31).

In summary, this new bidirectional amplicon pyrosequencing approach allows integrated evaluation of pyrosequencing results from the phylogenetic placement of representative assembled dominating amplicon sequences to T-RF matching. All raw and trimmed reads generated in this study have been deposited in NCBI's Gene Expression Omnibus (9) and are accessible through GEO Series accession number GSE25449. The selected amplicon contigs used for phylogenetic analysis have been deposited at GenBank under the accession numbers HQ625653 to HQ625672.

### 3.4. Results

#### 3.4.1 Exposure of aquifer sediments to $^{13}\text{C}$ -toluene

Fig. 3.1 shows the evolution of major redox species during SIP incubation. Increasing concentrations of sulphide, with a rapid rise up to 2.8 mM between the 10<sup>th</sup> and 12<sup>th</sup> week were paralleled by a steep increase in  $^{13}\text{CO}_2$  (up to ~12 atom percent, AT%) in sulphate-amended  $^{13}\text{C}$ -toluene microcosms. In contrast, iron(III)-amended microcosms showed a primary increase of  $\text{Fe}^{2+}$  up to ~9 mM during the first six weeks, followed by a secondary, slower increase to up to ~15 mM until the end of the experiment. Only this secondary increase of  $\text{Fe}^{2+}$  was connected to a rise in  $^{13}\text{CO}_2$  concentrations, albeit to much lower ratios (only ~4 AT%) than under sulphate amendment.  $^{12}\text{C}$ -toluene microcosms showed comparable dynamics of reduced electron acceptors.

The time-course of toluene consumption was not detectable due to the presence of the XAD7 carrier resin, as described before (32). Although toluene was present with a nominal total concentration of ~1 mM, desorbed free aqueous concentrations varied around ~50  $\mu\text{M}$  for most of the incubation time. Complete toluene depletion was observed in the sulphate-reducing incubations after the 13<sup>th</sup> week, while ~35  $\mu\text{M}$  remained detectable in the iron-reducing incubations by the end of the experiment (15<sup>th</sup> week). Autoclaved controls did not show

significant abiotic reactions, with sulphide concentration not exceeding  $\sim 0.1$  mM, and iron(II) concentration not exceeding  $\sim 4.6$  mM. As observed previously for electron balances in similar SIP microcosms (32), sulphate microcosms ended with  $\sim 60\%$  of the electrons from the added toluene recovered in sulphide and  $\sim 85\%$  of the added labelled carbon recovered as  $^{13}\text{CO}_2$ . In iron incubations, only  $\sim 42\%$  of the added electrons from toluene were recaptured in ferrous iron, and less than 30% of the carbon from  $^{13}\text{C}$ -toluene was recovered as  $^{13}\text{CO}_2$  (both assuming complete toluene oxidation).

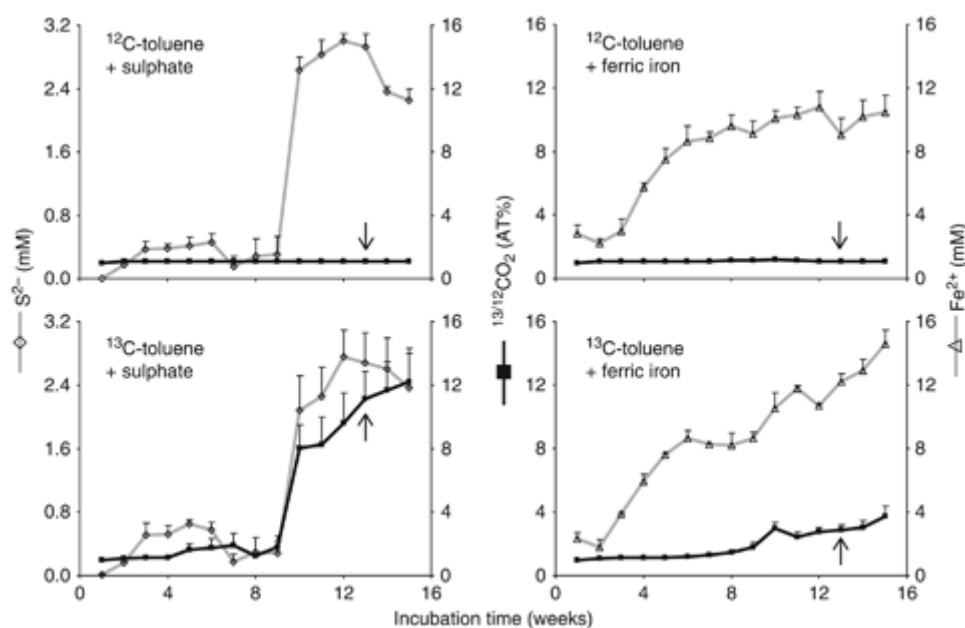


Fig. 3.1: Production of sulphide,  $^{13}\text{CO}_2$  and ferrous iron during degradation of  $^{13}\text{C}_7$ -toluene in comparative SIP microcosms.  $^{13}\text{C}/^{12}\text{C}$  isotopic composition of  $\text{CO}_2$  is indicated in atom per cent (AT%). Means of triplicate measurements are given + standard error. Arrows indicate the time point chosen for DNA-SIP analyses.

### 3.4.2 Detection and identification of $^{13}\text{C}$ -labelled degraders

One late time point, when substantial respiration and mineralisation activities had been observed in both SIP incubation series (after 13 weeks), was selected for detection of labelled DNA by isopycnic ultracentrifugation. This choice was driven mainly by the iron-reducing microcosms, where significant shifts in  $^{13}\text{CO}_2$  were not detectable earlier. Nevertheless, clear buoyant density (BD) shifts compared to the respective  $^{12}\text{C}$ -control gradients and enrichment of bacterial DNA, especially in ‘intermediate’ gradient fractions, was appreciable in SIP-gradients from both incubation series (Fig. 3.2).

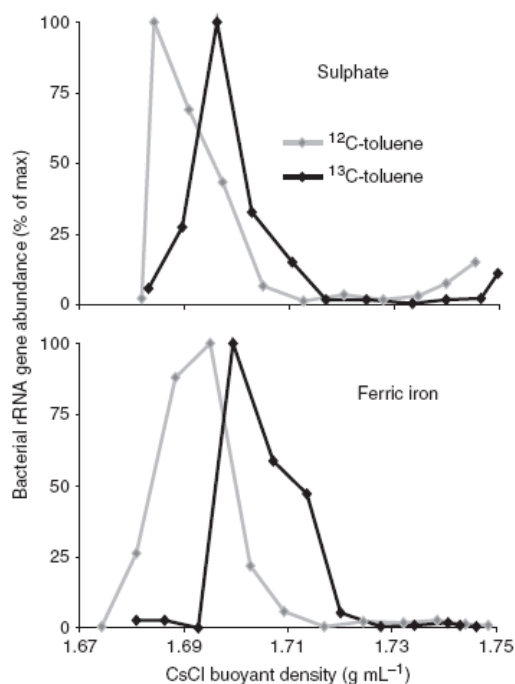


Fig. 3.2: Quantitative profiles of DNA distribution, measured via 16S rRNA qPCR, in comparative SIP gradients from microcosms amended with unlabelled (<sup>12</sup>C) toluene or <sup>13</sup>C<sub>7</sub>-toluene and sulphate (A) or ferric iron (B).

It was possible to detect clear distinctions between ‘light’ and ‘heavy’ DNA fractions of <sup>13</sup>C-gradients (Fig. 3.3) in bacterial community fingerprints. Thus, ‘intermediate’ and ‘heavy’ fractions of DNA from <sup>13</sup>C-toluene sediments showed a dominance of especially the 159 bp, but also the 146 and 177 bp T-RFs. At the same time, ‘light’ fractions showed selection for the 163 and 469 bp T-RFs. In contrast, all major T-RFs were detected in all gradient fractions from the sulphate-amended <sup>12</sup>C-toluene control. In the ferric iron SIP microcosms, bulk DNA from <sup>12</sup>C-control gradients was dominated mainly by two T-RFs, the 159 and 430 bp fragments. Also other fragments, such as the 288 bp T-RF, were detected in ‘lighter’, low GC-content DNA fractions (Fig. 3.3). In contrast, while ‘light’ bulk DNA in <sup>13</sup>C-gradients was still dominated by the 159 bp T-RF, the 288 bp and 430 bp fragments were of greater relative abundance in ‘intermediate’ and ‘heavy’ gradient fractions. Therefore, especially the latter seemed to represent microbes involved in ferric iron-dependent toluene degradation.

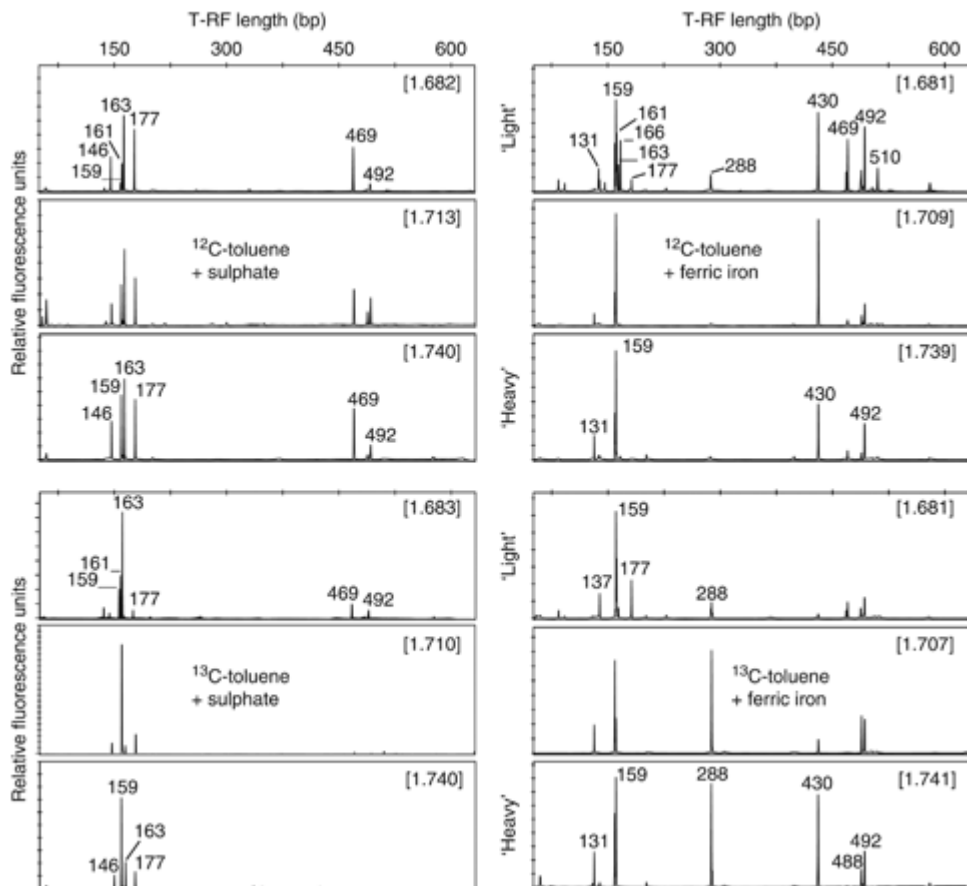


Fig. 3.3: Bacterial 16S rRNA gene T-RFLP fingerprints from density-resolved SIP gradient fractions of DNA from microcosms amended with unlabeled ( $^{12}\text{C}$ ) or  $^{13}\text{C}_7$ -toluene and comparative electron acceptors. The lengths (bp) of selected T-RFs are given. Numbers in parentheses are CsCl BDs ( $\text{g ml}^{-1}$ ) of gradient fractions.

To identify the bacterial lineages represented by T-RFs from density-resolved SIP gradient fractions, barcoded amplicon pyrosequencing (23, 26) of two representative bulk DNA extracts was performed. Table 3.1 summarises total pyrosequencing read, trimming and contig assembly statistics for the two amplicon pools, while Table 3.2 illustrates comprehensive affiliation of reads and that of deduced T-RFs.

### 3. Electron acceptor-dependent identification of key anaerobic toluene degraders at a tar-oil-contaminated aquifer by Pyro-SIP

Tab. 3.1: Number of reads and average read lengths produced in bidirectional pyrosequencing of \_520-bp bacterial 16S rRNA gene fragments from comparative SIP microcosm DNA.

Electron acceptor	Sulphate	Ferric iron
Total forward reads*	1981	2441
Total reverse reads*	1781	2053
Average length total reads (bp)	496	492
Trimmed forward reads, > 250 bp	1653	1827
Trimmed reverse reads, > 250 bp	1169	1428
Average length trimmed reads (bp)	355	358
Amplicon contigs†	67	64

\* The two samples were sequenced among 14 distinct MID-barcoded amplicons on 1/8 FLX picotiter plate.

† Criteria for the assembly of full-length (\_520 bp) amplicon contigs are described in the text.

SIP microcosm communities were mainly composed of reads within the *Delta*-, *Beta*- and *Epsilonproteobacteria*, and also the *Clostridia*. Sulphate-amended samples showed high relative abundances of sequences within the *Desulfobulbaceae* (29%), *Desulfosporosinus* spp. (21%) and *Sulfuricurvum* spp. (13%). In contrast, abundant reads affiliated to *Thermincola* spp. (16%), unclassified *Desulfobacterales* (9%), the *Rhodocyclaceae* (7%), *Comamonadaceae* (13%) and *Actinobacteria* (4%) constituted clear community distinctions detectable in the ferric iron SIP incubations.



### 3. Electron acceptor-dependent identification of key anaerobic toluene degraders at a tar-oil-contaminated aquifer by Pyro-SIP

Tab. 3.2: Phylogenetic affiliation of trimmed reads produced in pyrosequencing of bacterial 16S rRNA gene fragments retrieved from comparative SIP microcosm DNA

Phylogenetic affiliation*	Sulphate		Ferric iron		T-RF (bp) <sup>†</sup>
	Reads	%	Reads	%	
<b>Bacteria</b>	2822		3254		
<b>Unclassified Bacteria</b>	143	<b>5.1</b>	169	<b>5.2</b>	NA
<b>Proteobacteria</b>	1869	<b>66.2</b>	2034	<b>62.5</b>	
<b>Unclassified Proteobacteria</b>	19	<b>0.7</b>	12	<b>0.4</b>	NA
<b>Alphaproteobacteria</b>	3	<b>0.1</b>	20	<b>0.6</b>	NA
<b>Betaproteobacteria</b>	30	<b>1.1</b>	959	<b>29.5</b>	NA
Unclassified Betaproteobacteria	10	0.4	294	9.0	NA
Rhodocyclaceae	1	0.0	231	7.1	430
Comamonadaceae	17	0.6	414	12.7	ND
Curvibacter spp.	0	0.0	130	4.0	488
Rhodoferax spp.	1	0.0	115	3.5	492
<b>Gammaproteobacteria</b>	52	<b>1.8</b>	87	<b>2.7</b>	NA
<b>Deltaproteobacteria</b>	925	<b>32.8</b>	852	<b>26.2</b>	NA
Unclassified Deltaproteobacteria	8	0.3	262	8.1	NA
Desulfobulbaceae	817	29.0	233	7.2	159
Unclassified Desulfobacterales	9	0.3	289	8.9	159
Desulfovibrionaceae	32	1.1	37	1.1	ND
Geobacteraceae	6	0.2	11	0.3	160
<b>Epsilonproteobacteria</b>	840	<b>29.8</b>	104	<b>3.2</b>	NA
Helicobacteraceae	838	29.7	97	3.0	NA
Sulfuricum spp.	375	13.3	35	1.1	163, 469
Unclassified Helicobacteraceae	454	16.1	61	1.9	ND
<b>Firmicutes</b>	662	<b>23.5</b>	867	<b>26.6</b>	NA
<b>Clostridia</b>	654	<b>23.2</b>	861	<b>26.5</b>	NA
Unclassified Clostridiales	28	1.0	140	4.3	NA
Thermincola spp.	0	0.0	512	15.7	288
Desulfosporosinus spp.	589	20.9	41	1.3	146, 177
Unclassified Peptococcaceae	1	0.0	156	4.8	ND
<b>Acidobacteria</b>	3	<b>0.1</b>	3	<b>0.1</b>	NA
<b>Actinobacteria</b>	19	<b>0.7</b>	143	<b>4.4</b>	131
<b>Bacteroidetes</b>	20	<b>0.7</b>	14	<b>0.4</b>	NA
<b>Chloroflexi</b>	92	<b>3.3</b>	20	<b>0.6</b>	NA
<b>Spirochaetes</b>	10	<b>0.4</b>	4	<b>0.1</b>	NA

\* Phylum- or division-level read abundances (bold) include genus- or lineage-specific read abundances (nonbold).

† Characteristic T-RFs were predicted for important lineages via assembled amplicon contigs, but are given as T-RFs actually observed in the electropherograms and as verified in (Winderl et al., 2008). Commas separate more than one characteristic T-RF for a lineage. NA, not applicable for this level; ND, not detected for this lineage.

The phylogenetic placement of important amplicon contigs assembled from dominating pyrosequencing reads is illustrated in Fig. 3.4. In combination with T-RFs previously predicted and measured for cloned bacterial rRNA genes from the same site (31), a comprehensive affiliation of T-RFs detected in density-resolved DNA gradient fractions to defined lineages was possible. Almost all the peaks present in the electropherograms could actually be matched to pyrosequencing read data.

3. Electron acceptor-dependent identification of key anaerobic toluene degraders at a tar-oil-contaminated aquifer by Pyro-SIP

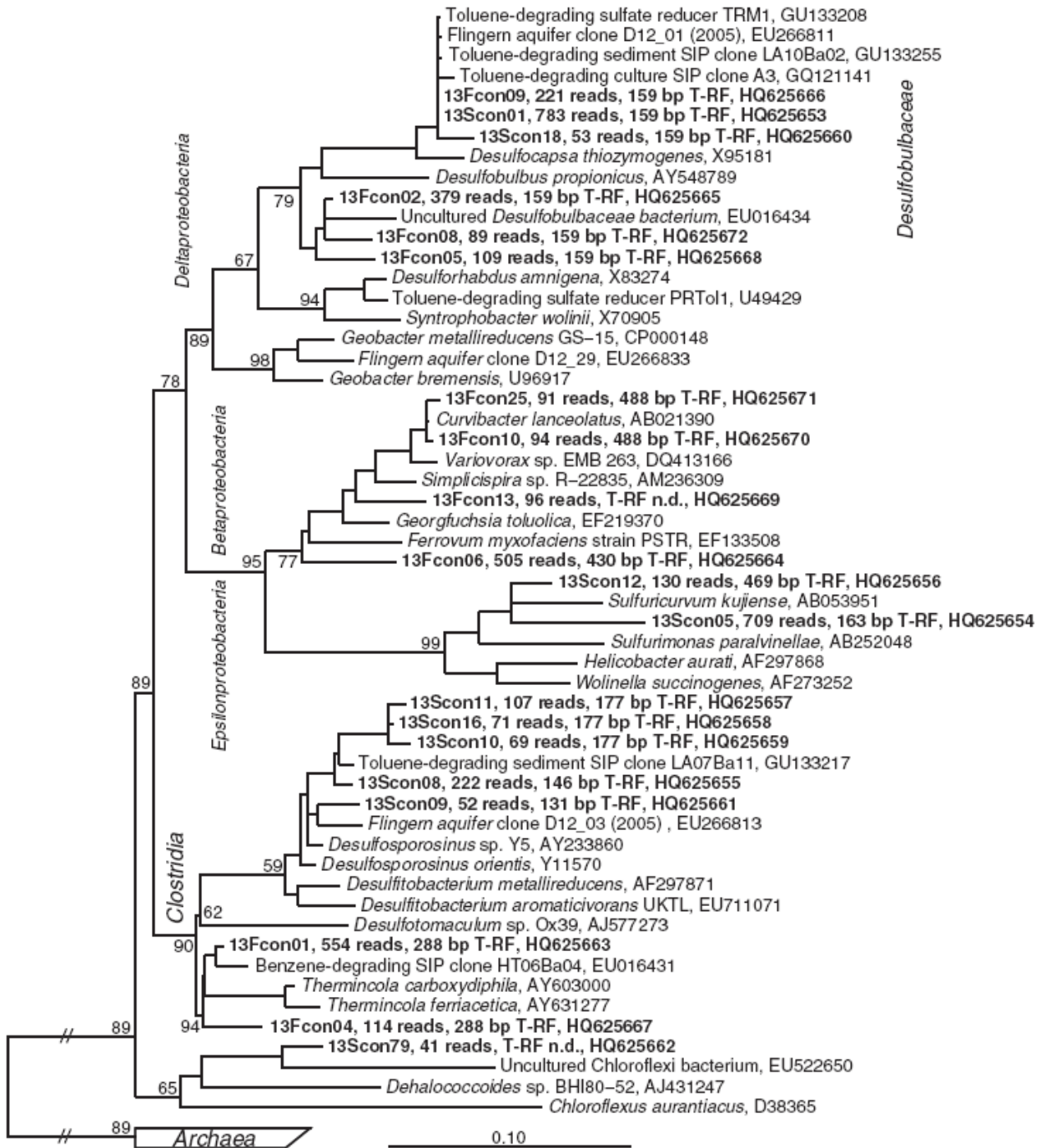


Figure 3.4: Phylogenetic affiliation of selected assembled pyrosequencing contigs (given in bold) of <sub>520</sub>-bp bacterial 16S rRNA gene amplicons from comparative SIP microcosms. Contig naming indicates treatment (e.g. 13F, 13S) as well as comprised total reads and predicted T-RFs (bp). T-RFs were predicted from sequence data, but are given as T-RFs actually measured in electropherograms and as verified in (Winderl et al., 2008). ND, no MspI restriction site in amplicon contig. The tree was reconstructed with the quartet puzzling and the subsequent addition of shorter sequences. Percentages at nodes show branching confidence values deduced from 10 000 intermediate trees. GenBank accession numbers are indicated. Scale bar, 10% sequence divergence, branch lengths to outgroup have been scaled down to 25%.

Thus, the 159, 146 and 177 bp T-RFs identified as  $^{13}\text{C}$ -labelled under sulphate amendment represented amplicons originating from members of the *Desulfobulbaceae* and *Desulfosporosinus* spp. (Table 3.2). In contrast, the 163 and 469 bp T-RFs dominating in ‘light’ fractions were affiliated to *Sulfuricurvum* spp. The 288 bp and 430 bp fragments with increased abundance in ‘heavy’ ferric iron SIP DNA represented amplicons related to *Thermincola* spp. and within the *Rhodocyclaceae*. In contrast, the 159 bp T-RF dominating in ‘light’ fractions of the same treatments was affiliated to a second cluster of unclassified *Desulfobulbaceae*, which was distinct to the labelled sequence types from the same family found under sulphate reduction.

However, the primary *Desulfobulbaceae*-related sequence type dominating in sulphate-reducing SIP microcosms was also detected in iron-reducing incubations, albeit much less abundant (Table 3.2, Fig. 3.4).

### 3.4.3 *BssA* genes detected in SIP gradient fractions

Finally, we aimed to affiliate the *bssA* genes previously detected *in situ*, tentatively named “F1-lineage” (33), to either key sulphate- or iron-reducing toluene degraders detected in SIP incubations. For this, we performed *bssA*-targeted T-RFLP fingerprinting of density-resolved DNA gradient fractions, to screen for and identify *bssA* sequence types via T-RFs. For the hitherto unidentified “F1-lineage” of *bssA* genes, *TaqI* restriction of amplicons produces a 478 bp T-RF, which was found to dominate the fractions of density-resolved DNA from sulphate- and iron-reducing SIP microcosms (Fig. 3.5). Additionally, an as-yet unidentified 248 bp T-RF was found in DNA fractions from sulphate treatments, and a further unidentified 77 bp T-RF in fractions from iron treatments.

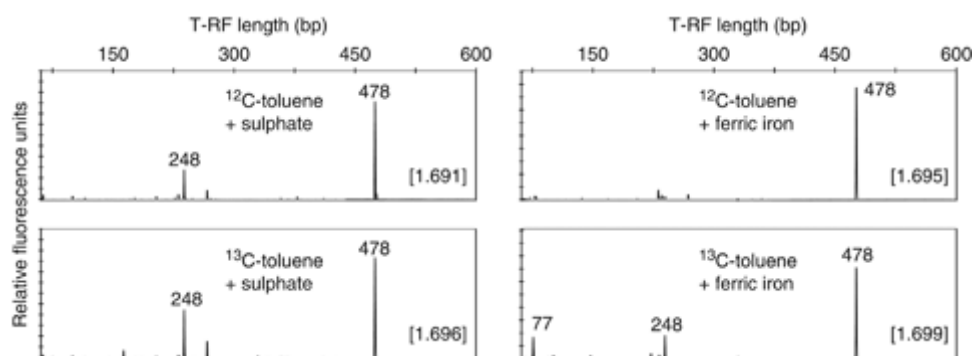


Fig. 3.5: Bacterial *bssA* gene-based T-RFLP fingerprints of representative density-resolved SIP gradient fractions after 13 weeks of incubation with unlabeled toluene and comparative electron acceptor amendment. The lengths (bp) of selected T-RFs are given. Numbers in parentheses are CsCl BDs ( $\text{g ml}^{-1}$ ) of gradient fractions.

### 3.5. Discussion

The aim of this study was to unravel whether *Desulfobulbaceae* or *Geobacteraceae*-related putative toluene degraders detected at the highly active lower fringe of a contaminant plume (31) are actually important in on-site toluene degradation, and to affiliate the previously detected “F1-lineage” of *bssA* genes (33) to one of these lineages. This objective was pursued using a novel combination of DNA-SIP and high-throughput pyrosequencing of amplicons from SIP microcosms. For the first time, this strategy was used in combination with T-RFLP fingerprinting of SIP gradient DNA to identify relevant degraders.

We used freshly sampled sediments containing a diverse *in situ* aquifer degrader community as inoculum, which contrasts our study with other recent reports, where SIP has been applied to less complex laboratory cultures of anaerobic BTEX degraders (4, 12, 16, 25). Both parallel SIP incubations required considerable lag-phases before biodegradation became noticeable, as previously observed before (32) and attributed to transfer and adaptation amongst degraders during SIP incubation. In addition, the lack of recovered  $\text{CO}_2$  and electrons from the added toluene may indicate parallel involvement of fermenters and methanogens in toluene breakdown, which cannot be excluded, but seems unlikely, since sulphate and ferric iron were added in non-limiting quantities for toluene oxidation.

Once activated, the selective role of electron acceptor availability was especially apparent for sulphate-reducing degraders, where high sulphate reduction and toluene oxidation rates were observed over a short period of time. SIP in combination with amplicon pyrosequencing revealed

that degraders within the *Desulfobulbaceae*, a lineage well known to dominate at the lower plume fringe *in situ* (3, 31), and for which cultivated toluene-degrading isolates (22) and enrichments (4) have been described, were highly represented in the ‘heavy’ DNA fractions from sulphate-reducing microcosms. Thus their central role in sulphidogenic toluene degradation *in situ* is unambiguously demonstrated. Moreover, the low abundance of *Geobacter*-related sequences (0.2%) in amplicon libraries from these incubations clearly precludes an affiliation of the “F1” *bssA* lineage to degraders within the *Geobacteraceae*. Therefore, an affiliation of the “F1” *bssA* lineage to the detected degraders within the *Desulfobulbaceae* seems warranted, even though a phylogenetically distinct *bssA* sequence type has previously been observed for other degraders within the *Desulfobulbaceae* (18, 32). This strongly indicates another example of lateral gene transfer for this catabolic marker (28, 33), which clearly limits its identification potential for unknown catabolic homologues detected in environmental gene libraries. However, this affiliation must be interpreted with caution prior to isolation of a pure culture of these new *Desulfobulbaceae*-affiliated degraders, or at least (meta-) genomic sequence data linking both markers are obtained.

A secondary population of sulphate-reducing toluene degraders identified in SIP gradients was related to *Desulfosporosinus* spp. within the *Peptococcaceae*. Although detected, but not abundant in clone libraries previously generated from *in situ* sediment samples (31), the capacity of members of this genus for anaerobic toluene degradation has already been demonstrated (18, 32). Their detection as secondary degraders in SIP suggests the possibility of functional redundancy amongst sulphate-reducing toluene degraders *in situ*.

An important unlabelled lineage detected in the sulphate-reducing microcosms was *Sulfuricurvum* spp. within the *Epsilonproteobacteria*. These microbes are normally capable of sulphide oxidation coupled to reduction of nitrate or oxygen (6, 14). Although traces of nitrate could have been present in our microcosms, they would not have sustained abundant sulphide oxidizing populations, as indicated by pyrosequencing reads. Intriguingly, similar *Epsilonproteobacteria* have recently been detected in sulphate-reducing, toluene- and benzene-degrading enrichment cultures (24), where their function also remained enigmatic (12).

In iron-reducing SIP microcosms, specific toluene degradation activities and electron recoveries appeared much lower, unsurprisingly, as added toluene was apparently not completely oxidized during incubation. The dominating labelled phylotype of iron-reducing toluene degraders detected in SIP was related to the genus *Thermincola* within the *Peptococcaceae* (288 bp T-RF). Relatives of this lineage have recently also been identified as iron-reducing benzene

degraders (16), but their involvement in toluene degradation has not been described to date. Another labelled phylotype detected in our DNA gradients was within the *Rhodocyclaceae*. Recently, a novel iron-reducing betaproteobacterial toluene degrader, *Georgfuchsia toluolica* has been isolated (30) from a BTEX-contaminated aquifer. The sequence type represented by the 430 bp T-RF clustered close to *Ferrovum myxofaciens* (11) and *G. toluolica* within the *Rhodocyclaceae*. Therefore, the diversity of iron-reducing BTEX degraders within the *Betaproteobacteria* may also be larger than previously recognised.

Since the signatures of both *Georgfuchsia*- and *Thermincola*-related degraders (the 430 and 288 bp T-RFs) were hardly detectable in the respective aquifer sediments (31), this illustrates their enrichment as iron-reducing toluene degraders during our SIP incubation. In contrast, the *Geobacteraceae* shown to be dominant *in situ* (3, 31), and which were also abundant (~15% relative T-RF abundance at the lower plume fringe) in the samples used for SIP incubation (data not shown), do not appear directly involved in on-site toluene breakdown. Likely, these abundant *Geobacteraceae* catabolise some of the other electron donors potentially provided by the plume (e.g. hydrocarbons other than toluene, fatty acids). Also at the BTEX-contaminated aquifer from which *G. toluolica* was isolated (30), members of the *Geobacteraceae* are widespread and abundant, but not directly involved in toluene breakdown {Staats, 2011 #54}.

If *Geobacter* populations are not involved in toluene oxidation *in situ*, this again supports linking the “F1-lineage” of *bssA* genes (31) to the *Desulfobulbaceae* as key toluene degraders in the Flingern sediments. As mentioned above, these *Desulfobulbaceae*-related degraders were also found (albeit unlabelled) in the iron-reducing incubations. Therefore, detection of the “F1-lineage” sequence type in both DNA gradients seems warranted. At the same time, no known *bssA* sequence types were inferable from DNA gradients for the clostridial and betaproteobacterial toluene-degraders detected in surplus. Here, we cannot be sure that the primer pair utilized for *bssA*-fingerprinting is actually capable of detecting all relevant fumarate-adding gene lineages potentially present in our SIP microcosms. Although the primer set has been demonstrated to detect readily the *bssA* of most known iron- and sulphate-reducing toluene degraders (33), primer development and optimization for the detection of fumarate-adding catabolic genes is still an ongoing process.

In summary, our results unambiguously reveal the central role of *Desulfobulbaceae* for toluene degradation at the lower plume fringe at the Flingern contaminated aquifer. Second, we substantiate the absence of true iron-reducing toluene-degrading populations in the same zone, since only degraders not previously detected or abundant *in situ* were identified in SIP.

Interestingly, secondary toluene degraders within the *Peptococcaceae* detected under both sulphate- and iron-reducing conditions give rise to speculations about niche differentiation or functional redundancy amongst degradative potentials on site.

Finally, we show that new technologies such as amplicon pyrosequencing can be of substantial benefit for the assignment of catabolic capacities to defined lineages in SIP. Hence, amplicon pyrosequencing in combination with fingerprinting of density-resolved nucleic acids was established as a powerful new strategy in SIP gradient interpretation.

### 3.6. References

1. **Anderson, R. T., and D. R. Lovley.** 1997. Ecology and biogeochemistry of in situ groundwater bioremediation, p. 289-350, *Advances in Microbial Ecology*, PLENUM PRESS DIV PLENUM PUBLISHING CORP ed, vol. 15.
2. **Anneser, B., F. Einsiedl, R. U. Meckenstock, L. Richters, F. Wisotzky, and C. Griebler.** 2008. High-resolution monitoring of biogeochemical gradients in a tar oil-contaminated aquifer. *Applied Geochemistry* **23**:1715-1730.
3. **Anneser, B., G. Pilloni, A. Bayer, T. Lueders, C. Griebler, F. Einsiedl, and L. Richters.** 2010. High Resolution Analysis of Contaminated Aquifer Sediments and Groundwater-What Can be Learned in Terms of Natural Attenuation? *Geomicrobiology Journal* **27**:130 - 142.
4. **Bombach, P., A. Chatzinotas, T. R. Neu, M. Kästner, T. Lueders, and C. Vogt.** 2010. Enrichment and characterization of a sulfate-reducing toluene-degrading microbial consortium by combining *in situ* microcosms and stable isotope probing techniques. *FEMS Microbiol. Ecol.* **71**:237-246.
5. **Bosch, J., A. Fritzsche, K. U. Totsche, and R. U. Meckenstock.** 2010. Nanosized Ferrihydrite Colloids Facilitate Microbial Iron Reduction under Flow Conditions. *Geomicrobiology Journal* **27**:123 - 129.
6. **Campbell, B. J., A. S. Engel, M. L. Porter, and K. Takai.** 2006. The versatile epsilon-proteobacteria: key players in sulphidic habitats. *Nat Rev Micro* **4**:458-468.
7. **Christensen, T. H., P. L. Bjerg, S. A. Banwart, R. Jakobsen, G. Heron, and H.-J. Albrechtsen.** 2000. Characterization of redox conditions in groundwater contaminant plumes. *Journal of Contaminant Hydrology* **45**:165-241.
8. **DeSantis, T. Z., P. Hugenholtz, N. Larsen, M. Rojas, E. L. Brodie, K. Keller, T. Huber, D. Dalevi, P. Hu, and G. L. Andersen.** 2006. Greengenes, a Chimera-Checked 16S rRNA Gene Database and Workbench Compatible with ARB. *Appl. Environ. Microbiol.* **72**:5069-5072.
9. **Edgar, R., M. Domrachev, and A. E. Lash.** 2002. Gene Expression Omnibus: NCBI gene expression and hybridization array data repository. *Nucleic Acids Research* **30**:207-210.

10. **Hall, T. A.** 1999. BioEdit: a user-friendly biological sequence alignment editor and analysis program for Windows 95/98/NT. *Nucl. Acids. Symp. Ser.* **41**:95-98.
11. **Hallberg, K. B., K. Coupland, S. Kimura, and D. B. Johnson.** 2006. Macroscopic Streamer Growths in Acidic, Metal-Rich Mine Waters in North Wales Consist of Novel and Remarkably Simple Bacterial Communities. *Appl. Environ. Microbiol.* **72**:2022-2030.
12. **Herrmann, S., S. Kleinsteuber, A. Chatzinotas, S. Kuppardt, T. Lueders, H. H. Richnow, and C. Vogt.** 2010. Functional characterization of an anaerobic benzene-degrading enrichment culture by DNA stable isotope probing. *Environmental Microbiology* **12**:401-411.
13. **Kane, S. R., H. R. Beller, T. C. Legler, and R. T. Anderson.** 2002. Biochemical and genetic evidence of benzylsuccinate synthase in toluene-degrading, ferric iron-reducing *Geobacter metallireducens*. *Biodegradation* **13**:149-54.
14. **Kodama, Y., and K. Watanabe.** 2004. *Sulfuricurvum kujiense* gen. nov., sp. nov., a facultatively anaerobic, chemolithoautotrophic, sulfur-oxidizing bacterium isolated from an underground crude-oil storage cavity. *Int J Syst Evol Microbiol* **54**:2297-2300.
15. **Kunapuli, U., M. K. Jahn, T. Lueders, R. Geyer, H. J. Heipieper, and R. U. Meckenstock.** 2010. *Desulfitobacterium aromaticivorans* sp. nov. and *Geobacter toluenoxydans* sp. nov., iron-reducing bacteria capable of anaerobic degradation of monoaromatic hydrocarbons. *Int J Syst Evol Microbiol* **60**:686-695.
16. **Kunapuli, U., T. Lueders, and R. U. Meckenstock.** 2007. The use of stable isotope probing to identify key iron-reducing microorganisms involved in anaerobic benzene degradation. *ISME J.*
17. **Lane, D. J.** 1991. 16S/23S rRNA sequencing. E. Stackebrandt and M. Goodfellow (ed.), *Nucleic acid techniques in bacterial systematics*. John Wiley & Sons, New York, N.Y.
18. **Liu, A., E. Garcia-Dominguez, E. D. Rhine, and L. Y. Young.** 2004. A novel arsenate respiring isolate that can utilize aromatic substrates. *FEMS Microbiol. Ecol.* **48**:323-332.
19. **Lovley, D. R., and E. J. P. Phillips.** 1986. Organic Matter Mineralization with Reduction of Ferric Iron in Anaerobic Sediments. *Appl. Environ. Microbiol.* **51**:683-689.
20. **Ludwig, W., O. Strunk, R. Westram, L. Richter, H. Meier, Yadhukumar, A. Buchner, T. Lai, S. Steppi, G. Jobb, W. Forster, I. Brettske, S. Gerber, A. W. Ginhart, O. Gross, S. Grumann, S. Hermann, R. Jost, A. Konig, T. Liss, R. Lussmann, M. May, B. Nonhoff, B. Reichel, R. Strehlow, A. Stamatakis, N. Stuckmann, A. Vilbig, M. Lenke, T. Ludwig, A. Bode, and K.-H. Schleifer.** 2004. ARB: a software environment for sequence data. *Nucl. Acids Res.* **32**:1363-1371.
21. **Lueders, T.** 2010. Stable isotope probing of hydrocarbon-degraders, p. 4011-4026. *In* K. N. Timmis (ed.), *Handbook of Hydrocarbon and Lipid Microbiology*, vol. 5. Springer, Berlin, Heidelberg.
22. **Meckenstock, R. U.** 1999. Fermentative toluene degradation in anaerobic defined syntrophic cocultures. *FEMS Microbiology Letters* **177**:67-73.
23. **Miller, S. R., A. L. Strong, K. L. Jones, and M. C. Ungerer.** 2009. Bar-Coded Pyrosequencing Reveals Shared Bacterial Community Properties along the Temperature Gradients of Two Alkaline Hot Springs in Yellowstone National Park. *Appl. Environ. Microbiol.* **75**:4565-4572.
24. **Müller, S., C. Vogt, M. Laube, H. Harms, and S. Kleinsteuber.** 2009. Community dynamics within a bacterial consortium during growth on toluene under sulfate-reducing conditions. *FEMS Microbiology Ecology* **70**:586-596.



25. **Oka, A. R., C. D. Phelps, L. M. McGuinness, A. Mumford, L. Y. Young, and L. J. Kerkhof.** 2008. Identification of critical members in a sulfidogenic benzene-degrading consortium by DNA stable isotope probing. *Appl. Environ. Microbiol.* **74**:6476-6480.
26. **Quince, C., A. Lanzen, T. P. Curtis, R. J. Davenport, N. Hall, I. M. Head, L. F. Read, and W. T. Sloan.** 2009. Accurate determination of microbial diversity from 454 pyrosequencing data. *Nat Meth* **6**:639-641.
27. **Shinoda, Y., J. Akagi, Y. Uchihashi, A. Hiraishi, H. Yukawa, H. Yurimoto, Y. Sakai, and N. Kato.** 2005. Anaerobic degradation of aromatic compounds by *Magnetospirillum* strains: Isolation and degradation genes. *Bioscience Biotechnology and Biochemistry* **69**:1483-1491.
28. **Shinoda, Y., J. Akagi, Y. Uchihashi, A. Hiraishi, H. Yukawa, H. Yurimoto, Y. Sakai, and N. Kato.** 2005. Anaerobic degradation of aromatic compounds by *Magnetospirillum* strains: Isolation and degradation genes. *Biosci. Biotechnol. Biochem.* **69**:1483-1491.
29. **Wang, Q., G. M. Garrity, J. M. Tiedje, and J. R. Cole.** 2007. Naive Bayesian Classifier for Rapid Assignment of rRNA Sequences into the New Bacterial Taxonomy. *Appl. Environ. Microbiol.* **73**:5261-5267.
30. **Weelink, S. A. B., W. Van Doesburg, F. T. Saia, W. I. C. Rijpstra, W. F. M. Röling, H. Smidt, and A. J. M. Stams.** 2009. A strictly anaerobic betaproteobacterium *Georgfuchsia toluolica* gen. nov., sp. nov. degrades aromatic compounds with Fe(III), Mn(IV) or nitrate as an electron acceptor. *FEMS Microbiology Ecology* **70**:575-585.
31. **Winderl, C., B. Anneser, C. Griebler, R. U. Meckenstock, and T. Lueders.** 2008. Depth-Resolved Quantification of Anaerobic Toluene Degraders and Aquifer Microbial Community Patterns in Distinct Redox Zones of a Tar Oil Contaminant Plume. *Appl. Environ. Microbiol.* **74**:792-801.
32. **Winderl, C., H. Penning, F. von Netzer, R. U. Meckenstock, and T. Lueders.** 2010. DNA-SIP identifies sulfate-reducing Clostridia as important toluene degraders in tar-oil-contaminated aquifer sediment. *ISME J.*
33. **Winderl, C., S. Schaefer, and T. Lueders.** 2007. Detection of anaerobic toluene and hydrocarbon degraders in contaminated aquifers using benzylsuccinate synthase (bssA) genes as a functional marker. *Environmental Microbiology* **9**:1035-1046.

## 4. Disturbance ecology controls natural attenuation in contaminated aquifers

G. Pilloni<sup>1</sup>, A. Bayer<sup>1</sup>, B. Anneser<sup>1</sup>, M. Engel<sup>2</sup>, C. Griebler<sup>1</sup> and T. Lueders<sup>1</sup>

<sup>1</sup> Institute of Groundwater Ecology and <sup>2</sup> Department of Terrestrial Ecogenetics, Institute of Soil Ecology, Helmholtz Zentrum München- *German Research Center for Environmental Health*, Neuherberg, Germany.

Submitted to *Science*; now in preparation for re-submission to *Nature Geoscience*.

### 4.1. Abstract

Aquifers provide important ecosystem services, but their ecology is poorly understood. Especially, aquifers are perceived as stable environments, characterized by low reactivity and dynamics even after contamination. Here, we unravel how anaerobic hydrocarbon degraders in a contaminant plume unexpectedly react to hydraulic disturbance. Repetitive depth-resolved hydrogeochemical monitoring over four years showed an upshift of the plume and a transient collapse of biodegradation after pronounced dynamics of the groundwater table. Parallel degrader community analyses including pyrosequencing of bacterial rRNA genes revealed that after the collapse, an initial deltaproteobacterial degrader population was replaced by distinct clostridial degraders. Thus, functional redundancy “insured” natural attenuation against hydraulic disturbance. These findings highlight that aquifers are not steady-state, and call for a new understanding of the controls of hydraulic disturbance on microbes in groundwater ecosystems.

### 4.2. Introduction

The structure and function of microbial communities in both natural and anthropogenically impacted environments is governed by general ecological laws, yet a basic understanding of these principles is only beginning to gain momentum (12, 28). For groundwater, it is still unclear

whether the effects of anthropogenic or natural perturbation can be interpreted or predicted via concepts of disturbance ecology (20). Aquifers are generally considered as low-productivity and extremely stable environments (17), thus ecosystem disturbance might have much more pronounced effects on intrinsic biota and processes than in other, more productive and dynamic habitats (14).

A sound understanding of the ecological principles controlling microbial populations in aquifers is especially important in contaminated systems, where fastidious anaerobic microbes fulfill central ecosystem functions (6). At a heavily tar-oil contaminated aquifer in Germany, we have previously identified a highly active fringe zone underneath a stationary hydrocarbon plume (mainly toluene), where a distinct and highly specialized community of contaminant degraders had established (2, 33). This verified the concept that active degraders are not uniformly distributed within contaminant plumes, but develop at biogeochemical gradient zones where transverse dispersive mixing provides a constant supply of electron donors and acceptors (3). This local establishment of degrader populations can be regarded as a key factor contributing to the recovery of groundwater ecosystems upon contamination. Hypothesizing that such locally selected degrader populations may even be a prerequisite for effective biodegradation (33), the effects of added ecosystem disturbance on natural attenuation can now be tested. It is established (for other systems) that while such specialized communities with few dominating taxa (low diversity and evenness) can be highly effective in driving a given process, they are also especially prone to collapse and loose functionality under ecosystem stress (36).

Maybe the most important natural disturbance affecting contaminant plumes is hydraulically driven fluctuations of the groundwater table (GWT) (11). Hydrodynamics have been previously hypothesized to positively affect net reactive capacities in porous media by increasing the mixing (30). However, in contrast, disturbance ecology predicts a negative effect on net biodegradation, if locally established degrader populations cannot cope with such plume dynamics. Currently, although a small number of reports on microbial population variability in aquifers is available (15, 38), the effects of hydrodynamics on dedicated degrader populations have been completely neglected. Here, we close this prominent research gap and reveal unexpected effects of hydraulic disturbance on *in situ* populations of anaerobic hydrocarbon degraders.

### **4.3. Materials and Methods**

#### **4.3.1 Samples acquisition**

Groundwater and aquifer sediment samples were collected at Düsseldorf – Flingern aquifer (details in section 1.4) in February 2006, September 2008 and June 2009. Sediment samples taken with a direct-push drilling rig (Geoprobe, Salina, KS, USA) were frozen on-site, directly after retrieval of sub-cores from intact sediment liners, and transported to the lab. Sediments were analyzed in a range of approximately 5.5 to 10.5 m below ground surface (bgs), starting from the groundwater table (GWT) and over all major plume compartments (2, 33).

#### **4.3.2 Geochemical analyses of groundwater samples**

Water samples collected in February 2006 (2), September 2008 and June 2009 from a high-resolution multilevel well were monitored for geochemical parameters such as the distribution of contaminants and redox species as described earlier (1). Analysis of toluene-specific  $^{13}\text{C}/^{12}\text{C}$  isotope ratios were performed on NaOH-preserved samples and measured with gas chromatography-combustion-isotope ratio mass spectrometry (GC-C-IRMS, Thermo Fisher Scientific, Bremen, Germany) via purge & trap as previously described (19), with the gas chromatographic separation adapted to BTEX compounds. A DB624-column (Supelco, Bellefonte, Pennsylvania, USA) and an optimized temperature program (3.07 min at 60°C, 8.1°C/min to 129°C, 1°C/min to 134°C, 20°C/min to 180°C, 50°C/min to 230°C, hold 5 min) were used. The standard deviation for our isotopic measurements was much lower (Table A.1) than the total instrumental uncertainty of carbon isotope measurements and was therefore set to 0.5‰ as recommended by (31).

#### **4.3.3 DNA extraction**

DNA was extracted from ~0.8 g aliquots of sediment in 2 ml screw-cap vials containing ~0.2 ml of sterile zirconia-silica beads (a 1:1 mix of 0.1- and 0.7-mm diameter; Roth). Samples were suspended in 650 µl PTN buffer (120 mM Na<sub>2</sub>HPO<sub>4</sub>, 125 mM Tris, 0.25 mM NaCl [pH 8]) and incubated at 37°C for 15 min with 40 µl lysozyme (50 mg/ml) and 10 µl proteinase K (10 mg/ml). After the addition of 150 µl 20% SDS, incubation was continued with shaking (500

rpm) for 15 min at 65°C. Subsequently, the sediments were bead beaten (45 s at 6.5 m/s) Afterwards nucleic acids were sequentially purified by extraction with 1 volume of phenol-chloroform-isoamyl alcohol (25:24:1) and 1 volume of chloroform-isoamyl alcohol (24:1) and precipitated with 2 volumes of 30% polyethylene glycol by incubation at 4°C for 2 h and by centrifugation at 20,000 g and 20°C for 30 min. All reagents were from Sigma, if not otherwise stated. For each single extract, two replicate extractions were pooled in 50 µl of elution buffer (Qiagen) and stored frozen (-20°C) for downstream analyses.

#### **4.3.4 Microbial community fingerprinting**

Terminal restriction fragment length polymorphism (T-RFLP) analysis of bacterial 16S rRNA gene amplicons was performed with primers Ba27f-FAM and 907r and MspI digestion as previously described (33). Purified (Quiagen-Min Elute) amplicons were UV-quantified (Nanodrop) and about 40 ng were restricted and after, Dye-ex (Quiagen) desalting of the digested products, the fragments were subjected to capillary electrophoresis on a 3730 DNA Analyzer (Applied Biosystems). Primary electropherogram evaluation was performed using Gene-Mapper 5.1 software (Applied Biosystems). T-RF frequencies were inferred from peak heights. Signals with a peak height below 100 relative fluorescence units or with a peak abundance contribution below 1% were considered background noise and excluded from further analysis.

#### **4.3.5 Quantification of genetic signatures (qPCR)**

Real-time quantitative PCR (qPCR) measurements were performed on a MX3000P qPCR cyclor (Stratagene). For every year of sampling and each sediment depth, the three independent DNA extracts from sediment subsamples were quantified in three different dilutions to account for the possibility of PCR inhibition in less diluted templates.

Total bacterial 16S rRNA gene quantities were measured using a Sybr green PCR approach. We used standard *Taq* polymerase (Fermentas) assays in the presence of 0.1 X Sybr green (FMC Bio Products) and 2 µl DNA template. Initial denaturation (94°C, 3 min) was followed by 50 cycles of denaturation (94°C, 15 s), annealing (52°C, 15 s), and elongation (70°C, 30 s). Subsequently, a melting curve was recorded between 55°C and 94°C to discriminate between specific and unspecific amplification products. An almost-full-length

bacterial 16S rRNA gene amplicon of *Azoarcus* sp. strain T genomic DNA was quantified using the PicoGreen double-stranded DNA quantification kit (Molecular Probes) and utilized as standard DNA for qPCR in a concentration range between  $10^7$  and  $10^1$  copies/ $\mu$ l.

For *bssA* qPCR, a TaqMan system for the previously described “F1” cluster of unidentified *bssA* genes was used (33). *bssA* qPCR was performed with the TaqMan universal master mix kit (Applied Biosystems), as specified by the manufacturer, using three-step thermal cycling (95°C, 10 min; and 50 cycles of 95°C, 15 s; 55°C, 20 s; and 72°C, 30 s). Standardization in concentrations between  $10^7$  and  $10^1$  copies/ $\mu$ l was determined as previously described (33).

#### **4.3.6 16S rRNA amplicons ultra-deep pyrosequencing**

Selected bacterial 16S rRNA gene amplicon pools from five depths ranging between 6.4 and 8.4 m bgs were chosen for each year based on T-RFLP screening distinctness, and subjected to amplicon pyrosequencing (26, 29). Barcoded amplicons for multiplexing were prepared with the primers Ba27f (5'-aga gtt tga tcm tgg ctc ag-3') and Ba519r (5'-tat tac cgc ggc kgc tg-3') (21) extended as amplicon fusion primers with respective primer A or B adapters, key sequence and multiplex identifiers (MID) as recommended by 454/Roche (Penzberg, Germany). Amplicons were purified and pooled as specified by the manufacturer. Emulsion PCR (emPCR), purification of DNA-enriched beads and sequencing run were performed following protocols and using a 2<sup>nd</sup> generation pyrosequencer (454 GS FLX Titanium, Roche) as recommended by the developer. Quality filtering of the pyrosequencing reads was performed using the automatic amplicon pipeline of the GS Run Processor (Roche), with a slight modification concerning the valley filter (vfScanAllFlows false instead of TiOnly) to extract the sequences.

Afterwards, reads were further trimmed for quality using the Trim function of Greengenes (9), with the following setting: good quality score 20, window size 40 bp, window threshold 90%. Subsequently, reads were batched per sample based on MID-identifiers with BioEdit (16), and reads with inferior read length (<250 bp) were excluded from further analysis. Total community composition was classified via read affiliation using the RDP classifier (32) at a confidence threshold of 80%. Read abundance percentage of classified lineages was recorded. The RDP pyrosequencing pipeline (7) was also used for inferring total diversity and evenness indicators for quality trimmed read populations.

For downstream analysis of sequenced amplicon pools (UniFrac clustering, T-RF prediction, phylogenetic inference), matching sequences from forward- and reverse-reads were assembled

into contigs with the SeqMan II software (DNASTar) using assembly thresholds of at least 98% sequence similarity over a 50 bp match window. Contigs containing less than one forward or reverse read were not considered for further analyses, therefore our UniFrac clustering does not include information from extremely rare taxa or erratic sequence reads.

Contigs were aligned using the Align function of Greengenes (9) with standard settings, but a minimum match requirement of 250 bp. The resulting alignment was then subjected to UniFrac clustering for weighted similarity analysis of total bacterial communities as described in the respective web resource (23). For this, taxa were again normalized by the abundance of reads contributing to each contig. Finally, selected dominating assembled amplicon contigs were integrated into an ARB database (24) and used for T-RF prediction and the reconstruction of phylogenetic trees as described (33, 35).

Thus, for the first time, our newly established bidirectional amplicon pyrosequencing approach allows for a comprehensive and elaborate evaluation of pyrosequencing results up to the phylogenetic placement of representative assembled dominating amplicon sequences. Both all raw and trimmed reads generated in this study have been deposited in NCBI's Gene Expression Omnibus (10) and are accessible through GEO Series accession number GSE25345. The selected amplicon contigs have been deposited to NCBI's GenBank under the accession numbers from HQ596373 to HQ596401.

#### 4.4. Results and Discussion

During our four-year field sampling campaign, substantial dynamics of the GWT were observed at the site. Especially, a pronounced drop of the water table of almost 40 cm after July 06 was followed by a constant uprise of almost 60 cm until March 09 (Fig. 4.1).



Fig. 4.1: On-site fluctuations of the GW-table during the period of investigation as measured by a water table logging in a monitoring well closely adjacent to the location of high-resolution water and sediment sampling. The 4 time points of sediment and groundwater sampling are indicated. Field data from Sep. 05 has been reported in (33).

High-resolution depth-resolved monitoring revealed marked hydrogeochemical dynamics in parallel (Fig. 4.2 A-C). Most importantly, in Sep. 08, after the pronounced down- and upshift of the GWT, maximum toluene concentrations in the plume core surprisingly doubled, and plume localization clearly moved upward (Fig. 4.2A). In 2009, localization of the plume was still similar, but toluene concentrations in the core had then dropped again, by >80% compared to 2008.



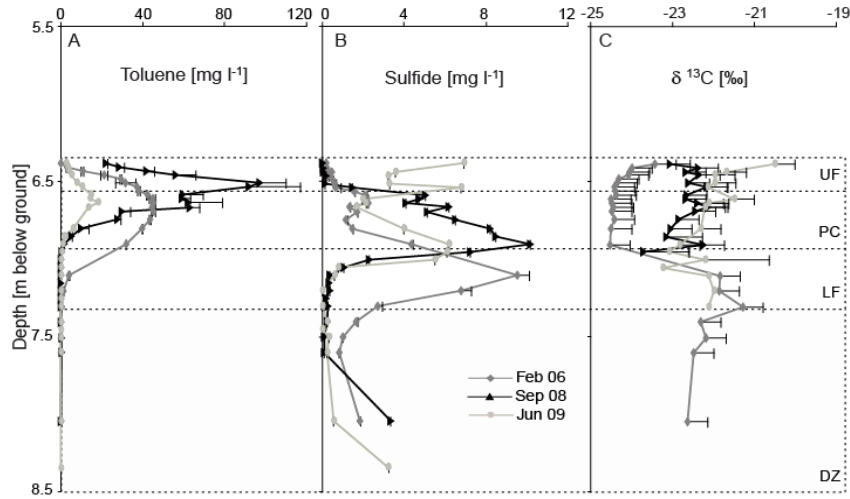


Fig. 4.2: Depth profiles of toluene (A) and sulphide concentrations (B), and toluene stable isotope ratios (C) in groundwater of the Flingern aquifer at three successive time points. Error bars indicate standard deviation (positive only) of duplicate measurements. Plume compartments were defined as in (33) and are averaged over the successive years; the dynamics of the GWT of  $\pm 0.3$  m are not illustrated here, but are shown in Fig. 3.1. Abbreviations are as follows: UF – upper plume fringe; PC – plume core; LF – lower plume fringe; DZ – deeper zone.

This pronounced reduction cannot be interpreted as a mere effect of changing hydraulics (i.e. dilution), since the concentrations of other detected contaminants (e.g. benzene, naphthalene) remained constant or even increased between 2008 and 09.

Rather, these dynamics appeared connected to changes in biodegradation, which was further strengthened by the dynamics of contaminant stable isotope ratios. In 2006, the  $\delta^{13}\text{C}$ -values of toluene (Fig. 4.2C) showed characteristic enrichment towards the lower plume fringes. This corroborated toluene depletion in this zone by active biodegradation (25), which was consistent also with peaks of sulphide concentrations in corresponding depths (Fig. 4.2B). In Sep. 08, however, isotope fractionation at the plume fringes was no longer apparent, indicative of a collapse of biodegradation connected to the plume shift. At the same time, total average  $\delta^{13}\text{C}$ -isotope ratios of toluene over depth increased by  $\sim 2\%$ . This points towards the intrusion of a secondary contaminant source with distinct isotopic signature (4), likely connected to the rise of the GWT, but cannot be linked to dynamics of biodegradation. In 2009, toluene stable isotope fractionation patterns indicative of biodegradation had reestablished, especially at the upper plume fringe.

Connected to these pronounced spatial and temporal dynamics of plume biogeochemistry, we uncovered marked fluctuations for intrinsic bacterial communities. Multivariate statistics of

bacterial T-RFLP fingerprints showed a characteristic community pattern especially at the lower plume fringe, but also a reduction of the distinctness of this pattern in 2009 (Fig. 4.3).

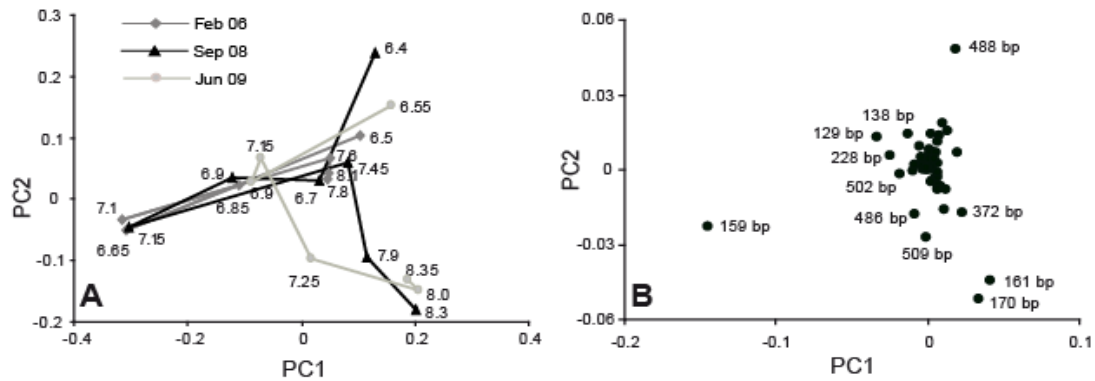


Fig. 4.3: Principal component ordination of the overall variance in depth-resolved bacterial community composition as analyzed by T-RFLP fingerprinting (A). Depths at which fingerprints were retrieved are given next to the ordination points. Ordination was averaged over three replicate fingerprints per data point. Inferred PC factors 1 and 2 accounted for 37.9% and 15% of total variance, respectively. (B) Loading plot of inferred PC factors on specific T-RFs. The identities (bp) of selected T-RFs with characteristic factor loading are given. Multivariate statistics as described previously (33).

Congruent to our previous observations for 2005, these communities were dominated especially by the 159 bp T-RF, but also the 129 and 228 bp fragments, identified to represent members of the *Desulfobulbaceae*, *Geobacteraceae*, and *Peptococcaceae*, respectively (33). This was especially apparent when comparing the relative abundance of these three T-RFs over depth and years (Fig. 4.4). However, while the 129 bp peak (*Geobacteraceae*) was relatively stable in abundance at the lower fringe over time (Fig. 4.4A), the 159 bp T-RF (*Desulfobulbaceae*) was strongly reduced in June 09 (Fig. 4.4B), while the 228 bp T-RF (*Peptococcaceae*) significantly increased in contrast (Fig. 4.4C).

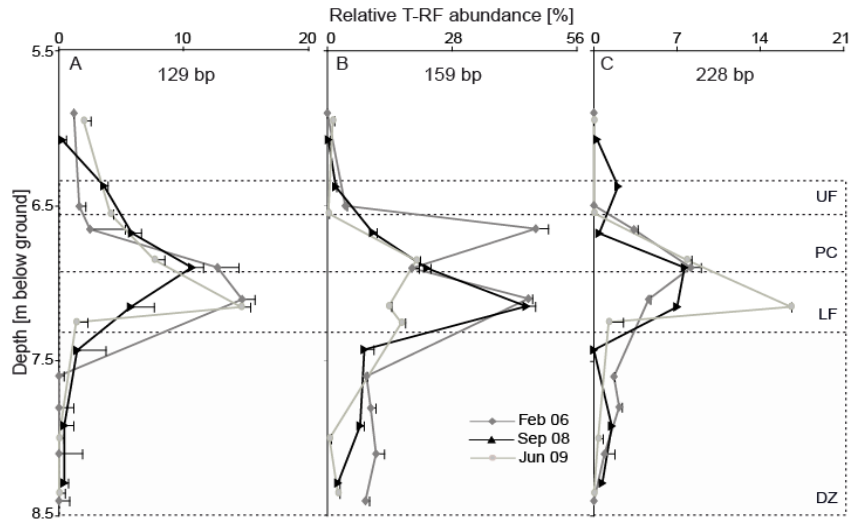


Fig. 4.4: Relative abundance of selected T-RFs characteristic for the sulfidogenic zone degrader community over depth. The T-RFs represent populations of (A) 129 bp - *Geobacter* spp.; (B) 159 bp - *Desulfobulbaceae*; and (C) 228 bp - *Peptococcaceae* detected at the site (33). Error bars indicate standard error (positive only) for averages of triplicate DNA-extracts fingerprints.

These qualitative dynamics of community patterns were flanked by even more pronounced quantitative dynamics of sedimentary total bacterial rRNA gene counts, and of site-specific anaerobic toluene degradation genes measured via a previously published qPCR assay for deltaproteobacterial benzylsuccinate synthase  $\alpha$ -subunit (*bssA*) genes (33). The importance of the lower plume fringe for toluene degradation was clearly demonstrated by the fact that this zone always carried high absolute, and highest relative amounts of degradation genes (Fig. 4.5).

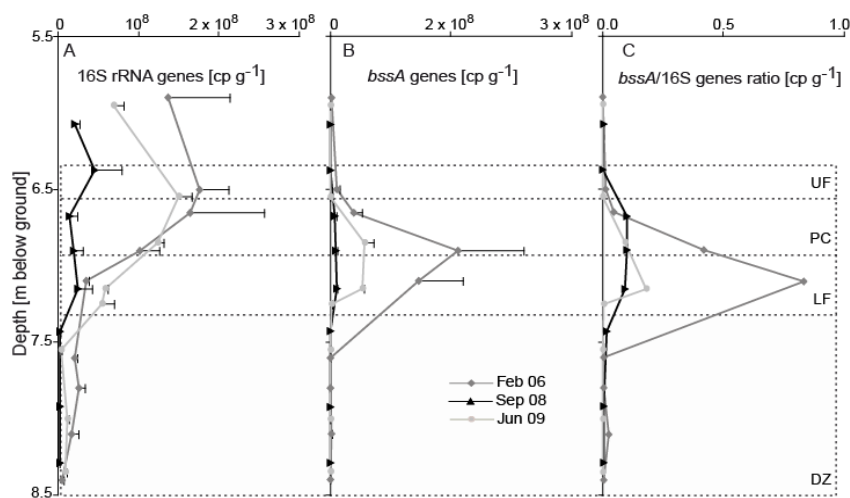


Fig. 4.5: Depth-resolved quantitative distribution of bacterial 16S rRNA genes (A) and *bssA* genes (B) of on-site anaerobic toluene degraders. (C): ratio of *bssA* vs. 16S rRNA genes over depth. Shown are average gene  $\text{cp g}^{-1}$  sediment (wet weight) plus standard error (positive only) of qPCR measurements from triplicate DNA extracts.

However, compared to the high maximum catabolic gene counts of  $>10^7$  per g of sediment observed for this zone in 2005 (33) and 06 (Fig. 4.5B), a dramatic quantitative collapse of these gene populations of  $\sim 99\%$  was observed in 2008. At the same time, compared to 2006, 16S rRNA gene counts dropped to  $\sim 10\text{-}20\%$  over large parts of the plume in 2008. In 2009 the previous 16S rRNA gene depth profile had mostly recovered, while *bssA* gene counts recovered to only  $\sim 30\%$ .

To provide even more comprehensive insights into these unexpected aquifer ecosystem dynamics, we used massively parallel pyrosequencing of bacterial rRNA gene amplicons. Barcoded pyrosequencing is particularly appropriate to provide superior detail on the diversity and structure of natural microbial populations (8, 13). However it has not been applied to aquifer ecosystems to date. Here, we established bidirectional sequencing of bacterial rRNA gene amplicons ( $\sim 520$  bp) with second-generation pyrosequencing technology. We sequenced 15 amplicon pools from 5 depths over different plume compartments taken in 2006, 08 and 09. More than 135,000 pyrosequencing reads (Tab. 4.1) with an average length of  $\sim 350$  bp (after stringent quality trimming), were obtained and used for community characterization.

Tab. 4.1: Number of reads and average read lengths produced in bidirectional pyrosequencing of  $\sim 520$  bp bacterial 16S rRNA gene fragments retrieved in time- and depth-resolved sampling of the Flingern aquifer.

Sediment samples	Feb. 2006					Sep. 2008					June 2009				
Depth [m]	6.5	6.65	6.9	7.1	8.1	6.4	6.7	6.9	7.15	8.3	6.55	6.85	7.15	7.25	8.35
Plume zone <sup>1</sup>	UF	PC	LF	LF	DZ	UF	PC	LF	LF	DZ	UF	PC/LF	LF	LF/DZ	DZ
Total reads, for	7911	2306	3116	2588	3015	3543	3857	3202	3898	3991	3611	4097	1951	3588	1786
Total reads, rev	16072	2387	3165	5119	6294	3551	7581	3199	7687	7190	7202	3812	3966	3551	3554
Av. length total reads	475	510	507	494	486	495	490	503	494	490	481	501	495	498	492
Trimmed reads, f >250 bp	5558	1892	2522	1944	2104	2880	2772	2557	2787	2908	2579	2402	1335	2067	1299
Trimmed reads, r >250 bp	13342	2109	2777	4336	5283	3175	6313	2083	6431	6052	6154	2485	3239	2265	3071
Av. length trimmed reads	350	371	360	337	339	365	346	364	336	336	346	359	339	357	336
Amplicon contigs <sup>2</sup>	3535	365	419	822	1479	571	1414	490	1022	1576	1390	916	786	1044	578

<sup>1</sup> Plume compartments are defined as in Fig. 4.2.

<sup>2</sup> Criteria for the assembly of full-length ( $\sim 520$  bp) amplicon contigs are described above (par. 4.3.6).

A first screening of total bacterial community variability via UniFrac (23) revealed three major clusters of samples, largely discriminating between populations from the upper plume fringe, the plume core and lower plume fringe, and samples from the deeper zone (Fig. 4.6).

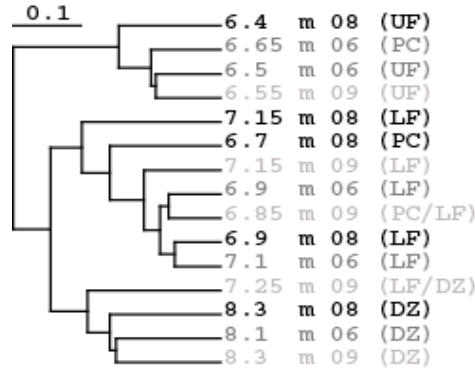


Fig. 4.6: UniFrac clustering (23) of community similarity over depth at three successive time points of sampling. Sample depth, year, and plume compartment are indicated. The scale bar indicates 10% community divergence.

The diversity and evenness of sequenced amplicon pools was clearly reduced in plume core and lower fringe samples in 2006 and 08 (Fig. 4.7). Also for T-RF diversity, absolute minima were reached at the lower fringe for these years (Fig. 4.7A), as observed before in 2005 (33). In contrast, both diversity and evenness indices were more evenly distributed over depth in 2009.

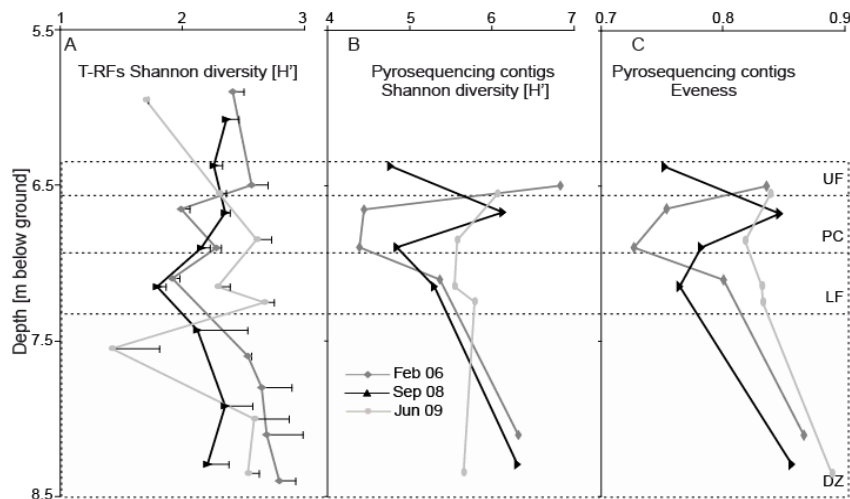


Fig. 4.7: Depth-resolved shifts in diversity of (A) bacterial T-RFLP fingerprints and (B) pyrosequencing contigs, and of (C) evenness of pyrosequencing contigs over plume compartments of the Flingern aquifer at three successive time points of sampling.

Again, these results highlight the high level of specialization of the degrader populations at the lower fringe, but point also towards a reorganization of plume zone microbiota after hydraulic disturbance, which we further detailed by sequencing read affiliation.

Over the years, pyrosequencing reads from the upper fringe were dominated by members of the *Alpha*-, *Beta*- and *Gammaproteobacteria*, as well as the *Acidobacteria* (Fig. 4.8). While a clade of unclassified *Betaproteobacteria* was always abundant (~13%), marked dynamics were observed between the years e.g. for reads related to *Thiobacillus* spp., *Azoarcus* spp., *Pseudomonas* spp., a group of unclassified *Gammaproteobacteria*, as well as for sequences within the *Acidobacteria*.

Samples taken at the lower fringe and also in the plume core were dominated by reads of the *Deltaproteobacteria*, *Betaproteobacteria*, and *Clostridia* (Fig. 4.8, Fig. 4.9). Within the *Betaproteobacteria*, a high abundance of unclassified *Comamonadaceae* related to *Simplicispira* spp. and also other unaffiliated *Betaproteobacteria* (~12% each) disappeared in 2008, but partly recovered again in 2009. But consistent with our T-RFLP results, sequencing reads of unclassified *Desulfobulbaceae* and relatives of *Geobacter* spp. were especially prominent in these samples. *Geobacter* spp. read abundance was very stable (12 – 15%) at the lower fringe, and almost not detectable in other depths. In contrast, an extremely high abundance of reads within the *Desulfobulbaceae* (~26% in average in 2006 and 08) collapsed to only ~6% in 2009. At the same time, amplicons related to *Desulfosporosinus* spp. within the *Peptococcaceae* (*Clostridia*) constantly increased in abundance, from only ~9% in 2006 to ~24% in 2009. Interestingly, recent evidence revealed the importance of members of both lineages (*Desulfobulbaceae*, *Desulfosporosinus* spp.) as sulphate-reducing toluene-degraders in the subsurface (5, 22, 34, 35).

Finally, amplicon pools from the deeper zone were also dominated by *Deltaproteobacteria* and *Clostridia*, but also *Chloroflexi* and exceptionally high ratios of unclassifiable *Bacteria* (up to 44%). The *Deltaproteobacteria*, however, were mostly affiliated to the *Desulfobacteraceae*, as well other unclassified *Deltaproteobacteria*, and also reads related to *Desulfosporosinus* spp. were detected at max. 2% abundance. Thus, the microbiota in these depths was clearly distinct from the degrader populations detected at the lower fringe.

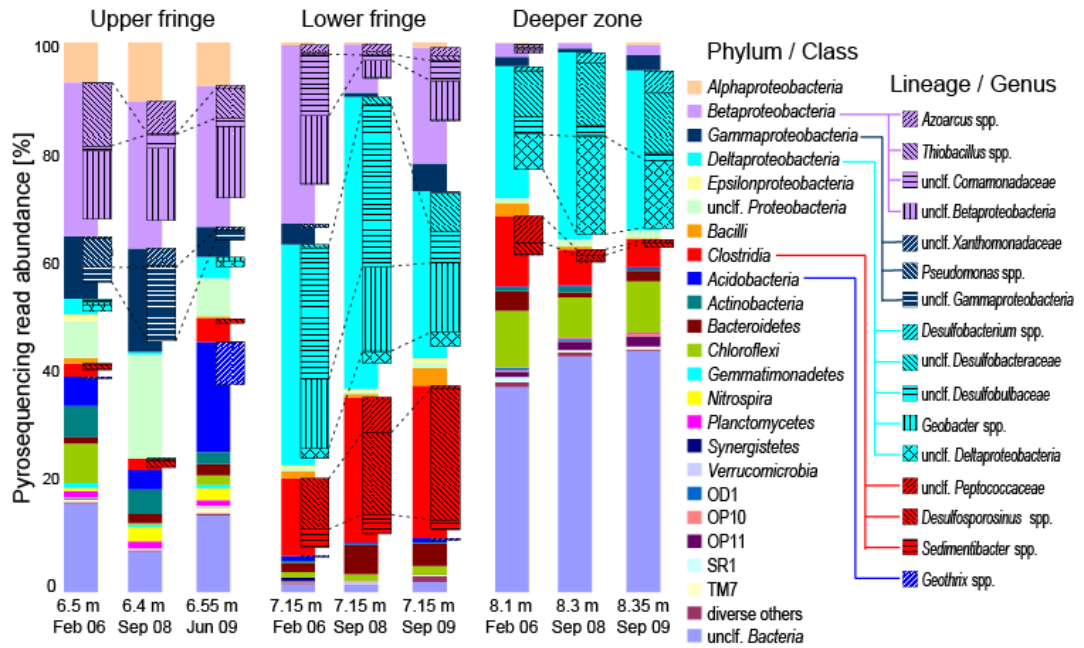


Fig. 4.8: Temporal dynamics of bacterial communities in important plume zones of the Flingern aquifer as revealed by amplicon pyrosequencing of bacterial 16S rRNA gene fragments. Total communities are dissected on a Phylum / Class-level, while selected dominating and dynamic lineages are specifically highlighted, where possible to Genus-level. Read affiliation was done using the RDP classifier (7) at a confidence threshold of 80%.

In conclusion, at a level of biogeochemical as well as bacterial community detail unprecedented to date, we provide comprehensive evidence that aquifers are much more dynamic habitats for microbes than currently perceived, especially at the micro- and mesoscale. In fact, hydraulic aquifer ecosystem dynamics were coupled to severe effects within intrinsic contaminant degrader populations and respective degradation processes. Prior to the disturbance, a highly selected, low evenness degrader community established at the lower plume fringe was responsible for anaerobic toluene degradation. Due to the direct relationship of the Flingern *Desulfobulbaceae* amplicon sequences to known toluene-degrading isolates and respective degraders identified via stable isotope probing (Fig. 4.9), these *Desulfobulbaceae* were the most likely primary toluene degraders at the site.

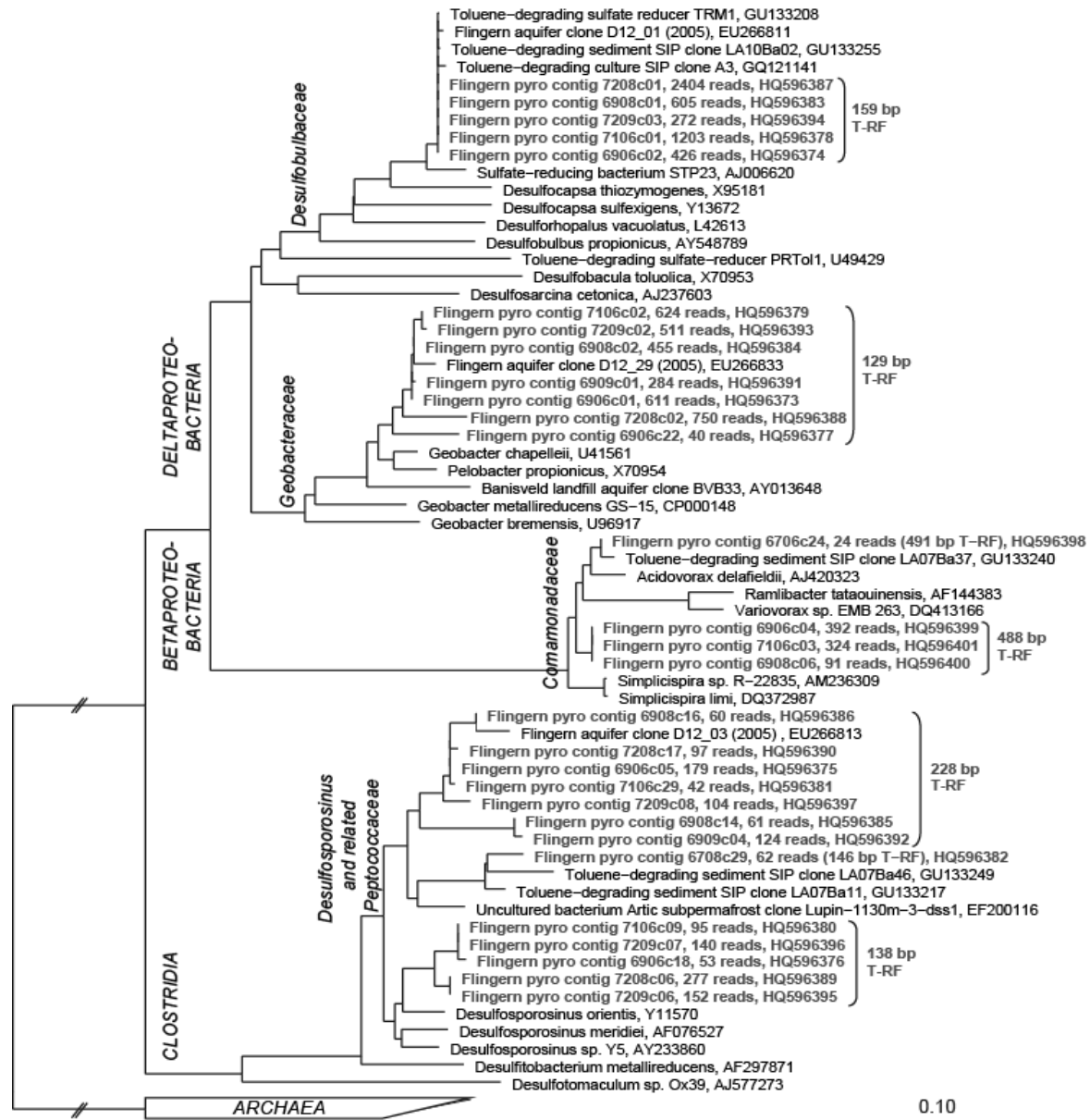


Fig. 4.9: Phylogenetic affiliation of selected assembled pyrosequencing contigs of ~520 bp bacterial 16S rRNA gene fragments retrieved from different depths of the Flingern aquifer at three successive time points of sampling. The tree was reconstructed using full-length reference sequences and Neighbor Joining algorithms as implemented in ARB (24), and subsequent addition of shorter sequences without changing overall tree topology. GenBank accession numbers are indicated. The scale bar represents 10% sequence divergence, branch lengths to the outgroup have been scaled down to 25%.

After the down- and upshift of the contaminant plume, however, this degrader community did not remain stable, neither in abundance, structure, or function. We hypothesize that the observed collapse of the community at the lower fringe was connected to an exchange of dominating degrader lineages, from members of the *Desulfobulbaceae* to *Desulfosporosinus* spp. This population swap was evident from both T-RFLP and pyrosequencing data and consistent



with the independent lines of evidence from contaminant stable isotopes and *bssA* qPCR. However, the quantitative collapse of the degrader community as indicated by a significant reduction of *bssA* and also total bacterial rRNA gene counts as observed in 2008 was not directly reflected in profound relative bacterial community shifts in the same year. This was expected, however, because a quantitative community collapse will only become apparent on relative level when other, originally less dominating members of the community re-establish.

Most notably however, the establishment of an ecologically and phylogenetically distinct, but functionally redundant population of sulphate-reducing toluene degraders within the *Clostridia* seemed to, on a longer time scale, restore functionality and thus “insure” the important processes of natural attenuation (27, 37) against disturbance. This data clearly contributes to a better understanding of central diversity-stability relationships (18) in aquifer ecosystems. Specific ecological features such as sporulation may contribute to an improved survival and subsequent re-activation of clostridial contaminant degraders under ecosystem stress (34). Our observations show that shifts in hydrogeochemical gradients were, *in situ*, coupled to dynamics in degrader populations and activity in contaminated aquifers. Thus, hydraulic disturbance caused a transient reduction in net biodegradation activities by negatively impacting established degrader communities.

These unique field data will help to develop a better conceptual understanding of the ecological controls of groundwater contaminant degradation. If the frequency of such intrinsic disturbances of natural attenuation can be estimated, much more sound predictions of the time scales required for aquifer ecosystem recovery after contamination will become possible.

#### 4.5. References

1. **Anneser, B., F. Einsiedl, R. U. Meckenstock, L. Richters, F. Wisotzky, and C. Griebler.** 2008. High-resolution monitoring of biogeochemical gradients in a tar oil-contaminated aquifer. *Appl. Geochem.* **23**:1715-1730.
2. **Anneser, B., G. Pilloni, A. Bayer, T. Lueders, C. Griebler, F. Einsiedl, and L. Richters.** 2010. High Resolution Analysis of Contaminated Aquifer Sediments and Groundwater-What Can be Learned in Terms of Natural Attenuation? *Geomicrobiol. J.* **27**:130 - 142.
3. **Bauer, R. D., P. Maloszewski, Y. Zhang, R. U. Meckenstock, and C. Griebler.** 2008. Mixing-controlled biodegradation in a toluene plume -- Results from two-dimensional laboratory experiments. *J. Contam. Hydrol.* **96**:150-168.

4. **Blessing, M., T. C. Schmidt, R. Dinkel, and S. B. Haderlein.** 2009. Delineation of Multiple Chlorinated Ethene Sources in an Industrialized Area—A Forensic Field Study Using Compound-Specific Isotope Analysis. *Environ. Sci. Technol.* **43**:2701-2707.
5. **Bombach, P., A. Chatzinotas, T. R. Neu, M. Kästner, T. Lueders, and C. Vogt.** 2010. Enrichment and characterization of a sulphate-reducing toluene-degrading microbial consortium by combining *in situ* microcosms and stable isotope probing techniques. *FEMS Microbiol. Ecol.* **71**:237-246.
6. **Carmona, M., M. T. Zamarro, B. Blazquez, G. Durante-Rodriguez, J. F. Juarez, J. A. Valderrama, M. J. L. Barragan, J. L. Garcia, and E. Diaz.** 2009. Anaerobic Catabolism of Aromatic Compounds: a Genetic and Genomic View. *Microbiol. Mol. Biol. Rev.* **73**:71-133.
7. **Cole, J. R., Q. Wang, E. Cardenas, J. Fish, B. Chai, R. J. Farris, A. S. Kulam-Syed-Mohideen, D. M. McGarrell, T. Marsh, G. M. Garrity, and J. M. Tiedje.** 2009. The Ribosomal Database Project: improved alignments and new tools for rRNA analysis. *Nucl. Acids Res.* **37**:D141-145.
8. **Costello, E. K., C. L. Lauber, M. Hamady, N. Fierer, J. I. Gordon, and R. Knight.** 2009. Bacterial Community Variation in Human Body Habitats Across Space and Time. *Science* **326**:1694-1697.
9. **DeSantis, T. Z., Jr., P. Hugenholtz, K. Keller, E. L. Brodie, N. Larsen, Y. M. Piceno, R. Phan, and G. L. Andersen.** 2006. NAST: a multiple sequence alignment server for comparative analysis of 16S rRNA genes. *Nucl. Acids Res.* **34**:W394-399.
10. **Edgar, R., M. Domrachev, and A. E. Lash.** 2002. Gene Expression Omnibus: NCBI gene expression and hybridization array data repository. *Nucleic Acids Research* **30**:207-210.
11. **Fretwell, B. A., W. G. Burgess, J. A. Barker, and N. L. Jefferies.** 2005. Redistribution of contaminants by a fluctuating water table in a micro-porous, double-porosity aquifer: Field observations and model simulations. *J. Contam. Hydrol.* **78**:27-52.
12. **Fuhrman, J. A.** 2009. Microbial community structure and its functional implications. *Nature* **459**:193-199.
13. **Galand, P. E., E. O. Casamayor, D. L. Kirchman, and C. Lovejoy.** 2009. Ecology of the rare microbial biosphere of the Arctic Ocean. *P. Natl. Acad. Sci. U.S.A.* **106**:22427-22432.
14. **Griebler, C., and T. Lueders.** 2009. Microbial biodiversity in groundwater ecosystems. *Freshwater Biol.* **54**:649-677.
15. **Haack, S. K., L. R. Fogarty, T. G. West, E. W. Alm, J. T. McGuire, D. T. Long, D. W. Hyndman, and L. J. Forney.** 2004. Spatial and temporal changes in microbial community structure associated with recharge-influenced chemical gradients in a contaminated aquifer. *Environ. Microbiol.* **6**:438-448.
16. **Hall, T. A.** 1999. BioEdit: a user-friendly biological sequence alignment editor and analysis program for Windows 95/98/NT. *Nucl. Acids. Symp. Ser.* **41**:95-98.
17. **Hancock, P. J., A. J. Boulton, and W. F. Humphreys.** 2005. Aquifers and hyporheic zones: Towards an ecological understanding of groundwater. *Hydrogeol. J.* **13**:98-111.
18. **Ives, A. R., and S. R. Carpenter.** 2007. Stability and Diversity of Ecosystems. *Science* **317**:58-62.
19. **Kuhn, T. K., K. Hamonts, J. A. Dijk, H. Kalka, W. Stichler, D. Springael, W. Dejonghe, and R. U. Meckenstock.** 2009. Assessment of the Intrinsic Bioremediation Capacity of an Eutrophic River Sediment Polluted by Discharging Chlorinated Aliphatic Hydrocarbons: A Compound-Specific Isotope Approach. *Environ. Sci. Technol.* **43**:5263-5269.
20. **Lake, P. S.** 2000. Disturbance, patchiness, and diversity in streams. *J. North Am. Benth. Soc.* **19**:573-592.
21. **Lane, D. J.** 1991. 16S/23S rRNA sequencing. E. Stackebrandt and M. Goodfellow (ed.), *Nucleic acid techniques in bacterial systematics.* John Wiley & Sons, New York, N.Y.

22. **Liu, A., E. Garcia-Dominguez, E. D. Rhine, and L. Y. Young.** 2004. A novel arsenate respiring isolate that can utilize aromatic substrates. *FEMS Microbiol. Ecol.* **48**:323-332.
23. **Lozupone, C. A., M. Hamady, S. T. Kelley, and R. Knight.** 2007. Quantitative and Qualitative {beta} Diversity Measures Lead to Different Insights into Factors That Structure Microbial Communities. *Appl. Environ. Microbiol.* **73**:1576-1585.
24. **Ludwig, W., O. Strunk, R. Westram, L. Richter, H. Meier, Yadhukumar, A. Buchner, T. Lai, S. Steppi, G. Jobb, W. Forster, I. Brettske, S. Gerber, A. W. Ginhart, O. Gross, S. Grumann, S. Hermann, R. Jost, A. Konig, T. Liss, R. Lussmann, M. May, B. Nonhoff, B. Reichel, R. Strehlow, A. Stamatakis, N. Stuckmann, A. Vilbig, M. Lenke, T. Ludwig, A. Bode, and K.-H. Schleifer.** 2004. ARB: a software environment for sequence data. *Nucl. Acids Res.* **32**:1363-1371.
25. **Meckenstock, R. U., B. Morasch, C. Griebler, and H. H. Richnow.** 2004. Stable isotope fractionation analysis as a tool to monitor biodegradation in contaminated acquifers. *J. Contam. Hydrol.* **75**:215-255.
26. **Miller, S. R., A. L. Strong, K. L. Jones, and M. C. Ungerer.** 2009. Bar-Coded Pyrosequencing Reveals Shared Bacterial Community Properties along the Temperature Gradients of Two Alkaline Hot Springs in Yellowstone National Park. *Appl. Environ. Microbiol.* **75**:4565-4572.
27. **Naeem, S., and S. Li.** 1997. Biodiversity enhances ecosystem reliability. *Nature* **390**:507-509.
28. **Prosser, J. I., B. J. M. Bohannan, T. P. Curtis, R. J. Ellis, M. K. Firestone, R. P. Freckleton, J. L. Green, L. E. Green, K. Killham, J. J. Lennon, A. M. Osborn, M. Solan, C. J. van der Gast, and J. P. W. Young.** 2007. The role of ecological theory in microbial ecology. *Nat. Rev. Microbiol.* **5**:384-392.
29. **Quince, C., A. Lanzen, T. P. Curtis, R. J. Davenport, N. Hall, I. M. Head, L. F. Read, and W. T. Sloan.** 2009. Accurate determination of microbial diversity from 454 pyrosequencing data. *Nat. Methods* **6**:639-641.
30. **Rolle, M., C. Eberhardt, G. Chiogna, O. A. Cirpka, and P. Grathwohl.** 2009. Enhancement of dilution and transverse reactive mixing in porous media: Experiments and model-based interpretation. *J. Contam. Hydrol.* **110**:130-142.
31. **Sherwood Lollar, B., S. K. Hirschorn, M. M. G. Chartrand, and G. Lacrampe-Couloume.** 2007. An Approach for Assessing Total Instrumental Uncertainty in Compound-Specific Carbon Isotope Analysis: Implications for Environmental Remediation Studies. *Anal. Chem.* **79**:3469-3475.
32. **Wang, Q., G. M. Garrity, J. M. Tiedje, and J. R. Cole.** 2007. Naive Bayesian Classifier for Rapid Assignment of rRNA Sequences into the New Bacterial Taxonomy. *Appl. Environ. Microbiol.* **73**:5261-5267.
33. **Winderl, C., B. Anneser, C. Griebler, R. U. Meckenstock, and T. Lueders.** 2008. Depth-Resolved Quantification of Anaerobic Toluene Degraders and Aquifer Microbial Community Patterns in Distinct Redox Zones of a Tar Oil Contaminant Plume. *Appl. Environ. Microbiol.* **74**:792-801.
34. **Winderl, C., H. Penning, F. von Netzer, R. U. Meckenstock, and T. Lueders.** 2010. DNA-SIP identifies sulphate-reducing Clostridia as important toluene degraders in tar-oil-contaminated aquifer sediment. *ISME J.*
35. **Winderl, C., S. Schaefer, and T. Lueders.** 2007. Detection of anaerobic toluene and hydrocarbon degraders in contaminated aquifers using benzylsuccinate synthase (bssA) genes as a functional marker. *Environ. Microbiol.* **9**:1035-1046.

36. **Wittebolle, L., M. Marzorati, L. Clement, A. Balloi, D. Daffonchio, K. Heylen, P. De Vos, W. Verstraete, and N. Boon.** 2009. Initial community evenness favours functionality under selective stress. *Nature* **458**:623-626.
37. **Yachi, S., and M. Loreau.** 1999. Biodiversity and ecosystem productivity in a fluctuating environment: The insurance hypothesis. *P. Natl. Acad. Sci. U.S.A.* **96**:1463-1468.
38. **Yagi, J. M., E. F. Neuhauser, J. A. Ripp, D. M. Mauro, and E. L. Madsen.** 2009. Subsurface ecosystem resilience: long-term attenuation of subsurface contaminants supports a dynamic microbial community. *ISME J.* **4**:131-143.

## 5. General conclusions and outlooks

Two major elements of novelty are presented in this thesis that advance our current perception of the ecology of natural attenuation going on at contaminated groundwater sites. First, I unambiguously identify, using DNA-SIP, the sulphate-reducing microbes actually responsible for toluene-oxidation at the sulfidogenic lower plume fringe of the Flingern site. Second, via an unprecedented time series of on site depth-resolved microbial community monitoring, I unravel previously totally unrecognized dynamics and ecological disturbance effects within on-site degrader populations that are driven mainly by hydraulic fluctuations of the groundwater table.

A primary event of depth-resolved sampling of groundwater and sediment at the tar-oil contaminated aquifer in Düsseldorf-Flingern was performed in Sep. 2005 (17). Under those circumstances, a highly active gradient zone beneath the contaminant plume was demonstrated, where an apparently specialized population of degraders related to the *Desulfobulbaceae* and also *Geobacteraceae* was responsible for degradation activity (8). This degradation activity, as revealed by *bssA* catabolic genes (1), seemed to be phylogenetically linked to relatives of the genus *Geobacter* (17). This interpretation was however not supportable by on-site geochemical data which indicated an aquifer with only minor importance of ferric iron reduction (7), and with a lower plume fringe highly characterized by sulfidogenic processes (10).

At a second sampling time point in Feb. 2006 (3), the presence of the same lineages in this particularly active zone was confirmed (chapter 2). Depth-resolved fingerprinting of bacterial communities in water and sediments revealed that only ~50% of all detected T-RFs were shared between water and sediment samples. This is evidence that even if closely corresponding depths are sampled, the two compartments are distinct, and that not all aquifer microbes are equally detectable in both. This comparison provide valuable insights on the ecology of the different microbes, as exemplified e.g. by the comparative distribution pattern of the *Geobacter*-related T-RF (figure 2.5B). This T-RF was practically not detected in groundwater, which can be attributed to the preference of these microbes to insoluble electron acceptors such as ferric iron and elemental sulphur, and hence to a lifestyle attached to mineral surfaces (16). In contrast, other microbes putatively more dependent on dissolved electron acceptors, such as the *Desulfobulbaceae* relatives (figure 2.5 C), were consistently distributed with depth in both sediment and water samples, but always detected in higher ratios in groundwater.

Moreover, the maximal abundance of this T-RF was surprisingly congruent to the peak of sulphide (Fig. 2.1B), as indication that the distribution of these specific microbes is clearly correlated to the localization of sulphate reducing processes within the Flingern aquifer. Over depth, the non-shared T-RFs appeared mainly in the deeper PAH zone (56% of all singletons). Thus, the upper zones dominated by the BTEX plume seem to impose much stronger selective pressures on the microorganisms, leading to a more uniform appearance of bacteria in both compartments.

A SIP incubation study with fresh sediment sampled in Sep. 2008 under comparative electron acceptor availability (sulphate vs. ferric iron) was performed under close to *in-situ* conditions to unravel whether either desulfobulbal or geobacterial putative toluene degraders detected at the highly active lower fringe of a contaminant plume (17) are actually important in on-site toluene degradation, and to affiliate the previously detected “F1-lineage” of *bssA* genes (17) to either of these two lineages. Combined with the use of labelled-toluene, the SIP-DNA approach described in chapter 3 gave the opportunity to unambiguously affiliate the key player of toluene degradation to members of the *Desulfobulbaceae* closely related to the TRM1 cluster also identified in other studies (6, 18). Furthermore, the incubation under sulphate and iron reducing conditions, emphasized by the absence of any *Geobacter* enrichment, permitted to exclude its involvement in on site degradation and to hypothesize the observed (17) clustering of *bssA* genes to this lineage as a probable effect of a lateral gene transfer. The dominating presence of a 478 bp *bssA* T-RF (figure 3.5) in all the DNA-fractions (presenting always also the *Desulfobulbaceae* 16S signature, 159 bp, figure 3.3) is a clear indication supporting this hypothesis. This should, however, be interpreted with caution, as long as genes from a pure culture of these new desulfobulbal degraders, or at least (meta-) genomic sequence data are not available.

Also the relevance of members of *Peptococcaceae* within the *Clostridia* under both electron-accepting regimes was revealed, accordingly to recent observations also from other sites (13, 18). Generally, the SIP experiment described in chapter 3 leads to important ecological conclusions regarding: (i) the linking between observed processes *in situ* (sulphate reduction) and microbes actually responsible for those processes (*Desulfobulbaceae*) within a selected community; (ii) even if not related to toluene degradation, the presence of *Geobacter* in the aquifer lower fringe is unlikely to be related to iron(III) reduction, due to the scarce availability of this electron acceptor *in situ* (3). Therefore, elemental sulphur ( $S^0$ ) could be another likely

electron acceptor for *Geobacter* (15) and it could be abiotically produced as reaction of  $S^{2-}$  (from sulphate reduction) with oxidized sedimentary metals (5); (iii) the absence of a true iron reducing microbial community associated to on-site BTEX degradation, but the possibility of their enrichment could be regarded as further potential for degradation even with (iv) redundancy of functionalities. This was true under both redox conditions, with *Clostridia* presenting the same catabolic traits to known proteobacterial degraders.

The importance of the low diversity and evenness of the community responsible for toluene degradation at the lower plume fringe of Flingern aquifer was especially highlighted by the on site temporal observations described in chapter 4. Here, for the first time, I unravel the unexpected effects of hydraulic disturbance on *in situ* populations of anaerobic hydrocarbon degraders. As mechanical parameter, fluctuation of the water table was shown to be closely interconnected with dramatic changes in on site geochemistry, and also a driver of re-organization in the structure and function of microbes actually responsible for remediation *in situ*. The observed collapse of degradation activities in Sep. 08 was not an obvious consequence, since numerical simulations and experiments in laboratory model systems suggested a positive effect of hydrodynamics on net biodegradation by increasing the mixing (4, 9, 12). Here however, I report how an established, “specialized” population of desulfobulbal toluene degraders at the lower fringe collapses, first quantitatively and then also qualitatively, after a down- and upshift of the contaminant plume. The low resistance of this community against disturbance could have been related to unfavourable conditions and possibly toxic effect of the increased toluene concentration (figure 4.2 B).

After the collapse, an increased abundance of *Desulfosporosinus* degraders during the last year of sediment sampling (Jun. 2009) indicated that this functional redundant degrader lineage replaced the original *Desulfobulbaceae*, which constitutes further evidence of the relevance of *Clostridia* in anaerobic hydrocarbon degradation *in situ*. The presence of functional redundancy can be regarded as “insurance” (19) of the environment against disturbance. The environmental resilience to fluctuations, conserving functionality of the environment, could have been related to improved resistance of *Clostridia* connected to ecological features such as sporulation.

The recovery of degradation activities gained by a re-arranged degrader community in Jun. 09 is an event never reported before for groundwater. Generally, an environment like the Flingern aquifer, subjected to a dramatic event of disturbance (release of contaminant) reached

with time a new level of stability (establishment of adapted microbial population), which was then very sensible to further, rather minor disturbance events (fluctuation of the water table).

My approach included also, for the first time, bidirectional barcoded amplicon pyrosequencing of aquifer microbiota. A protocol for the analyses established in this thesis and successfully applied to both SIP and on-site degraders dynamic investigations (chapters 3 and 4), allowed to clearly link pyrosequencing results to community fingerprinting. Thus, the relative abundances analyses of sequencing trimmed reads (table 3.2 and figure 4.8) constituted a cross-check, but with enhanced information, of what predicted via T-RFLP. Furthermore, the reconstruction of high quality full length (~520 bp) amplicon contigs, allowed a much more precise phylogenetic affiliation of the sequences with their accurate placement in phylogenetic trees (figures 3.4 and 4.9). The analyses presented here were never applied to groundwater ecosystems to date and, combined with the other qualitative and quantitative techniques on time and space series, constitutes an unprecedented detailed level of investigation for aquifers.

In summary, these findings highlight that aquifers are not steady-state and extremely stable environments as currently perceived. Rather, they call for a new understanding of the ecological controls of microbes involved in aquifer contaminant degradation. In the present thesis, a new relevance for general ecological concepts such as “disturbance ecology” (2, 14) for this very important, but dramatically under-investigated ecosystem below our feet is promoted. Hydraulic disturbance in groundwater is affected by seasonal levels of recharge and depletion mainly related to rainfall and evaporation events. Climate changes, affecting the global water cycle, could influence groundwater hydraulic regimes and impact on established biota. Including the results of the present thesis in models accounting the effect of climate changes in water cycles (11), it will make possible a much more sound prediction of the time scales required for aquifer ecosystem recovery at contaminated sites.

## 5.1. References

1. **Achong, G. R., A. M. Rodriguez, and A. M. Spormann.** 2001. Benzylsuccinate Synthase of *Azoarcus* sp. Strain T: Cloning, Sequencing, Transcriptional Organization, and Its Role in Anaerobic Toluene and m-Xylene Mineralization. *J. Bacteriol.* **183**:6763-6770.



2. **Angeler, D. G., and W. Goedkoop.** Biological responses to liming in boreal lakes: an assessment using plankton, macroinvertebrate and fish communities. *Journal of Applied Ecology* **47**:478-486.
3. **Anneser, B., G. Pilloni, A. Bayer, T. Lueders, C. Griebler, F. Einsiedl, and L. Richters.** 2010. High Resolution Analysis of Contaminated Aquifer Sediments and Groundwater-What Can be Learned in Terms of Natural Attenuation? *Geomicrobiology Journal* **27**:130 - 142.
4. **Bauer, R. D., P. Maloszewski, Y. Zhang, R. U. Meckenstock, and C. Griebler.** 2008. Mixing-controlled biodegradation in a toluene plume -- Results from two-dimensional laboratory experiments. *Journal of Contaminant Hydrology* **96**:150-168.
5. **Beller, H. R., D. Grbic-Galic, and M. Reinhard.** 1992. Microbial degradation of toluene under sulfate-reducing conditions and the influence of iron on the process. *Appl. Environ. Microbiol.* **58**:786-793.
6. **Bombach, P., A. Chatzinotas, T. R. Neu, M. Kästner, T. Lueders, and C. Vogt.** 2010. Enrichment and characterization of a sulfate-reducing toluene-degrading microbial consortium by combining *in situ* microcosms and stable isotope probing techniques. *FEMS Microbiol. Ecol.* **71**:237-246.
7. **Botton, S., and J. Parsons.** 2007. Degradation of BTX by dissimilatory iron-reducing cultures. *Biodegradation* **18**:371-381.
8. **Christensen, T. H., P. L. Bjerg, S. A. Banwart, R. Jakobsen, G. Heron, and H.-J. Albrechtsen.** 2000. Characterization of redox conditions in groundwater contaminant plumes. *Journal of Contaminant Hydrology* **45**:165-241.
9. **Cirpka, O. A., and A. J. Valocchi.** 2007. Two-dimensional concentration distribution for mixing-controlled bioreactive transport in steady state. *Advances in Water Resources* **30**:1668-1679.
10. **Coates, J. D., R. T. Anderson, J. C. Woodward, E. J. P. Phillips, and D. R. Lovley.** 1996. Anaerobic Hydrocarbon Degradation in Petroleum-Contaminated Harbor Sediments under Sulfate-Reducing and Artificially Imposed Iron-Reducing Conditions. *Environmental Science & Technology* **30**:2784-2789.
11. **D'Agostino, D. R., L. G. Trisorio, N. Lamaddalena, and R. Ragab.** 2010. Assessing the results of scenarios of climate and land use changes on the hydrology of an Italian catchment: modelling study. *Hydrological Processes* **24**:2693-2704.
12. **Dobson, R., M. H. Schroth, and J. Zeyer.** 2007. Effect of water-table fluctuation on dissolution and biodegradation of a multi-component, light nonaqueous-phase liquid. *Journal of Contaminant Hydrology* **94**:235-248.
13. **Kunapuli, U., T. Lueders, and R. U. Meckenstock.** 2007. The use of stable isotope probing to identify key iron-reducing microorganisms involved in anaerobic benzene degradation. *ISME J.*
14. **Lake, P. S.** 2000. Disturbance, patchiness, and diversity in streams. *J. North Am. Benth. Soc.* **19**:573-592.
15. **Méthé, B. A., K. E. Nelson, J. A. Eisen, I. T. Paulsen, W. Nelson, J. F. Heidelberg, D. Wu, M. Wu, N. Ward, M. J. Beanan, R. J. Dodson, R. Madupu, L. M. Brinkac, S. C. Daugherty, R. T. DeBoy, A. S. Durkin, M. Gwinn, J. F. Kolonay, S. A. Sullivan, D. H. Haft, J. Selengut, T. M. Davidsen, N. Zafar, O. White, B. Tran, C. Romero, H. A. Forberger, J. Weidman, H. Khouri, T. V. Feldblyum, T. R. Utterback, S. E. Van Aken, D. R. Lovley, and C. M. Fraser.** 2003. Genome of *Geobacter sulfurreducens*: Metal Reduction in Subsurface Environments. *Science* **302**:1967-1969.

16. **Weber, K. A., L. A. Achenbach, and J. D. Coates.** 2006. Microorganisms pumping iron: anaerobic microbial iron oxidation and reduction. *Nat Rev Micro* **4**:752-764.
17. **Winderl, C., B. Anneser, C. Griebler, R. U. Meckenstock, and T. Lueders.** 2008. Depth-Resolved Quantification of Anaerobic Toluene Degraders and Aquifer Microbial Community Patterns in Distinct Redox Zones of a Tar Oil Contaminant Plume. *Appl. Environ. Microbiol.* **74**:792-801.
18. **Winderl, C., H. Penning, F. von Netzer, R. U. Meckenstock, and T. Lueders.** 2010. DNA-SIP identifies sulfate-reducing Clostridia as important toluene degraders in tar-oil-contaminated aquifer sediment. *ISME J.*
19. **Yachi, S., and M. Loreau.** 1999. Biodiversity and ecosystem productivity in a fluctuating environment: The insurance hypothesis. *Proceedings of the National Academy of Sciences of the United States of America* **96**:1463-1468.





## **Authorship clarifications**

### **Chapter 2: “High resolution analysis of contaminated aquifer sediments and groundwater- what can be learned in terms of natural attenuation?”**

The contributions of the PhD candidate to this work were the following:

The idea and concept for the experimental design were carried out by Dr. Bettina Anneser, Dr. Christian Griebler and the PhD candidate. Dr. Bettina Anneser, Anne Bayer, Dr. Florian Einsiedl and Dr. Christian Griebler performed the analyses and evaluated the results related to the on site geochemistry. The PhD candidate performed the microbial fingerprinting, calculated the statistics and evaluated the results together with Dr. Tillmann Lueders. The manuscript was published on *Geomicrobiology Journal*, 27:130-142 (2010).

### **Chapter 3: “Electron acceptor-dependent identification of key anaerobic toluene degraders at a tar-oil contaminated aquifer by Pyro-SIP.”**

The contributions of the PhD candidate to this work were the following:

The concept for the experiment was developed by Dr. Tillmann Lueders. The experimental design was done by the PhD candidate and Dr. Tillmann Lueders. All the measurements were performed by the PhD candidate, except the *bssA* T-RFLP (Frederick von Netzer) and the 16 S rRNA analyses on the inoculum DNA (Katrin Hörmann). The evaluation, statistical data analyses and their graphical illustration were done by the PhD candidate independently. Dr. Tillmann Lueders and the PhD candidate interpreted and discussed the results together. Stable isotope measurements were facilitated by Dr. Martin Elsner laboratory staff. Dr. Marion Engel (Department of Soil Ecology, Helmholtz Centre Munich) provided technical expertise on amplicon pyrosequencing. The manuscript was written by the PhD candidate and Dr. Tillmann Lueders and submitted (06/12/2010) by the corresponding author Dr. Tillmann Lueders to *FEMS Microbiology Ecology*. The paper was accepted on March, 2<sup>nd</sup> 2011.

### **Chapter 4: “Disturbance ecology controls natural attenuation in contaminated aquifers.”**

The contributions of the PhD candidate to this work were the following:

The concept for the experiment was developed by Dr. Tillmann Lueders and Dr. Christian Griebler. The experimental design and the sampling at the Düsseldorf-Flingern aquifer were managed by the PhD candidate, Anne Bayer, Dr. Bettina Anneser, Dr. Tillmann Lueders and Dr. Christian Griebler. The access to the sampling site was facilitated by Lars Richters and Stadtwerke Düsseldorf. The molecular biology analyses (DNA extraction, T-RFLP fingerprinting, qPCR and amplicon pyrosequencing) were done by the PhD candidate. Dr. Marion Engel

(Department of Soil Ecology, Helmholtz Centre Munich) provided technical expertise on amplicon pyrosequencing. The geochemical analyses (concentration of toluene, sulphide and toluene isotope ratios) and the results evaluation were done by Anne Bayer, Dr. Bettina Anneser and Dr. Christian Griebler. The evaluation, statistical data analyses and their graphical illustration were done by the PhD candidate independently. Dr Tillmann Lueders and the PhD candidate interpreted and discussed the results together. The draft of the manuscript was written by the PhD candidate, edited and improved by the other co-authors, corrected and optimized by Dr. Tillmann Lueders. The manuscript was submitted by the corresponding author Dr. Tillmann Lueders to *Science* (13/10/2010) and it is now in preparation for re-submission to *Nature Geoscience*.

## **Publications in peer reviewed journals**

- M. Coci, G. W. Nicol, **G. N. Pilloni**, M. Schmid, M. P. Kamst-van Agterveld, P. L. E. Bodelier and H. J. Laanbroek, **Quantitative Assessment of Ammonia-Oxidizing Bacterial Communities in the Epiphyton of Submerged Macrophytes in Shallow Lakes**, APPLIED AND ENVIRONMENTAL MICROBIOLOGY, 76: 1813–1821 (2010).
- B. Anneser, **G. Pilloni**, A. Bayer, T. Lueders, C. Griebler, F. Einsiedl and L. Richters, **High Resolution Analysis of Contaminated Aquifer Sediments and Groundwater—What Can be Learned in Terms of Natural Attenuation?**, GEOMICROBIOLOGY JOURNAL, 27(2): 130-142 (2010).
- **G. Pilloni**, F. von Netzer and T. Lueders, **Electron acceptor-dependent identification of key anaerobic toluene degraders at a tar-oil contaminated aquifer by Pyro-SIP**, FEMS MICROBIOLOGY ECOLOGY (accepted 2 March 2011).
- **G. Pilloni**, A. Bayer, B. Anneser, M. Engel, C. Griebler and T. Lueders, **Disturbance ecology controls natural attenuation in contaminated aquifers**, NATURE GEOSCIENCE (in preparation).

## **Appendix**

## Supporting data tables

**Table A.1:** Depth profiles of toluene, sulphide and toluene isotope ratio in groundwater (aq.) of the Flingern aquifer in successive years of sampling as shown in **Fig. 4.2**. All measurements by Anne Bayer (Helmholtz München-IGOE). Std dev = standard deviation, b.d.l = below detection limit.

Depth [m]	Toluene, aq [mg/l]		Sulfide, aq [mg/l]		d13C Toluene [‰]	
	Average	Std dev	Average	Std dev	Average	Std dev
<b>Feb-06</b>						
6.39	0.00	0.00	0.18	0.00	-23.42	0.13
6.41	2.83	0.19	0.24	0.00	-24.00	0.03
6.44	10.72	0.65	0.48	0.00	-24.06	0.16
6.46	21.09	1.62	0.27	0.04	-24.07	0.36
6.49	29.45	0.34	0.51	0.04	-24.32	0.02
6.51	31.60	5.00	0.60	0.08	-24.35	0.07
6.54	36.91	0.40	0.66	0.25	-24.42	0.10
6.56	38.08	0.65	1.58	0.04	-24.40	0.02
6.59	42.12	0.26	2.06	0.13	-24.37	0.07
6.61	44.75	1.39	2.15	0.08	-24.51	0.09
6.64	45.38	0.88	2.26	0.00	-24.49	0.06
6.67	44.66	0.46	1.34	0.04	-24.44	0.05
6.70	45.34	0.95	1.70	0.04	-24.49	0.02
6.75	43.53	0.34	1.13	0.08	-24.43	0.05
6.81	39.80	0.19	1.46	0.04	-24.50	0.14
6.91	31.97	0.19	4.35	0.08	-24.53	0.03
7.11	4.08	0.08	9.54	0.59	-21.84	0.07
7.21	1.32	0.00	6.79	0.51	-21.86	0.27
7.31	0.35	0.01	2.71	0.21	-21.28	0.11
7.41	0.21	0.00	1.67	0.08	-22.31	0.02
7.51	0.15	0.02	1.01	0.00	-22.19	0.04
7.61	0.08	0.01	0.80	0.04	-22.49	0.06
8.05	0.00	0.00	1.82	0.04	-22.64	0.09
<b>Sep-08</b>						
6.39	21.98	0.78	0.00	0.00	-23.07	0.50
6.41	28.36	2.64	0.03	0.00	-22.38	0.50
6.44	41.97	3.94	0.06	0.00	-22.68	0.50
6.46	56.02	9.86	0.19	0.00	-22.35	0.50
6.51	97.27	12.66	0.13	0.00	-22.62	0.53
6.54	91.76	25.10	1.46	0.00	-22.16	0.50
6.59	59.57	9.96	5.05	0.00	-22.65	0.50
6.61	59.22	4.14	4.70	0.01	-22.69	0.50
6.64	62.25	16.68	4.07	0.00	-22.39	0.64
6.67	63.16	4.54	6.17	0.00	-22.14	0.50
6.70	29.99	4.23	5.12	0.00	-22.44	0.50
6.75	27.65	1.75	6.51	0.01	-22.85	0.50
6.81	9.98	3.71	8.20	0.00	-23.03	0.50
6.86	5.31	0.09	8.45	0.00	-23.15	0.87
6.91	1.56	0.12	10.17	0.00	-22.24	0.50
6.96	0.23	0.23	7.21	0.00	-23.71	1.10
7.01	0.18	0.04	2.29	0.01	b.d.l.	b.d.l.
7.06	0.19	0.00	1.05	0.00	b.d.l.	b.d.l.
7.11	0.10	0.03	0.35	0.00	b.d.l.	b.d.l.
7.16	0.13	0.04	0.32	0.00	b.d.l.	b.d.l.
7.21	0.11	0.06	0.38	0.00	b.d.l.	b.d.l.
7.26	0.17	0.01	0.19	0.00	b.d.l.	b.d.l.
7.31	0.15	0.04	0.25	0.00	b.d.l.	b.d.l.
7.41	0.17	0.02	0.22	0.00	b.d.l.	b.d.l.
7.51	0.23	0.09	0.10	0.00	b.d.l.	b.d.l.
7.61	0.25	0.08	0.10	0.00	b.d.l.	b.d.l.
8.05	0.21	0.07	3.34	0.00	b.d.l.	b.d.l.
9.05	0.23	0.14	0.03	0.00	b.d.l.	b.d.l.



Table A.1 (continued).

Jun-09						
6.39	2.47	0.01	6.90	0.00	-20.51	0.50
6.44	4.01	0.29	3.59	0.00	-21.69	0.50
6.46	5.22	0.69	3.21	0.00	-21.97	0.50
6.51	7.80	0.13	3.27	0.00	-21.96	0.50
6.54	10.33	0.45	6.77	0.00	-22.14	0.50
6.61	14.27	0.34	1.97	0.01	-21.50	0.50
6.64	18.33	4.54	2.13	0.01	-22.13	0.50
6.67	13.25	1.78	1.65	0.03	-22.21	0.50
6.81	5.97	0.02	3.97	0.01	-22.32	0.50
6.91	0.65	0.04	6.17	0.00	-22.84	0.50
6.96	0.33	0.02	6.07	0.00	-23.10	0.50
7.01	0.16	0.06	5.50	0.00	-22.21	1.58
7.06	0.09	0.00	0.79	0.00	-23.25	0.50
7.11	0.13	0.00	0.60	0.00	-22.13	0.50
7.21	0.08	0.00	0.00	0.00	-22.00	0.50
7.31	0.09	0.00	0.00	0.00	-22.11	0.50
7.41	0.08	0.01	0.22	0.00	b.d.l.	b.d.l.
7.46	0.07	0.01	0.00	0.00	b.d.l.	b.d.l.
7.51	0.08	0.01	0.32	0.00	b.d.l.	b.d.l.
7.61	0.06	0.00	0.22	0.01	b.d.l.	b.d.l.
8.05	0.00	0.00	0.54	0.00	b.d.l.	b.d.l.
8.35	0.00	0.00	3.21	0.04	b.d.l.	b.d.l.
9.05	0.05	0.00	0.54	0.00	b.d.l.	b.d.l.

**Table A.2:** Principal component ordination of the overall variance in depth-resolved bacterial community composition retrieved from T-RFLP fingerprinting over year as shown in **Fig. 4.3 A**.

Depth_year	Factor 1	Factor2
6.50_06	0.103	0.102
6.65_06	-0.317	-0.056
6.90_06	-0.115	0.019
7.10_06	-0.325	-0.040
7.60_06	0.049	0.064
7.80_06	0.043	0.028
8.10_06	0.047	0.037
6.38_08	0.130	0.240
6.67_08	0.029	0.026
6.90_08	-0.127	0.030
7.15_08	-0.311	-0.053
7.43_08	0.079	0.056
7.92_08	0.114	-0.103
8.29_08	0.203	-0.190
6.55_09	0.158	0.152
6.85_09	-0.093	0.024
7.15_09	-0.077	0.065
7.25_09	0.015	-0.105
8.00_09	0.206	-0.158
8.35_09	0.189	-0.140
<b>% tot Var</b>	<b>37.85</b>	<b>15.05</b>

**Table A.3:** Loading plot of inferred principal component factors on specific T-RFs as in **Fig. 4.3 B**.

<b>T-RF [bp]</b>	<b>61</b>	<b>66</b>	<b>70</b>	<b>73</b>	<b>77</b>	<b>87</b>	<b>89</b>	<b>92</b>
<b>Factor 1</b>	0.012	0.007	0.002	0.003	0.002	-0.005	0.000	-0.002
<b>Factor 2</b>	-0.008	0.003	0.002	0.007	0.008	0.009	0.000	0.002
<b>T-RF [bp]</b>	<b>109</b>	<b>117</b>	<b>120</b>	<b>122</b>	<b>125</b>	<b>129</b>	<b>134</b>	<b>138</b>
<b>Factor 1</b>	0.001	-0.004	0.000	0.001	0.009	-0.033	0.010	-0.012
<b>Factor 2</b>	0.001	0.002	0.002	0.006	-0.007	0.013	0.018	0.014
<b>T-RF [bp]</b>	<b>141</b>	<b>146</b>	<b>148</b>	<b>154</b>	<b>159</b>	<b>161</b>	<b>164</b>	<b>170</b>
<b>Factor 1</b>	-0.002	0.001	0.003	0.008	-0.145	0.041	-0.003	0.034
<b>Factor 2</b>	0.000	0.002	0.014	0.014	-0.023	-0.044	0.004	-0.052
<b>T-RF [bp]</b>	<b>184</b>	<b>187</b>	<b>202</b>	<b>206</b>	<b>212</b>	<b>225</b>	<b>228</b>	<b>242</b>
<b>Factor 1</b>	0.003	0.012	0.003	0.004	-0.009	-0.009	-0.024	-0.002
<b>Factor 2</b>	0.004	-0.016	0.000	-0.004	-0.001	0.002	0.006	0.001
<b>T-RF [bp]</b>	<b>259</b>	<b>263</b>	<b>271</b>	<b>276</b>	<b>279</b>	<b>282</b>	<b>286</b>	<b>288</b>
<b>Factor 1</b>	-0.003	0.003	0.001	0.014	-0.003	-0.004	0.002	0.002
<b>Factor 2</b>	0.000	0.007	0.004	0.015	0.001	0.005	0.001	0.003
<b>T-RF [bp]</b>	<b>305</b>	<b>372</b>	<b>431</b>	<b>437</b>	<b>454</b>	<b>469</b>	<b>472</b>	<b>477</b>
<b>Factor 1</b>	0.000	0.023	0.005	0.000	0.000	0.000	0.004	0.007
<b>Factor 2</b>	0.001	-0.017	0.007	0.001	0.000	0.000	-0.004	0.011
<b>T-RF [bp]</b>	<b>486</b>	<b>488</b>	<b>492</b>	<b>494</b>	<b>498</b>	<b>502</b>	<b>505</b>	<b>509</b>
<b>Factor 1</b>	-0.008	0.019	0.020	-0.001	0.002	-0.018	0.007	-0.001
<b>Factor 2</b>	-0.018	0.048	0.007	0.001	0.004	-0.002	-0.006	-0.027
<b>T-RF [bp]</b>	<b>513</b>	<b>518</b>	<b>520</b>	<b>526</b>	<b>534</b>	<b>604</b>		
<b>Factor 1</b>	0.005	0.007	0.004	0.007	0.002	0.007		
<b>Factor 2</b>	-0.003	-0.003	0.004	-0.001	-0.005	-0.008		

**Table A.4:** Comparative abundance distribution profiles of specific T-RFs over depth and in different sampling time point as reported in **Fig. 4.4**. Averaged measurements from independent triplicate DNA extracts are reported; Std.Err. = standard error.

Depth_year	T-RF [bp]					
	129		159		228	
	Average	Std.Err.	Average	Std.Err.	Average	Std.Err.
5.90_06	1.19	0.00	0.00	0.00	0.00	0.00
6.50_06	1.62	0.50	3.99	0.50	0.00	0.00
6.65_06	2.47	2.85	46.80	2.85	3.36	0.39
6.90_06	12.72	1.67	18.89	1.67	8.18	0.87
7.10_06	14.67	1.08	45.00	1.08	4.60	0.18
7.60_06	0.00	0.40	8.72	0.40	1.72	0.02
7.80_06	0.00	1.18	9.73	1.18	2.13	0.27
8.10_06	0.00	1.93	10.96	1.93	0.87	0.87
8.40_06	0.00	0.82	8.57	0.82	0.00	0.00
9.20_06	0.00	3.39	13.44	3.39	0.00	0.00
6.08_08	0.26	0.33	0.33	0.33	0.23	0.23
6.37_08	3.58	0.35	1.87	0.35	2.03	0.23
6.67_08	5.87	0.77	10.27	0.77	0.46	0.23
6.90_08	10.67	0.89	22.40	0.89	7.65	0.23
7.15_08	5.72	1.92	44.72	1.92	6.96	0.32
7.43_08	1.47	2.28	8.21	2.28	0.00	0.00
7.92_08	0.44	0.78	7.42	0.78	1.51	0.08
8.29_08	0.44	0.37	2.43	0.37	0.69	0.42
8.82_08	2.71	1.15	2.48	1.15	0.00	0.00
9.30_08	2.90	0.40	6.32	0.40	0.00	0.00
5.95_09	2.00	0.61	1.17	0.61	0.00	0.00
6.55_09	4.16	0.22	0.22	0.22	0.00	0.00
6.85_09	7.67	0.80	20.05	0.80	7.83	0.41
7.15_09	14.61	0.76	13.74	0.76	16.60	0.06
7.25_09	1.35	0.97	16.69	0.97	1.24	1.24
8.00_09	0.00	0.45	0.45	0.45	0.39	0.39
8.35_09	0.00	0.49	2.31	0.49	0.00	0.00
8.60_09	0.00	4.63	7.92	4.63	0.00	0.00
9.40_09	0.00	0.41	2.51	0.41	0.00	0.00

**Table A.5:** Depth distribution over the three year of sampling of bacterial 16S rRNA genes and specific *bssA* genes of the F1-cluster measured via qPCR and averaged over independent triplicate DNA extracts, as shown in **Fig. 4.5**. Std.Err. = standard error.

Depth_year	16S x5.5 [cp/g]	Stderr x5.5	bss A [cp/g]	Std.Err.	Ratio
5.90_06	1.4E+08	7.7E+07	1.9E+05	1.2E+05	0.00
6.50_06	1.8E+08	3.6E+07	2.1E+06	9.2E+05	0.01
6.65_06	1.6E+08	9.2E+07	7.8E+06	2.6E+06	0.05
6.90_06	1.0E+08	2.5E+07	4.2E+07	2.2E+07	0.42
7.10_06	3.5E+07	3.8E+06	2.9E+07	1.5E+07	0.83
7.60_06	2.1E+07	3.4E+06	1.1E+05	8.6E+04	0.01
7.80_06	2.6E+07	8.0E+06	9.2E+04	5.7E+04	0.00
8.10_06	1.7E+07	8.1E+06	4.1E+05	3.8E+05	0.02
8.40_06	5.5E+06	2.6E+06	2.9E+04	2.1E+04	0.01
8.80_06	7.3E+06	2.5E+06	1.6E+05	1.4E+05	0.02
9.20_06	5.7E+06	2.9E+06	4.8E+04	3.3E+04	0.01
6.08_08	2.1E+07	5.7E+06	5.9E+04	3.7E+04	0.00
6.37_08	4.6E+07	3.3E+07	2.2E+04	2.0E+04	0.00
6.67_08	1.4E+07	1.1E+07	1.4E+06	5.3E+05	0.10
6.90_08	1.9E+07	1.3E+07	1.9E+06	4.3E+05	0.10
7.15_08	2.5E+07	1.8E+07	2.3E+06	2.2E+05	0.09
7.43_08	3.0E+06	1.2E+06	5.6E+04	5.2E+04	0.02
7.92_08	2.3E+06	8.7E+05	1.1E+04	1.1E+04	0.00
8.29_08	2.1E+06	1.0E+06	7.4E+03	6.5E+03	0.00
8.82_08	2.0E+06	8.8E+05	1.1E+04	5.8E+03	0.01
9.30_08	1.2E+06	8.2E+05	2.2E+03	1.9E+03	0.00
5.95_09	7.0E+07	1.2E+07	1.4E+03	5.0E+01	0.00
6.55_09	1.5E+08	1.7E+07	4.4E+03	1.2E+03	0.00
6.85_09	1.2E+08	7.8E+06	1.1E+07	3.1E+06	0.09
7.15_09	5.9E+07	3.1E+06	1.1E+07	6.3E+05	0.18
7.55_09	5.4E+07	1.6E+07	3.2E+05	3.0E+05	0.01
7.25_09	3.8E+06	1.2E+06	4.5E+02	1.5E+02	0.00
8.00_09	1.2E+07	2.7E+06	5.7E+02	5.6E+01	0.00
8.35_09	9.2E+06	2.8E+06	2.0E+02	5.6E+01	0.00
8.60_09	8.8E+06	2.3E+06	1.1E+03	3.5E+02	0.00
9.40_09	1.2E+07	4.4E+06	2.7E+02	7.0E+01	0.00

Appendix

**Table A.6:** Percentages of sequences retrieved from amplicon pyrosequencing on sediment samples of the subsequent years of sampling. Shown is the phylum/class level and, for characteristic/dynamic lineages, genus level, as reported in Fig. 4.8.

Phlogeny	6.5_06	6.5_08	6.6_09	7.1_06	7.2_08	7.2_09	8.1_06	8.3_08	8.3_09
unclassified_Bacteria	16.1	7.4	13.9	1.5	1.4	1.9	37.3	42.9	43.9
TM7	0.4	0.0	0.8	0.1	0.0	0.1	0.2	0.3	0.3
SR1	0.0	0.0	0.0	0.0	0.0	0.0	0.8	0.2	0.2
OP11	0.1	0.0	0.1	0.1	0.1	0.1	1.0	1.5	1.9
OP10	0.1	0.0	0.1	0.0	0.1	0.0	0.3	0.2	0.4
OD1	0.2	0.0	0.0	0.0	0.0	0.0	0.4	0.2	0.0
Verrucomicrobia	0.1	0.3	0.3	0.0	0.0	0.0	0.0	0.0	0.0
Synergistetes	0.0	0.0	0.0	0.7	0.1	0.1	0.0	0.1	0.0
Planctomycetes	1.1	1.3	0.9	0.0	0.0	0.0	0.1	0.2	0.2
Nitrospira	0.5	2.6	2.2	0.0	0.0	0.0	0.0	0.0	0.0
Leptospirillum	0.0	2.1	2.0	0.0	0.0	0.0	0.0	0.0	0.0
Gemmatimonadetes	0.9	0.5	0.6	0.0	0.0	0.0	0.0	0.0	0.0
Chloroflexi	7.1	0.2	1.7	1.0	1.2	1.5	10.3	7.4	9.3
unclassified_Anaerolineaceae	6.7	0.0	1.5	1.0	1.2	1.5	9.6	6.8	8.9
Bacteroidetes	1.2	1.7	2.1	1.6	5.3	4.1	3.5	0.9	2.0
unclassified_ "Bacteroidetes"	0.4	0.3	0.8	0.8	3.5	2.0	2.5	0.8	1.4
Proteiniphilum	0.1	0.0	0.1	0.6	1.4	1.7	0.8	0.0	0.0
Actinobacteria	5.6	4.4	2.2	0.4	0.2	0.2	0.8	1.1	0.5
Acidobacteria	5.3	3.6	20.1	0.9	0.3	0.8	0.2	0.2	0.2
unclassified_Holophagaceae	0.9	0.1	5.6	0.4	0.2	0.2	0.0	0.0	0.0
Geothrix	0.4	0.1	7.7	0.2	0.1	0.4	0.0	0.0	0.0
Firmicutes	3.6	2.3	5.0	15.7	27.3	31.9	15.9	7.3	5.5
Clostridia	2.4	2.0	4.2	14.1	26.4	27.8	12.8	6.5	5.1
Sedimentibacter	0.1	0.1	0.0	3.2	3.4	1.7	0.2	0.0	0.0
Desulfosporosinus	0.9	1.3	0.8	9.2	14.9	23.7	2.0	1.0	0.8
unclassified_Peptococcaceae 2	0.1	0.3	0.2	0.0	6.2	0.5	4.7	1.1	0.6
Bacilli	1.0	0.1	0.5	1.3	0.6	3.1	2.3	0.6	0.2
Proteobacteria	57.4	75.7	49.8	78.0	63.9	59.3	29.2	37.1	35.6
unclassified_ "Proteobacteria"	6.7	18.8	6.8	0.5	0.4	1.0	0.9	1.3	1.4
Epsilonproteobacteria	1.2	0.0	0.1	0.5	0.5	0.8	0.1	0.0	0.0
Deltaproteobacteria	2.9	0.5	3.9	40.2	53.1	30.4	24.0	34.0	29.1
unclassified_Deltaproteobacteria	1.2	0.1	1.0	1.7	2.1	2.6	6.3	17.6	12.2
Geobacter	0.3	0.1	0.6	12.4	15.3	12.4	0.1	0.2	0.0
unclassified_Desulfobulbaceae	0.7	0.1	0.2	23.6	29.1	5.7	3.1	1.8	1.3
unclassified_Desulfobacteraceae	0.0	0.0	0.1	0.5	1.3	6.9	8.2	11.3	10.9
Desulfobacterium	0.0	0.0	0.0	0.0	0.0	0.1	0.8	1.8	3.9
Gammaproteobacteria	11.4	18.8	5.5	3.8	0.8	5.0	1.7	0.7	2.8
unclassified_Gammaproteobacteria	2.7	13.3	1.8	0.0	0.0	0.2	0.2	0.1	0.0
Pseudomonas	5.1	0.3	0.1	0.6	0.1	0.1	0.0	0.2	0.2
unclassified_Xanthomonadaceae	0.3	3.1	0.4	0.0	0.0	0.0	0.0	0.0	0.0
Betaproteobacteria	27.9	26.8	25.7	32.5	8.8	21.1	2.4	1.0	1.9
unclassified_Betaproteobacteria	12.3	12.9	12.8	12.3	3.0	7.1	0.4	0.2	0.0
unclassified_Comamonadaceae	0.8	2.5	1.5	11.0	1.0	3.6	0.2	0.2	0.2
Thiobacillus	11.5	0.3	5.2	0.3	0.6	0.9	0.4	0.2	0.1
Azoarcus	0.0	5.7	0.7	1.3	1.4	1.5	0.5	0.2	0.0
Alphaproteobacteria	7.3	10.7	7.9	0.5	0.3	0.9	0.2	0.1	0.5
unclassified_Rhizobiales	2.2	2.1	1.3	0.1	0.0	0.2	0.1	0.0	0.2
Methylocystis	0.0	1.4	1.8	0.0	0.0	0.0	0.0	0.0	0.0

**Table A.7:** Production of sulphide and  $^{13}\text{CO}_2$  in SIP microcosms related to transformation of labelled vs. unlabelled toluene as shown in **Fig. 3.1**. St.Err. = standard error.

Week	$\text{CO}_2$ AT% Aver.	$\text{CO}_2$ St.Err.	Sulfide mM Aver.	Sulfide St.Err.
<b><math>^{12}\text{C}</math> toluene + sulfate</b>				
1	1.00	0.00	0.00	0.00
2	1.08	0.00	0.18	0.06
3	1.08	0.00	0.37	0.10
4	1.08	0.00	0.38	0.05
5	1.08	0.00	0.42	0.11
6	1.08	0.00	0.46	0.10
7	1.08	0.00	0.16	0.13
8	1.08	0.00	0.28	0.22
9	1.08	0.00	0.31	0.22
10	1.08	0.00	2.64	0.16
11	1.08	0.00	2.83	0.18
12	1.08	0.00	3.00	0.09
13	1.08	0.00	2.93	0.16
14	1.08	0.00	2.36	0.07
15	1.11	0.02	2.25	0.15
<b><math>^{13}\text{C}</math> toluene + sulfate</b>				
1	1.00	0.00	0.01	0.01
2	1.08	0.00	0.17	0.01
3	1.11	0.03	0.51	0.14
4	1.16	0.07	0.52	0.11
5	1.65	0.37	0.65	0.05
6	1.71	0.60	0.57	0.10
7	1.92	0.72	0.18	0.09
8	1.22	0.04	0.29	0.19
9	1.81	0.35	0.28	0.22
10	8.05	1.45	2.09	0.43
11	8.22	1.75	2.26	0.36
12	9.59	1.93	2.76	0.33
13	11.11	1.74	2.68	0.37
14	11.64	1.79	2.60	0.39
15	12.22	1.79	2.36	0.50

**Table A.8:** Production of ferrous iron and  $^{13}\text{CO}_2$  in SIP microcosms related to transformation of labelled vs. unlabelled toluene as shown in **Fig. 3.1**. St.Err. = standard error.

<b>Week</b>	<b>CO<sub>2</sub> AT% Aver.</b>	<b>CO<sub>2</sub> St.Err.</b>	<b>Iron (II) mM Aver.</b>	<b>Iron (II) St.Err.</b>
<b><math>^{12}\text{C}</math> toluene + ferric iron</b>				
1	1.00	0.00	2.81	0.55
2	1.08	0.00	2.21	0.31
3	1.08	0.00	3.00	0.76
4	1.08	0.00	5.75	0.26
5	1.09	0.00	7.49	0.73
6	1.10	0.01	8.60	1.02
7	1.10	0.02	8.82	0.40
8	1.12	0.02	9.63	0.67
9	1.14	0.03	9.13	0.80
10	1.19	0.05	10.10	0.46
11	1.11	0.04	10.32	0.48
12	1.08	0.00	10.81	0.96
13	1.08	0.00	9.05	1.01
14	1.09	0.00	10.22	0.98
15	1.10	0.00	10.45	1.10
<b><math>^{13}\text{C}</math> toluene + ferric iron</b>				
1	1.00	0.00	2.32	0.39
2	1.10	0.01	1.80	0.47
3	1.11	0.01	3.87	0.11
4	1.12	0.01	5.94	0.46
5	1.16	0.03	7.63	0.09
6	1.21	0.05	8.67	0.44
7	1.27	0.09	8.25	0.08
8	1.46	0.18	8.19	0.78
9	1.78	0.30	8.66	0.37
10	2.98	0.39	10.52	1.01
11	2.44	0.32	11.78	0.16
12	2.74	0.29	10.70	0.10
13	2.86	0.34	12.22	0.50
14	3.02	0.42	12.94	0.66
15	3.74	0.65	14.58	0.88



**Table A.9:** Quantitative detection, by means of real time PCR, of 16S rDNA genes in 12 CsCl fractions from  $^{12}\text{C}$ - and  $^{13}\text{C}$ -toluene SIP microcosms amended with sulphate. The measured DNA quantities as copies/ $\mu\text{l}$  were converted to percentages of max, as also reported in **Fig. 3.2 A**.

<b>CsCl [g/ml]</b>	<b>16S rRNA [cp/<math>\mu\text{l}</math>]</b>	<b>% of max</b>
<b><math>^{12}\text{C}</math> toluene + sulfate</b>		
1.7453	1.68E+04	15
1.7398	8.13E+03	7
1.7344	3.23E+03	3
1.7278	2.09E+03	2
1.7202	3.74E+03	3
1.7126	1.31E+03	1
1.7049	7.17E+03	6
1.6972	4.81E+04	43
1.6906	7.64E+04	69
1.6841	1.11E+05	100
1.6819	2.46E+03	2
1.5562	5.05E+03	5
<b><math>^{13}\text{C}</math> toluene + sulfate</b>		
1.7496	3.13E+04	11
1.7463	6.58E+03	2
1.7398	5.04E+03	2
1.7333	1.06E+03	0
1.7246	4.43E+03	2
1.7169	5.06E+03	2
1.7104	4.29E+04	15
1.7027	9.34E+04	33
1.6961	2.84E+05	100
1.6896	7.78E+04	27
1.6830	1.65E+04	6
1.6554	1.74E+04	6

**Table A.10:** Quantitative detection, by means of real time PCR, of 16S rDNA genes in 12 CsCl fractions from  $^{12}\text{C}$ - and  $^{13}\text{C}$ -toluene SIP microcosms amended with ferric iron. The measured DNA quantities as copies/ $\mu\text{l}$  were converted to percentages of max, as also reported in **Fig. 3.2 B**.

CsCl [g/ml]	16S rRNA [cp/ $\mu\text{l}$ ]	% of max
<b><math>^{12}\text{C}</math> toluene + ferrihydrite</b>		
1.7485	2.39E+03	1
1.7442	4.07E+03	1
1.7387	9.20E+03	3
1.7322	5.88E+03	2
1.7246	7.23E+03	2
1.7169	1.83E+03	1
1.7093	1.97E+04	6
1.7027	7.43E+04	22
1.6950	3.44E+05	100
1.6885	3.02E+05	88
1.6808	9.05E+04	26
1.6742	1.20E+03	0
<b><math>^{13}\text{C}</math> toluene + ferrihydrite</b>		
1.7463	1.37E+03	0
1.7431	3.52E+03	1
1.7409	5.53E+03	2
1.7344	3.53E+03	1
1.7278	1.94E+03	1
1.7202	1.84E+04	5
1.7137	1.67E+05	47
1.7071	2.08E+05	59
1.6994	3.55E+05	100
1.6928	3.49E+02	0
1.6863	9.80E+03	3
1.6808	1.02E+04	3

## Lebenslauf - Giovanni Piloni

- 03.07.1980      geboren in Augusta (Italien)
- 1994 – 2000      Abitur am Andrea Saluta-Gymnasium in Augusta
- 2000 – 2006      Biologiediplom an der Catania Universität (Italien)
- 2005              Diplomarbeit an der Niederländisches Institut für Ökologie (NIOO-KNAW, Nieuwersluis, den Niederlanden) am Lehrstuhl für mikrobielle Ökologie:  
“Echological-niches differentiation of ammonia oxidizing bacteria in freshwater shallow lake sediments” betreut durch Prof. Dr. Stefania Stefani (Catania Universität) und Dr. Manuela Coci (NIOO-KNAW)
- März 2007 –      Europass Bühnenprogramm "Leonardo Da Vinci" am Archipelagos
- August 2007      IMERAS, Icaria, Griechenland
- September 2007 – Doktorand in der Arbeitsgruppe molekular Ökologie am Institut für
- Dezember 2010      Grundwasserökologie in Neuherberg, betreut durch Dr. Tillmann Lueders und Prof. Dr. Rainer Meckenstock

## **Selected contributions to national and international scientific meetings**

(first authorship only):

- Microbial community dynamics in a tar-oil contaminated aquifer as driven by geochemical and hydraulic change - **G. Pilloni**, T. Lueders (Axiom-Vibe Workshop “Electron transfer processes at biogeochemical gradients” March 4-7, 2008, Helmholtz UFZ, Leipzig, Germany).

- Ecological – niches Differentiation of Ammonia Oxidizing Bacteria in Freshwater Shallow lake Sediments - **G.N. Pilloni**, M. Coci, S. Stefani, H.J. Laanbroek (VAAM Conference, 9-11 March 2008, Frankfurt, Germany).

- Microbial community dynamics of key contaminant degraders and sulphate reducers in a tar-oil contaminated aquifer as driven by hydrogeochemical change - **G.Pilloni**, T.Riedel, A.Bayer, C.Griebler and T.Lueders (VAAM Conference, 8-11 March 2009, Bochum, Germany).

- Distribution and dynamics of contaminant degraders and redox guilds in stationary and non-stationary contaminant plumes - **G.Pilloni** and T. Lueders (StE Micro- Italian Society of Microbial Ecology- Workshop, 5-8 May 2009, Verbania, Italy).

- A ROLE FOR OLIGOCHAETE-ENDOSYMBIOTIC MICROBES IN SULPHUR-CYCLING IN CONTAMINATED AQUIFERS? - **G. Pilloni**, T. Riedel, K. Euringer, C. Kellermann and T. Lueders (Workshop VAAM Special Group “Symbiotic Interactions”, Helmholtz Muenchen, 19-20 November 2009, Neuherberg, Germany).

- HOW DYNAMIC IS STABLE? UNEXPECTED REACTIVITY OF KEY CONTAMINANT DEGRADERS TO HYDRAULIC FLUCTUATIONS IN A TAR-OIL CONTAMINATED AQUIFER - **G. Pilloni**, A. Bayer, B. Anneser, C. Griebler and T. Lueders (13<sup>th</sup> International Symposium on Microbial Ecology-ISME13, 22-27 August 2010, Seattle, USA).

---

## Acknowledgments

If it is true good time runs fast, this assumption could be easily applied to the period of my PhD at the IGÖ. I still cannot believe, in fact, 3 years (+ almost 3 months) are already gone. For this I would like to acknowledge everyone who was with me during all these days and made possible this achievement. Thus, I want to thank all my colleagues at the Institute of Groundwater Ecology of the Helmholtz-Zentrum München (once known as GSF...) and, in particular, Tillmann Lueders, who gave me the job and guided me during the entire journey. I have learnt a lot from him and I am seriously indebted for all the patience and time-availability he always reserved and also for the discussions on opposite points of views we have had. I also want to thank Rainer Meckenstock, for agreeing with Tillmann about giving me the job, and also for all the discussions, feedbacks, ideas and motivation ("doing great science while having fun!") he was always able to distribute. To both, moreover, I have to express my appreciation for allowing me to do what I liked how I liked, in an environment maybe so productive for me also because full of freedom on managing my own activities.

All this thesis relied on the sampling we did on Düsseldorf-Flingern: this would not have been possible without the collaboration of Bettina Anneser, Christian Griebler and, in particular, Anne Bayer, who shared with me the joys and pains of the samples' analyses. For this also the DFG research group 'Analysis and Modeling of Diffusion/Dispersion-limited Reactions in Porous Media' (FOR 525) must be acknowledged, for the funding and for the fruitful discussions during the meetings.

I want also to express my sincere appreciation to all my colleagues of the "Molekulare Ökologie Arbeitsgruppe" and in particular to Katrin Hörmann, for re-establishing (and maintaining) the lab-managing and Frederick von Netzer, who is also the author of the German abstract of this thesis. Many thanks to the hard-working students (Tanja Riedel and Ilgin Yildiz) who collaborated with me; if Tanja recently started a PhD, this probably means something good has been done here!

After days of exhausting lab work, the time spent in the office was also great and for this my thanks are for my actual (Anne Bayer, Katrin Hörmann, Marko Hünninger and Clemens Karwautz) and previous (Bettina Anneser, Claudia Kellermann, Katrin Euringer, Nidal Abu Laban and Robert Bauer) room mates, who created always a nice environment with chats, discussions, laughs and hysterias.

For the laughs and good time thanks to Armin Meyer and Franz Bergmann, also for the "late" lunch breaks with the other more or less occasional attendees. Also, the parties and the hangouts with them and everyone else from the institute will be always unforgettable memories for me. Related to the hangouts in Munich (or the evenings at home when too cold!), a big thank to Antonio, Victor, Olga, Alessandra, Damiano, Silvia, Federico, Edoardo and Spyros for all the nice moments we spent together (the guys also for the weekend football matches!).

During these 3 years my family (which is a Sicilian one, but not "that" one) was always very close, encouraging and motivating me; therefore a big "grazie" goes to my mother, my father, my brother and my grandmother.

Last in this list but first in my heart there is Diyan Chen, for being emotionally so close even if geographically so far! I really hope this will be a further step for a better matching between our relationship and respective own careers.

Finally, it must be mentioned this experience (shared by Italian scientists all over the world) would have not been probably possible without the collaboration of more than 15 years of senseless politics (but, basically, a one-man show!) about research and university.